uOttawa

L'Université canadienne
Canada's university

FACULTÉ DES ÉTUDES SUPÉRIEURES ET POSTOCTORALES

uOttawa

L'Université canadienne
Canada's university

FACULTY OF GRADUATE AND POSDOCTORAL STUDIES

Philippe Malouf

AUTEUR DE LA THÈSE / AUTHOR OF THESIS

M.A.Sc. (Chemical Engineering)

GRADE / DEGREE

Department of Chemical Engineering

FACULTÉ, ÉCOLE, DÉPARTEMENT / FACULTY, SCHOOL, DEPARTMENT

Study of the Relationship of Rheology, Morphology and Biomass Concentration of Trichderma reesei Fermentation

TITRE DE LA THÈSE / TITLE OF THESIS

Dr. Jules Thibault

DIRECTEUR (DIRECTRICE) DE LA THÈSE / THESIS SUPERVISOR

CO-DIRECTEUR (CO-DIRECTRICE) DE LA THÈSE / THESIS CO-SUPERVISOR

EXAMINATEURS (EXAMINATRICES) DE LA THÈSE / THESIS EXAMINERS

Dr. Jason Zhang

Dr. Arturo Macchi

Gary W. Slater

Le Doyen de la Faculté des études supérieures et postdoctorales / Dean of the Faculty of Graduate and Postdoctoral Studies

Study of the Relationship of Rheology, Morphology and Biomass Concentration of *Trichoderma reesei* Fermentation

by

Philippe Malouf

A thesis submitted to the Faculty of Graduate and Postdoctoral Studies in partial fulfillment of the requirement for the degree of

Master of Applied Science

in

Department of Chemical and Biological Engineering

University of Ottawa

Your file Votre référence
ISBN: 978-0-494-48477-7
Our file Notre référence
ISBN: 978-0-494-48477-7

Abstract

Bioethanol produced from cellulosic materials, abundantly found as wastes, appears to be a viable alternative to fossil fuels. Cellulose is a glucose polymer and must undergo a hydrolysis step by cellulase enzymes prior to be used for bioethanol production. In order to make bioethanol more cost competitive, all aspects of the production are being examined, including trying to improve the production of these enzymes using a filamentous microorganism, *Trichoderma reesei*. Filamentous fungi broth is widely known for being highly viscous, which limits transport properties, thus hindering the production of cellulase. Therefore, the overall objective of this work is to understand the intimate relationship that exists between enzyme production, morphology of microorganism, rheology of the broth and operating conditions. In this work, the rheology of the fermentation broth is examined in order to understand its impact on the other process variables.

As a preliminary step, the choice of an appropriate rheological instrument was discussed. Fed-batch fermentation runs were performed in two bioreactors: a stirred tank bioreactor with an agitation speed of 200, 300, 400 and 500 RPM and a reciprocating plate bioreactor agitated at 0.25, 0.50, 0.75 and 1.00 Hz. Herschel-Bulkley equation described relatively well rheological data. The effect of morphology and biomass concentration (X) on the consistency index (K) was studied separately. Biomass reconstitution experiments showed that biomass exponent α, in K/X^{α}, remained constant. K/X^{α} varied during the course of the fermentation runs, underlying the importance of including a morphological parameter in the prediction of K. Although several morphological parameters were analyzed, K/X^{α} was found to correlate well with the average roundness, when the batch and

the fed-batch data were considered separately. Parity plot analysis of the models showed good prediction of the experimental *K*.

Résumé

Le bioéthanol produit à partir des matériaux cellulosiques, qui abondent comme déchets, semble être une alternative viable aux combustibles fossiles. La cellulose est un polymère de glucose devant subir une étape d'hydrolyse enzymatique par la cellulase avant d'être utilisée en bioéthanol via la fermentation. Afin de rendre le coût du bioéthanol concurrentiel, tous les aspects de la production doivent être examinés, y compris le sujet de cette thèse qui a pour but d'améliorer la production de ces enzymes produites par un micro-organisme filamenteux, *Trichoderma reesei*. Le bouillon de champignons filamenteux est habituellement très visqueux, limitant ainsi les phénomènes de transfert, de ce fait la production de la cellulase. Par conséquent, l'objectif de ce travail est de comprendre le rapport intime qui existe entre la production d'enzymes, la morphologie du micro-organisme, la rhéologie du bouillon de fermentation et les conditions de fonctionnement. Dans ce travail, la rhéologie du bouillon de fermentation est examinée plus particulièrement afin de comprendre son impact sur les autres variables du procédé. Dans un premier temps, le choix d'un instrument de mesure rhéologique approprié est discuté.

Des fermentations en mode semi-continu ont été menées dans deux bioréacteurs : un bioréacteur avec pâle de Rushton agité à 200, 300, 400 et 500 RPM et le bioréacteur à plateaux mobiles agité à des fréquences d'agitation de 0.25, 0.50, 0.75 et 1.00 Hz. Les données rhéologiques ont été décrites par l'équation de Herschel-Bulkley. L'effet de la morphologie et de la concentration de biomasse (X) sur le coefficient de consistance (K) a été étudié séparément. Les expériences faites avec une grande plage de la concentration de la biomasse ont montré que l'exposant de biomasse α, dans l'expression K/X^{α}, demeure

constant. Cependant, K/X^{α} varie durant la fermentation, montrant ainsi l'importance fondamentale d'inclure un paramètre morphologique pour prédire la valeur de K. Bien que plusieurs paramètres morphologiques ont été analysés, K/X^{α} a une plus forte corrélation avec la rondeur moyenne, quand les données en discontinu et en semi-continu étaient considérées séparément. Une analyse a démontrée une bonne prédiction de la valeur expérimentale de K.

Statement of Contribution of Collaborators

I hereby declare that I am the sole author of this thesis. I have performed the experimental design, all experiments and the associated data analysis relating to the rheological analyses.

My supervisor, Professor Jules Thibault, provided continual guidance throughout this work and made editorial comments and corrections to my written work. Professor Denis Rodrigue of Laval University contributed his expertise in rheology and made suggestions and corrections to improve the paper contained in Chapter 3.

Part of the experimental work was done in collaboration with Nilesh Patel and Viviane Choy. They helped in setting up the laboratory and conducting the experiments. Nilesh Patel is co-author of the paper of Chapter 3. I have contributed to the work of Nilesh Patel and I am co-author of a paper that will appear in his thesis submitted roughly at the same time.

Signature: _____ Date: 02-07-2008

Acknowledgements

I wish to express my sincere gratitude and respect to my advisor, Professor Jules Thibault, for his ideas, patience, advice throughout my Master's program, and for giving me an opportunity to work in my field of research interest at the Chemical and Biological Engineering Department. His support and encouragement are most appreciated.

I would like to thank Professor Denis Rodrigue (Laval University) for his assistance, guidance and willingness to take the time to make suggestions in the field of rheology. His knowledge and insight are greatly valued.

I am immensely grateful to Stewart Hunt from TA Instruments for establishing a collaboration allowing me to have access to their rheometer. Without his support, this research might not have been possible.

My particular gratitude goes to my research group partners, Nilesh Patel and Viviane Choy, for the days and nights spent in the laboratory, for keeping courage and perseverance amid the difficulties. I am thankful for their wonderful friendship.

I would like to thank the Chemical and Biological Engineering Department of the University of Ottawa. I am thankful to all professors, students and staff for their support and guidance throughout my MASc.

I am indebted to my friends for their suggestions, encouragement, motivation and guidance.

Finally, I would like to thank especially my beloved parents, Jean and Jeanette Malouf, and my sister, Diana, for their love, understanding, moral support, constant encouragement that they have given me throughout my academic career.

Table of Contents

List of Tables

List of Figures

Chapter 1

Introduction

1.1 Fermentation Historical Background

Fermentation has always been an important part of our lives in particular in the production of foods like bread and yoghurts, and beverages such as wine and beer. But how fermentation actually works was not understood until the work of Louis Pasteur in the later part of the nineteenth century and the research which followed. For a cell, fermentation is a way of getting energy without using oxygen. In general, fermentation involves the breaking down of complex organic substances into simpler ones. The microbial or animal cell obtains energy through glycolysis, splitting a sugar molecule and removing electrons from the molecule. The electrons are then passed to an organic molecule such as pyruvic acid. This results in the formation of a waste product that is excreted from the cell. Waste products formed in this way include ethyl alcohol, butyl alcohol, lactic acid, and acetone, the substances vital to our utilization of fermentation. For example, alcohol fermentation begins with glycolysis to produce two molecules of ethanol from every molecule of glucose. Alcohol fermentation is carried out by many bacteria and yeasts.

After Pasteur's discoveries, the uses of fermentation progressed rapidly in industry, as well as in other areas. Between 1900 and 1930, ethanol and butanol were the most important industrial fermentations in the world. But by the 1960s, chemical synthesis of alcohols and other solvents were less expensive and interest in fermentation diminished. However, chemical synthesis can be questioned. Chemical manufacture of organic

molecules such as alcohols and acetone relies on starting materials made from petroleum, a nonrenewable resource. Dependence on such resources could be considered non reliable due to its limitations and availability usually associated to politically unstable locations. Additionally, the use of petroleum has a detrimental impact on the environment.

In the past decade, interest in microbial fermentation is experiencing a revival. Plant starch, cellulose from agricultural waste, and whey from cheese manufacture are abundant and renewable sources of fermentable carbohydrates. Additionally, the portion of these materials that is not utilized represents solid waste that must be buried in dumps or treated as waste water. Microbial fermentations have other benefits. Unlike traditional chemical production, they do not use toxic reagents or require the addition of intermediate reagents. Microbiologists are now looking for naturally-occurring microbes that produce desired chemicals. In addition, thanks to the progress of biotechnology, they are now capable of engineering microbes to enhance production of these chemicals. In recent years, microbial fermentations have been revolutionized by the application of genetically-engineered organisms. Many fermentations use bacteria and fungi, but a growing number involve culturing mammalian cells.

According to the report by the National Research Council (1992), bioprocess engineering is "the subdiscipline within biotechnology that is responsible for translating life-science discoveries into practical products, processes, or systems capable of serving the needs of society". It is critical in moving newly discovered bioproducts into the hands of the consuming public. In addition, they define fermentation in industry as "any large-scale cultivation of microbes or other single cells, occurring with or without air". At the production and manufacturing level, large vessels called fermenters or bioreactors are used. A bioreactor may hold several liters to several thousand liters. Bioreactors are equipped

with aeration devices as well as nutrients, stirrers, and pH and temperature controls. During production, monitoring of these parameters is done, as well as growth in the bioreactors to ensure that conditions are optimum for cell growth and product formation. Bioreactors are used to make products such as insulin and human growth hormone from genetically-engineered microorganisms as well as products from naturally-occurring cells, such as the food additive xanthan. However, the most sought after products are biofuels, due to the environmental, economic and political implications.

1.2 Bioethanol production

Currently, production of fuel ethanol depends largely on corn grain and sugar cane. This industry, as well as the use of fuel ethanol itself, is rapidly expanding and beginning to increase prices of corn for feed and the downstream animal products. Cellulose as a substrate for ethanol has been of interest for several years, but recent events have called for a priority of research to commercialize the cellulose-to-ethanol biorefinery. Cost of lignocellulosic materials is lower than corn grain but processing for fermentation is more costly. The sugars in lignocellulose, which exist mostly as the polysaccharides cellulose and hemicellulose, are not readily available. Thus, pretreatment is required and is typically done by toxic chemicals. However, the last decade has seen intensive research in the production of cellulase enzymes, which is an alternative to the toxic chemicals. The enzymes are derived from microorganism, of which *Trichoderma reesei* (*T. reesei*) is the highest natural producer. The enzymes transform the cellulose into glucose, which makes it available for fermentation into ethanol. Although recent years has seen great progress in the production of these enzymes, thanks to genetic engineering and strain optimization

strategies, further research is required to make the price of ethanol more competitive with petroleum derived fuels.

1.3 Bioprocess Optimization

According to the textbook by Doran (1995), bioreactor performance should be optimized to reduce production cost. Four cost-determining factors in the process should be examined in order to devise strategies for bioreactor design necessary for cost reduction in the production of cellulase. The four factors are: research and development; raw materials; bioreactor operation; and downstream processing. In the case of cellulase production, bioreactor operation tends to be costly due to the microorganism. In fact, *Trichoderma reesei* is a filamentous fungus. Like many other moulds, *Trichoderma reesei* tends to form highly viscous non-Newtonian suspensions. This has a direct influence on some fermentation parameters such as culture broth composition, temperature, pH, shear stress, initial inoculum, dissolved oxygen and fungal morphology. In addition, the cell growth and the product formation are directly affected. Due to this complex interrelationship of operating parameters, it is important to consider morphology, enzyme production and process performance simultaneously (Schügerl et al., 1998). Thus, the strategy to decrease bioreactor operation cost is summarized in the diagram shown in Figure 1.1. Doran (1995) explains that to maximize volumetric productivity in order to minimize the reactor size, two approaches could be taken. On one side, maximizing productive cell concentration requires understanding the complex morphology of the fungi. On the other side, the production of high quantity and quality of enzyme entails the understanding of cellulase enzymes mode of function. Once the parameters are well understood, they can be related to other process parameters and reactor conditions to optimize production and decrease cost.

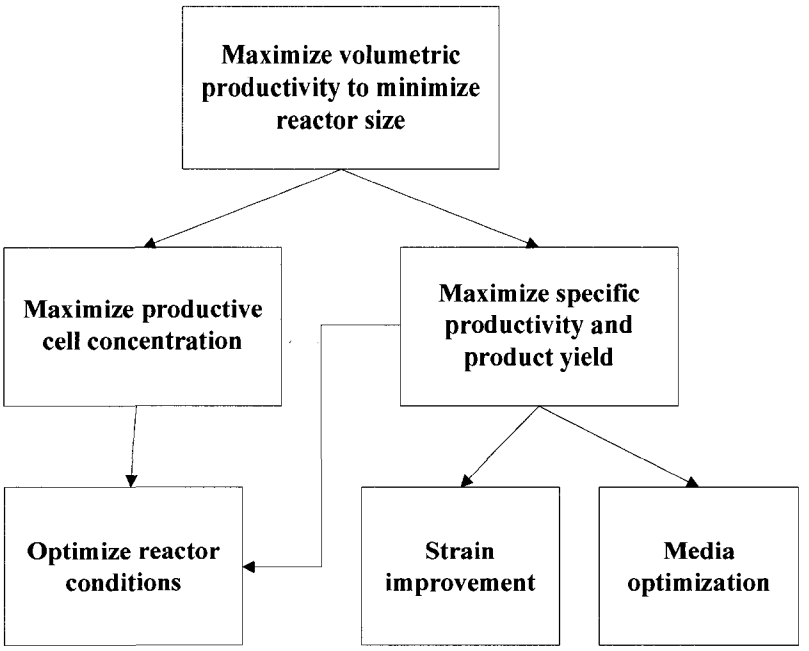

Figure 1.1 Strategy for bioreactor optimization. Adapted from Doran (1995).

The adaptation of the above approach results in the examination of cellulase production by *T. reesei* according to the strategy shown in Figure 1.2. As part of a group project done in close collaboration with our industrial partner, Iogen Corporation (Ottawa, Canada), the objectives are first to understand the intimate relationship that exists between the key process parameters of *T. reesei* during the course of fermentation and, second, to improve the production of enzymes. The results of this research will facilitate the development of strategies to optimize operating conditions for the production of enzymes secreted by *T. reesei* and to design more efficient bioreactors for these types of filamentous fungi, which will have a direct impact on the company's commercial potential to reach an enviable position in the international enzyme market.

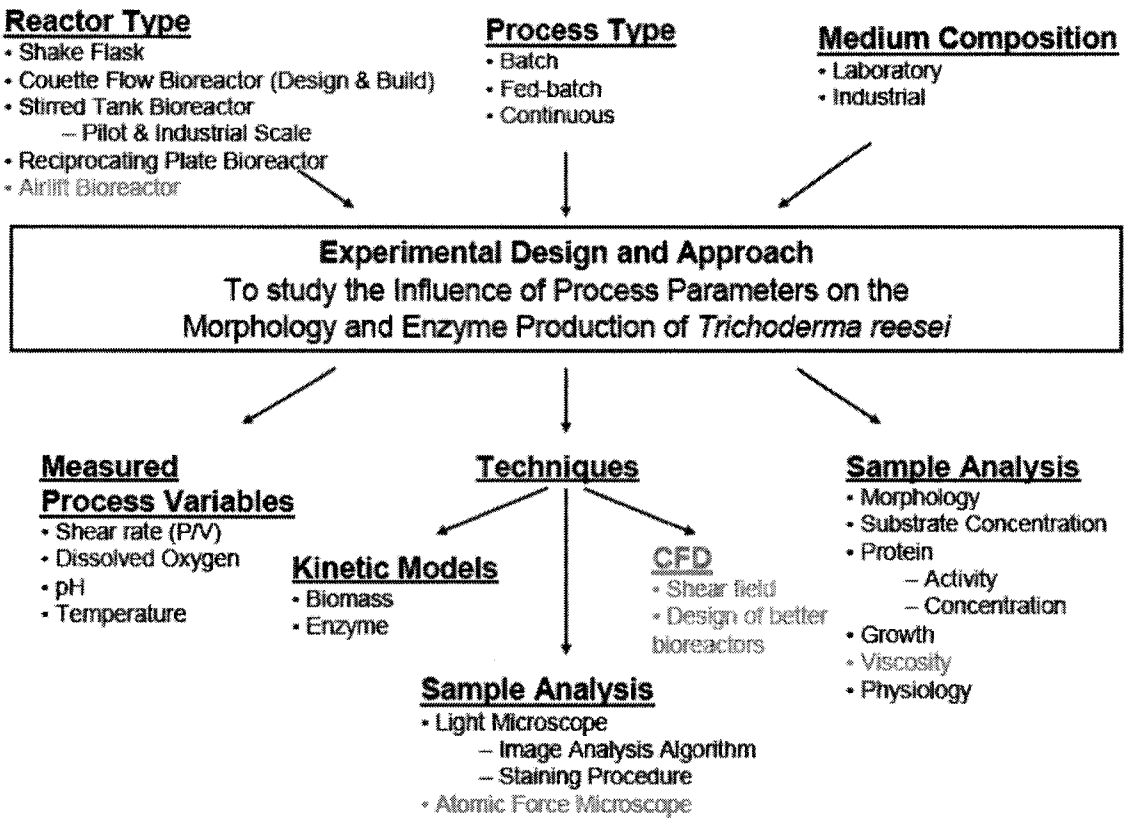

Figure 1.2 Diagram of the strategy to study the influence of process parameters on the morphology and enzyme production of *Trichoderma reesei.*

1.4 Thesis Objectives/Structure

Viscosity is an important aspect of rheology, the science of deformation and flow. Viscosity is the most important property affecting flow behavior of a fluid, and is related to the fluid's resistance to motion. It is determined by relating the velocity gradient in fluids to the shear force causing flow to occur. Viscosity has a marked effect on pumping, mixing, mass transfer, heat transfer and aeration of fluids. These in turn exert a major influence on bioprocess design and economics. Changes in rheology of fermentation broths are caused by variation of one or more of the following properties:

a. cell concentration;

b. cell morphology, including size, shape and mass;

c. flexibility and deformability of cells;

d. osmotic pressure of the suspending fluid;

e. concentration of polymeric substrate;

f. concentration of polymeric product; and

g. rate of shear.

Different members of our laboratory research group involved in this project had the responsibility to examine the different process parameters mentioned in Figure 1.2. However, due to its influence on process performance, a special consideration was given to the study of the fermentation broth rheology in this thesis. First, the measurement of rheological properties of fluid is closely examined. Second, the relationship between the rheology, the biomass concentration and the morphology of microorganisms is studied under different agitation conditions.

1.5 References

Doran, P.M. 1995. Bioprocess engineering principles. London: Academic Press. 439 p.

National Research Council (U.S.), Committee on Bioprocess Engineering, National Research Council (U.S.), Board on Biology, National Research Council (U.S.) and Commission on Life Sciences. 1992. Putting Biotechnology to Work: Bioprocess Engineering. Washington, D.C.: National Academy of Sciences. 133 p.

Schügerl, K., S.R.Gerlach and D. Siedenberg. 1998. Influence of the process parameters on the morphology and enzyme production of *Aspergilli*. Advances in Biochemical Engineering/Biotechnology, 60, pp. 195-266.

Chapter 2

Rheology Equipment Selection Process and Analysis Techniques

2.1 Historical Background

Although the study of rheology was established in the 1800 and in the first half of 1900's, its application to fermentation broth became an important field with the development of industrial fermentation in the second half of the 1900's century. It was well known, that good knowledge of broth flow properties is required in order to design and operate adequate bioreactors to carry out different types of fermentations (Steel and Maxon, 1962; Moo-Young et al., 1969). A fermentation broth is a complex structured suspension with properties varying during the course of a fermentation run. At the beginning of a run, the fermentation broth can have Newtonian properties. As the fermentation progresses, the fermentation broth may acquire non-Newtonian characteristics because the concentration of biomass and products increase. Due to this complexity, three decades were dedicated to research in view of defining the most appropriate measurement technique that would provide quantitative data. However, one of the major reasons for the slow progress in this area is the difficulty involved in measuring the rheological properties of suspensions such as mycelial broths. Some investigators argue that the disparities among rheological parameter estimates for a given broth result from the use of standard "absolute" rheological measurement devices - such as the concentric cylinder and pipeline viscometers - which are prone to particle settling and a "slip velocity" near the wall. Many researchers previously

addressed this problem with different techniques (Bongenaar et al., 1973; Leduy et al., 1974; Roels et al., 1974; Blanch and Bhavaraju, 1976; Charles, 1978; Metz et al., 1979; Fatile, 1985; Allen and Robinson, 1987, 1990). This work gathers information from previous research and applies previous findings to the measurement of fermentation broth of *Trichoderma reesei*.

2.2 Rheological Models in Fermentation Broths

Fluid mechanics can be defined by solving a set of constitutive equations, including a rheological model equation. A Newtonian behavior is the simplest of rheological models. The viscosity is defined as the relationship between the applied shear stress and the resulting movement of the fluid (shear rate).

$$\tau = \mu \times \dot{\gamma} \qquad 2.1$$

where μ is the viscosity (Pa.s), τ is the shear stress (Pa) and $\dot{\gamma}$ is the shear rate (s^{-1}).

Newtonian fluids have viscosities that are independent of the shear rate. The relationship becomes more complicated for non-Newtonian fluids. A special case of non-Newtonian fluids are pseudoplastic fluids, which have shear-thinning behavior. Shear-thinning fluids exhibit a decrease in viscosity with increasing shear rate. The viscosity in such fluids is thus shear-dependent, and in those cases, the viscosity is called the apparent viscosity. Mycelial fermentation broths commonly have marked pseudoplastic rheological characteristics (Deindoerfer and West, 1960; Charles, 1978; Metz et al., 1979; Olsvik and Kristiansen, 1994; Gibbs et al., 2000).

Four frequently used mathematical models for describing the rheology of fermentation broths are:

$$\text{Bingham (B)}: \quad \tau = \tau_{Y_B} + \mu \times \dot{\gamma} \tag{2.2}$$

$$\text{Power - Law (PL)}: \quad \tau = K_{PL} \times \dot{\gamma}^n \tag{2.3}$$

$$\text{Casson (C)}: \quad \sqrt{\tau} = \sqrt{\tau_{Y_C}} + K_C \times \sqrt{\dot{\gamma}} \tag{2.4}$$

$$\text{Hershel - Bulkley (HB)}: \quad \tau = \tau_{Y_{HB}} + K_{HB} \times \dot{\gamma}^n \tag{2.5}$$

where μ is the viscosity (Pa.s), τ is the shear stress (Pa), $\dot{\gamma}$ is the shear rate (s^{-1}), τ_{Y_B} is the Bingham yield stress, K_{PL} is the Power-Law consistency index, n is the flow index, τ_{Y_C} is the Casson yield stress, K_C is the Casson consistency index, $\tau_{Y_{HB}}$ is the Herschel-Bulkley yield stress and K_{HB} is the Herschel-Bulkley consistency index.

Fermentation broths are thus characterized in terms of time independent and non-viscoelastic models. Although experimental results have shown that time-dependent behavior may exist (Deindoerfer and West, 1960; Bonjenaar et al., 1973; Roels et al., 1974), no rheological models have been developed to characterize this occurrence in mould suspensions. The models are empirical equations used to fit to the experimental data and should be used with caution, since it is impossible to have full knowledge of shear stress vs. shear rate relations and the elastic properties in the different flow fields for non-Newtonian fluids.

The Bingham model is the Newtonian model with a yield stress. The yield stress is the minimum stress to be exceeded before the fluid will start to flow. The importance of the yield stress lies in the fact that the start-up power requirement in pumping through pipelines and mixers will be altered. In addition, well mixed caverns emerge inside the fermenters outside of which stagnant regions are present. In the specific case of *T. reesei*, Marten et al. (1996) gave a complete discussion on the effect of yield stress. Bingham model was used

previously by some authors to characterize rheology of fermentation broths of fungi (Deindoerfer and West, 1960; Allen and Robinson, 1990). A review of the different aspects of the yield stress phenomenon was given by Barnes (1999). He discussed yield stress for solids and liquids, and argued that a fluid can exhibit a range of yield stress and how yield stress can be measured. In the case of filamentous fermentations, Moo-Young et al. (1987) observed the polymer solutions were able to predict fermentations broth characteristics if no or low yield stress was observed in the fermentation broth, though was unsuccessful in the opposite case. The work by Leong-Poi and Allen (1992) applied the rotating vane technique for direct measurement of the yield stress of filamentous fermentation broths. In their work, they found that the static yield stress (measured by their method) had higher values than dynamic yield stress obtained by extrapolation of models that account for yield stress. At a later time, the work done by his colleague, Mohseni et al. (1997), showed that the difference of the static and the dynamic yield stress depended on the morphology of the mould tested. The more structured the filamentous fermentation broth, the greater this difference.

The Power Law model is the most generally used in the characterization of rheology of fermentation broths (Allen and Robinson, 1990; Ju et al., 1991; Olsvik et al., 1993; Queiroz et al., 1997; Badino Jr. et al., 1999; Riley et al., 2000; Pamboukian et Facciotti, 2005; Casas Lopez et al., 2005). This model describes well shear thinning fluids with no yield stress when the flow index (n) is below 1. An alternate model, Herschel-Bulkley (HB) model is an adaptation to the Power Law equation to include yield stress. The Casson model is a specific case of the HB model. They are both commonly used to describe rheology for fermentation broths. Though, HB and Casson models are thought to fit

experimental data at low shear rates better than the power law model (Bongenaar et al., 1973; Metz et al., 1979; Ghildyal et al., 1987; Marten et al., 1996).

In previous work, it was suggested via statistical studies that the use of any of the rheological models would characterize the experimental data evenly well, when the data ranged over only one or one-and-a-half decades (Scott Blair, 1966). Elsewhere, three models (Power Law, Casson and HB) were compared for the apparent viscosity of a *Penicillium chrysogemun* fermentation broth and found no significant difference over a limited range of shear rates (Reuss et al., 1982). Allen and Robinson (1990, 1991) showed that two- and three-parameter models did not have a significant difference in describing the experimental data in the shear rate range of 2 to 650 s^{-1}.

In mould suspension rheology, the viscosity is commonly described solely by the consistency index, K (Schügerl, 1981; Olsvik et Kristiansen, 1992a, 1992b). According to Allen and Robsinson (1990) and Olsvik et al. (1993), the flow index (n) is less influenced by the operational design than K. Nonetheless, n has larger effect on the shear stress due to the fact that n is an exponent. As a result, Olsvik et al. (1993) suggested that the use of K as a sole indicator of viscosity should be done with caution. This is possible when n is either constant or shows minor variation. Elsewhere, during studies on moulds *Penicillium*, *Aspergillus* and *Streptomyces*, correlations were found between the biomass concentration and the consistency index, while none were found in the case of the flow index (Allen and Robsinson, 1990).

2.3 Rheology Instruments

Fundamental rheological properties are independent of the instrument on which they are measured so different instruments should give the same rheological characteristics. This is an ideal concept and different instruments rarely yield identical results. To understand this shortcoming, it is essential to define rheology and viscosity. Viscosity describes a fluid's internal resistance to flow. As explained above, there are fluids which are called Newtonian, when their viscosities are constant, while others are non-Newtonian, where their viscosities depend on the shear rate. Some fluids may have solid-like properties such as elasticity, called viscoelastic. Rheology is the field of study which encompasses all these fluids. The existence of different properties within a fluid makes the measurement of the rheology a complicated task. Thus, it must be recognized from the outset that not all of the popular instruments measure viscosity, as an absolute value. However, they provide valuable flow behavior information which, in many cases is quite adequate so long as it is internally consistent. In some cases, such information is even more useful than actual viscosity data, like texture control in the food industry (Steffe, 1996). In general, the complex flow patterns employed in many instruments makes them unsuitable for rigorous measurement of viscosity. It is also important to note that even with instruments specifically designed to measure viscosity, considerable care must be exercised in analyzing data for non-Newtonian fluids. It is also important to recognize that in most cases, the empirical constants in any viscosity model are valid over only a limited range of shear rate and extrapolation beyond the range for which the constants were determined is usually risky. For example, the consistency index, K, of the Power Law model is obtained by extrapolation to 1 s^{-1}. Therefore, it is quite possible that K will have no real physical

significance at 1 s^{-1}. Also, the value of K will generally vary with the range of shear rate considered. Similar statements can be made regarding the flow index, n. Thus, viscosities should be determined over the range of shear rate that will be encountered in the process of interest. Finally, it should be noted that the choice of the most appropriate viscometer will be dictated, in part, by the range of shear rate to be studied.

2.4 Rheological Instrument Classes

Instruments for measuring elemental rheological properties of fluids are commonly placed into two general categories: rotational type and tube type (Steffe, 1996). Rotational instruments have different geometries, also known as fixtures, which is in contact with the sample being analyzed. The geometries typically found are the parallel plates, cone and plate, different variations of Couette (also know as concentric cylinders) and the mixer. Tube instruments are made up of glass capillary, high pressure capillary and pipes. Most are commercially available; others (mixer and pipe viscometers) are easily fabricated. Mixer rheometers include a variety of geometries like the vane (can have varying number of paddles and sizes), the ribbon impeller, etc... Costs vary tremendously from the inexpensive glass capillary viscometer to a very expensive rotational instrument capable of measuring dynamic properties and normal stress differences. Solids such as polymers, foods and gels are often tested in compression (between parallel plates), tension, or torsion. Rheometers are the instruments which measure rheological behavior of fluids. While, viscometers are instruments that only measure viscosity. The term viscometer is limited to the last type of measurements.

Rotational instruments can have two modes of operation: the steady shear (constant angular velocity) or/and oscillatory (dynamic) mode. Also, rheometers can function in either controlled stress mode or controlled rate mode. The controlled stress mode facilitates the collection of creep data, the analysis of materials at very low shear rates, and the investigation of yield stresses. This information is needed to describe the internal structure of materials. The controlled rate mode is most useful in obtaining data required in process engineering calculations. As well, rotational systems are commonly used to study time-dependent behavior because tube systems only allow one pass of the material through the apparatus. A detailed discussion of the oscillatory testing, the primary method for investigating the viscoelastic behavior of structured fluids can be found in other textbooks (Tanner, 2000; Steffe, 1996). All rotational instruments are typically configured such that a measuring fixture is in contact with the sample. The same fixture is attached to a drive and a torque sensor or the torque sensor is on the opposite fixture.

Mechanical differences exist between controlled rate and controlled stress instruments, which affect the capabilities and the cost of rotational instruments. The torque is essentially measured in a different manner. It is important to understand the physical characteristics of the torque sensor when considering measurements using a rotational viscometer, such as flow or yield stress. In simplified way, in controlled rate instruments, the motor drive and the torque sensor are separate, while in the controlled stress instruments, the motor drive and the torque sensor are on the same side. Two typical torque measuring concepts, used in controlled rate instruments, are illustrated in Figure 2.1. In one system, the force is transferred through the sample from the sample cup causing the deflection of a coiled spring. Spring deformation is measured and correlated to torque. Full scale wind-up (how much the cylinder must rotate before the full scale torque is measured)

is high for this type of system, often reaching as much as 80 degrees. A system with low wind-up is also illustrated in the same figure. In this system, the full scale deflection of a torsion bar is correlated to torque. Full scale deflection is achieved with very low wind-up values often in the range of 1 to 2 degrees.

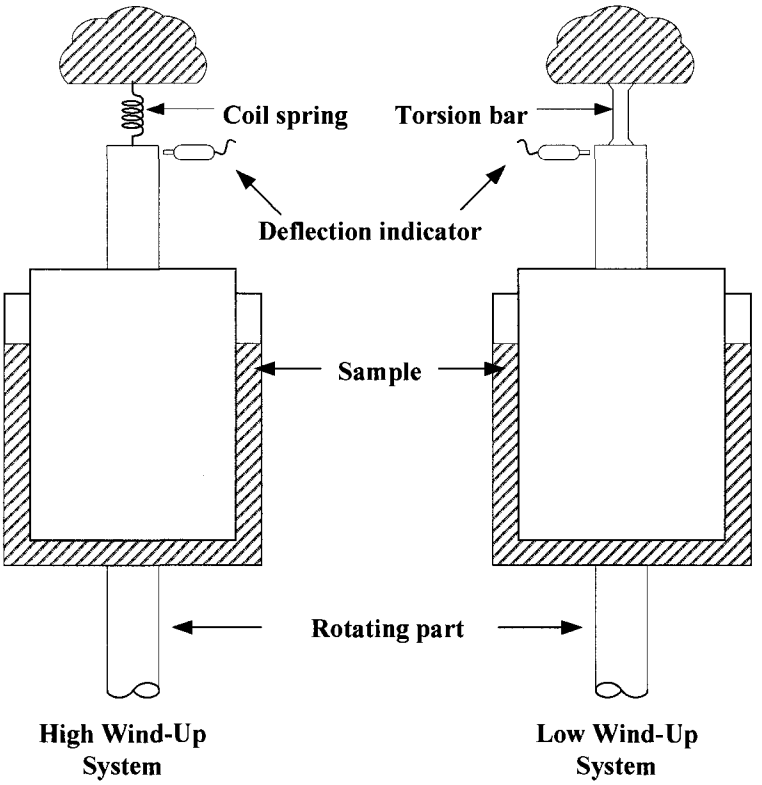

Figure 2.1 Strain Controlled Rheometer concentric cylinder (adapted from Steffe, 1996).

A controlled stress instrument is shown in Figure 2.2. It can use an air bearing or magnetic bearing to provide "frictionless" movement of the upper fixture and a drag cup motor to generate controlled torque on the shaft. Displacement is measured by a position indicator. For this type of instruments, wind-up is basically zero. In recent years, more sophisticated instruments were developed with both systems. In addition, technologies with air bearing are able to measure torques way below mechanical sensors. To further improve sensing, TA Instruments has developed rheometers with magnetic bearing instead of the air bearing, further increasing the shear stress and the shear rate ranges at which the instrument

can run tests. For further details on controlled stress rheometry, refer to the review on this matter by Barnes and Bell (2003).

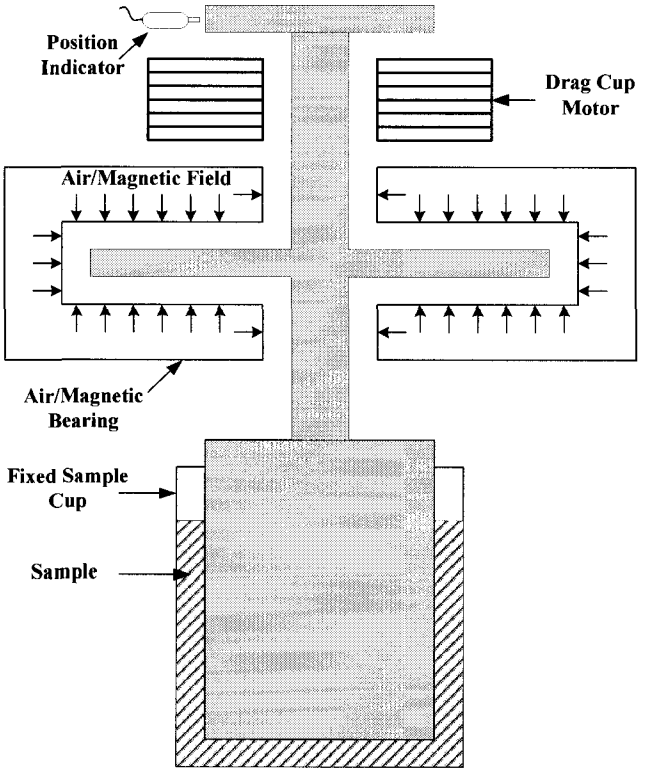

Figure 2.2 Controlled stress concentric cylinder rheometers (adapted from Steffe, 1996).

There are advantages and disadvantages associated with each instrument type. For example, gravity operated glass capillaries are only suitable for Newtonian liquids because the shear rate changes during a sample pass. Cone and plate systems with small cone angles require simple calculations to obtain shear rates. But, they are limited to moderate shear rates. Pipe and mixer viscometers can handle much larger particles than cone and plate, or parallel plate, devices. Problems associated with slip and degradation in structurally sensitive materials are minimized with mixer viscometers. Pipe viscometers can be constructed to withstand the rigors of the production plant conditions. It is frequently difficult to use a capillary viscometer to measure viscosities of fluids containing suspended particles. Among the problems most frequently encountered are settling of particles and

plugging of fine capillary tubes, particularly by filamentous fungi. When particles remain suspended and do not clog the capillary, complications can be introduced by the "tube pinch" effect which is the migration of small particles away from the wall to the center of the capillary. Capillary rheometers are also not well suited for measurement of the yield stress. As a result of these difficulties, capillary viscometers have not been used widely to study rheological properties of culture broths. Fatile (1985) measured the broth viscosity of *Aspergilus niger* fermentation with a pipe-flow viscometer. Allen and Robinson (1990) studied three different online pipeline viscometers for three mould suspensions: *Aspergilus niger*, *Penicillium chrysogenum* and *Streptomyces levoris*. They found that small diameter pipelines had slip problems, while larger diameter pipeline measurements were in close agreement with rotational instruments tested.

2.5 Rheometers and Fixtures used for Fermentation

The rheological measurements of fermentation broths were mainly done using rotational instruments. Tables 2.1 and 2.2 show an extensive list of publications where rheological instruments were used for fermentation broth. The different geometries used are also listed. The following section is a discussion on these different geometries. It can also be noted that Table 2.1 is dedicated to Brookfield Engineering rheometers due to the popularity and ease of use of this instrument. It is also clear from the two tables that the preferred geometries are the concentric cylinders and the vanes.

Table 2.1 Brookfield Engineering rheometers used in literature to measure fermentation broth rheology.

Authors	Date	Model	Torque Range	Geometry/Spindle	Comments/Characteristics
Oncu et al.	2007	DVII+	N/A	Concentric Cylinder	UL Adapter; Correction for pellets same size as annulus.
Brar et al.	2007	DVII+	N/A	Concentric Cylinder	SSA SC4-34, L2, ULA 18/50 ml cup (25°C); Shear rate 0.1-200 s^{-1}; Time dependent profile at 7.34 s^{-1}
Verma et al.	2006	DVII+	N/A	Concentric Cylinder	SSA SC4-34
O'Cleirigh et al.	2005	DVI+	N/A	Cone and Plate	Calibrated with Xanthan Gum
Mishra et al.	2005	DVI	N/A	N/A	Dial Viscometer
Lopez et al.	2005	DVII+	N/A	Vane and Cup	Measurement in glass vessel (35 mm D) filled (70 mm) Vane V72 (21.67 mm D × 43.33 mm H)
Pamboukian and Facciotti	2005	DVIII	LV	Concentric Cylinder	Speed 1-150 RPM, ULAdapter (0-322 s^{-1}; 1-5000cP), SSA-18 (0-330 s^{-1}; 1.3-30000 cP), SSA-31 (0- 85 s^{-1}; 12-30000 cP)
Benchapattarapong et al.	2005	Dial	N/A	HB#3	Dial; 0.17-33.33 s^{-1}; Qualitative measurements
Hwang et al.	2004	DVII+	LV	Concentric Cylinder	SSA
Bhargava et al.	2003	DVII+	N/A	Vane and Cup	4 blades vane (20 mm W x 30 mm H) in 250 mL beaker. Calibrated to correlate viscosity, torque, rpm
Richard and Margaritis	2003	DVII+	RV	N/A	N/A
Kim et al.	2003	DVII+	LV	Concentric Cylinder	SSA
Pollard et al.	2002	DVII+	LV	RV Disc spindles	RV disc spindles #2 and #6 immersed in a 500-mL cup
Cho et al.	2002	DVII+	LV	Concentric Cylinder	SSA
Roukas and Mantzouridou	2001	DVII	N/A	Concentric Cylinder	SSA SC4-18/13R
Sinha et al.	2001	DVII+	LV	Disc Spindle Impeller	
Thorne et al.	2000	DVII	LVT	N/A	
Gouveia et al.	2000	N/A	LV/RV	Concentric Cylinder	
Casas et al.	2000	N/A	LVT	Concentric Cylinder	Synchrolectric Model; SSA SC4-18, Calibrated
Chen et al.	1997	DVII	N/A	Concentric Cylinder	UL Adapter; Speeds: 12, 20, 30, 50, 60, 100 RPM
Badino Jr et al.	1997	DVIII	LV/RV	Vane/Helical Ribbon Impeller	Construction; Online; Calibrated to correlate viscosity, torque, rpm, shear rate, shear stress
Queiroz et al.	1997		LVT	Concentric Cylinder	SSA
Shi et al.	1993	Dial	LVT	N/A	

Table 2.2 Rheometers used in literature to measure fermentation broth rheology.

Author	Year	Make/Model	Comments/Characteristics
Chavez-Parga et al.	2007	Haake, Model CV20N	Helical Impeller to perform torque measurements
Lim	2006	ARES	Rheometrics Co. Ltd., USA
Müller et al.	2003	Bohlin CS Rheometer	Bohlin Rheologi, AB, Sweden; PC connected; C25 concentric cylinder (25 mm D); Cup (27.5 mm D); Sample (25 ml).
Chavarría-Hernández et al.	2003	Haake-5M viscometer, PV 20 Rotovisco	Concentric cylinders (inner D: 4 cm; annuli: 0.2 cm); Samples (45 mL) at 25 °C; Shear rates 67- 450 s^{-1} (upward direction).
Stoupis and Stewart	2002	Carri-Med Controlled Stress Rheometer CSL100	TA Instruments, Leatherhead, Surrey, UK; cone and plate (6 cm D, 1′ 59″); 1 min equilibration at 5°C, 1 min ascending shear rate to a preset shear stress value, and 1 min descending shear rate (constantly at 5°C).
Pollard et al.	2002	MC1 rotational viscometer	Paar Physica USA, Inc., Edison, N.J.; Concentric Cylinders: MS-Z1 (gap: 0.5 mm; sample (17 mL); viscosity 0.001–0.1 Pa.s)/MS-Z2 (gap: 1.9 mm; sample (100 mL), viscosity 0.02–15 Pa.s). Rushton impeller (six-bladed 0.025 m D; 3.0-L vessel; sample 2.6 L);
Bueno & Garcia-Cruz	2001	Rheotest 2.1 rheometer	RHEOTEST®GmbH in Medingen, Germany; Concentric cylinder
Hernández-Peñaranda et al.	2001	Haake RV2 viscometer	Concentric cylinders: NV and MVIP
Riley et al.	2000	Rheomat 30	Contraves, Zurich, Switzerland; six-blade Rushton in 600 ml beaker; sample (400 ml)
Casas et al.	2000	Bohlin Rheometer CS	Calibrated
Goudar et al.	1999	Bohlin CS Rheometer	Bohlin Instruments, Cranbury, NJ; Concentric cylinder C25; Sample 25 ml.
Gehrig et al.	1998	Home Made Rheometer	Baffled Couette rotary rheometers to prevent sedimentation
Toda et al.	1998	Rheometrics RFS-II	Equipped with a double cylindrical fixture.
Mohseni et al.	1995	Haake Rotovisco RV12/ RAA Analyser	Haake Buchler Instruments; Rheometrics Inc.; Direct vane method for yield stress measurement.
Marten et al.	1996	Rheometrics mechanical spectrometer (RMS-800)	Vane (40 mm H×17.6 mm D). Cup (47.6 mm D); Sample (90 ml-100ml); Shear Rate 0.1-10 s^{-1}. Viscoelastic Properties where measured.
Li et al.	1995	Rheotest 2.1 rheometer	RHEOTEST®GmbH in Medingen, Germany
Pedersen et al.	1993	Bohlin CS rheometer	Bohlin Reologi AB; Concentric cylinder: C25; Double gap: DG 40/50
Olsvik et al.	1993/		
Olsvik&Kristiansen	1992/	Rheomat (Constraves)	Online; Residence Time 90 s; Shear rate 10 – 50 s^{-1}; 6 bladed impeller
Kemblowski et al.	1985		
Allen and Robinson	1990	Haake Rotovisco RV12	Home Made: Helical Ribbon Impeller; 2 Turbine Impellers; 3 Pipelines
Fatile	1985	Home Made Pipeline	
Roels et al.	1974	Haake Rotovisco MK50	Vane (Turbine impeller)
Leduy et al.	1974	Model 35 Fann V-G Meter	Equipped with an R1-B1-F1 rotor-bob-spring combination; six different speeds: 3, 6, 100, 200, 300, and 600 rpm.
Bongenaar et al.	1973	Haake Rotovisco	Vane in 3 L glass beaker + Home Made Rheometer

2.5.1 Rotational Viscometers

As discussed earlier, rotational instruments can be adapted to use different fixtures for viscosity measurements. The sections below discuss specifically the fixtures that are most commonly used.

2.5.1.1 Concentric Cylinder Geometry

The concentric cylinders, also called the coaxial cylinders, have two versions: (1) the Searle system (when the inner cylinder is rotating while the outer cylinder is static) and (2) the Couette system (when the outer cylinder is rotating, while the inner cylinder is static). Figure 2.3 shows a typical concentric cylinder fixture. Equations (2.6) and (2.7) are used to calculate the viscosity for a Searle system (Shramm, 1998).

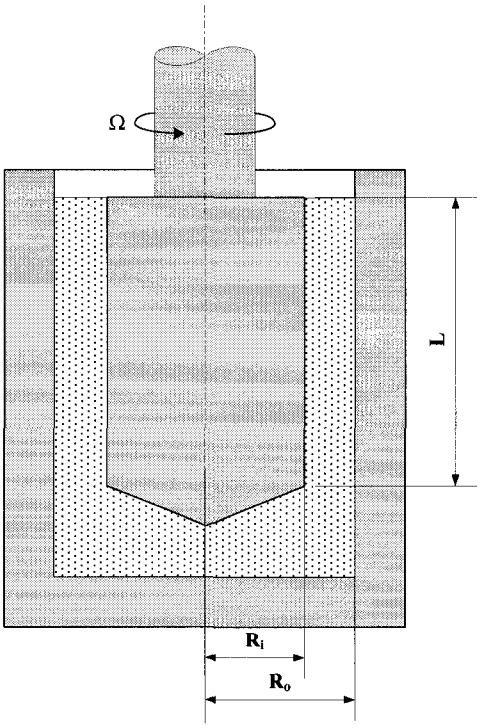

Figure 2.3 Typical Concentric Cylinder Fixture.

Shear rate calculation at the inner cylinder:

$$\dot{\gamma}_i = 2\Omega \frac{R_o^2}{R_o^2 - R_i^2} \tag{2.6}$$

$$\Omega = \frac{2\pi \times N}{60} \tag{2.7}$$

where $\dot{\gamma}_i$ is the shear rate (s^{-1}) at the inner cylinder of radius R_i (m), Ω is the angular velocity (rad/s), R_o is the outer cylinder radius (m), N is the inner cylinder rotational speed (min^{-1}). The shear rate $\dot{\gamma}_r$ within the annulus area is given by:

$$\dot{\gamma}_r = \frac{2\Omega}{r}\left(\frac{R_o^2}{R_o^2 - R_i^2}\right) \tag{2.8}$$

where r (m) is a radius between R_i and R_o. The shear stress τ_i (Pa) at radius R_i is given by:

$$\tau_i = \frac{M}{2\pi \times L \times R_i^2 \times C_f} \tag{2.9}$$

The shear stress τ_o (Pa) at radius R_o:

$$\tau_o = \frac{M}{2\pi \times L \times R_o^2 \times C_f} \tag{2.10}$$

The shear stress τ_r (Pa) at radius r:

$$\tau_r = \frac{M}{2\pi \times L \times r \times C_f} \tag{2.11}$$

where M (N.m) is the measured torque, L (m) is the cylinder height, C_f is the torque correction factor which incorporates cylinder end effects. The viscosity μ (Pa.s) is given by:

$$\mu = \frac{\tau_i}{\dot{\gamma}_i} \tag{2.12}$$

Therefore, the concentric cylinder fixture is a classical rotational viscometer. The above calculations show that the fixture provides a straightforward and accurate means for determining the Newtonian viscosity. While it can also be used for determining non-Newtonian viscosity, more complex calculations are required. The data should be collected at several rotational speeds. For more details regarding calculations, experimental procedures and various instrument correction factors, the reader is advised to consult rheology textbooks. Finally, it should be noted that when suspensions are tested in the Searle or Couette viscometer or any other rotational viscometer having a smooth rotating surface, a clear region forms in the immediate vicinity of the cylinder and there is often noticeable gravity settling of the particles. Hence, some questions exist as to whether such viscometers are entirely appropriate for testing whole culture broths. Nonetheless, concentric cylinders have the advantage over other rotational instruments in that they measure directly the viscosity. In order to retain this advantage, modified versions of the concentric cylinders have been investigated recently to address settling problems in suspensions. To address this problem, a flow rheometer based on the principles of helical flow was developed by Akroyd and Nguyen (2003). The rheometer they designed is a modified Couette flow system, whereby slurries are circulated through the concentric cylinders by the addition of an axial flow. The purpose of this axial flow is to prevent particles from settling and to maintain a homogeneous suspension. However, the addition of an axial flow component to Couette flow complicates the analysis procedure for non-Newtonian fluids particularly in wide gap geometries. Thus a specific emphasis in their study was placed on developing a correct analysis procedure for helical flow that eliminated the need for rudimentary calibration procedures. Although this settling was

investigated in concentric cylinder systems, further investigation is required for other problems.

2.5.1.2 Cone and Plate Viscometer

Another widely used type of fixture used in a rotational rheometer is the cone and plate. This fixture, which is illustrated in Figure 2.4, has the very convenient feature that for cone angles less than 3°, the shear rate throughout the fluid is essentially constant and given by:

$$\dot{\gamma} = \frac{\Omega}{\alpha} \qquad 2.13$$

where α is the cone angle (in radians).

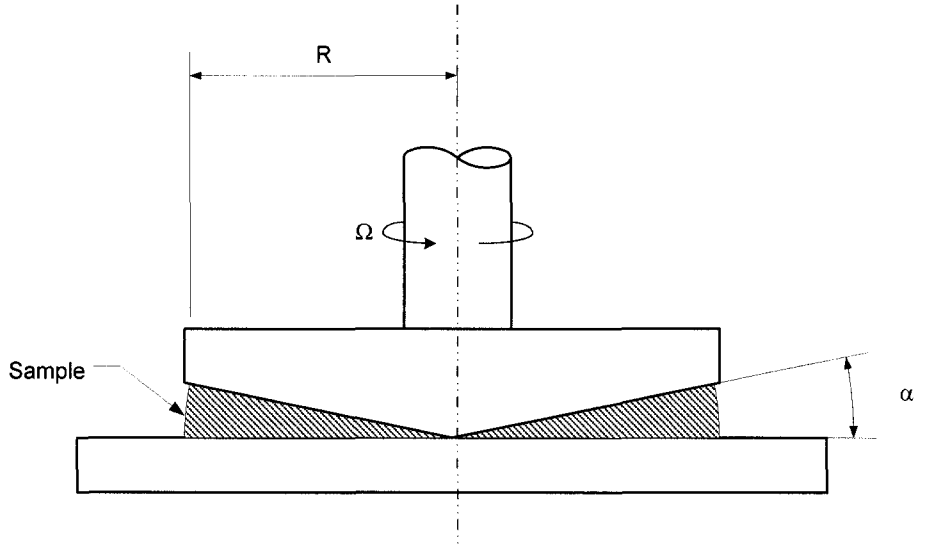

Figure 2.4 Cone and plate fixture.

The shear stress (at the surface of the cone) is given by:

$$\tau = \frac{3M}{2\pi R^3} \qquad 2.14$$

where M is the torque exerted on the cone and R is the radius of the cone. Thus, non-Newtonian flow curves can be obtained directly with relatively simple calculations. While the cone and plate fixture has been used extensively to study non-Newtonian fluids in general, its use in the study of rheological properties of culture broths has been limited (Mohseni et al., 1997; O'Cleirigh et al., 2005; Metz et al., 1979). In our laboratory, both the cone and plate and the parallel plate fixtures were tested. While the acrylic (which makes them transparent) fixtures rotated, the filamentous mould of *T. reesei* aggregated and separated from the fermentation broth medium. Then, the cell aggregates were expelled out of the fixtures; this will be discussed in future sections. Finally, other authors have observed phase separation near the rotating cone when suspensions were tested, but the separation did not appear to be as pronounced as in the cases of concentric cylinders and Brookfield spindles.

2.5.1.3 Mixer Viscometer

While standard rotational viscometers are versatile, reliable and widely employed, they are sometimes difficult to use for studying fermentation broths, particularly mycelial broths. Some of the difficulties were previously enumerated and are (Bongenaar et al., 1973; Roels et al., 1973; Allen and Robinson, 1987):

1. phase separation
2. formation of less dense region in immediate vicinity of rotating bob
3. non-homogeneity as a result of gravity settling

4. large particles about the same size as the gap impair accurate measurement of viscosity
5. destruction of particles in shear field.

Examples can be found in literature to illustrate the difficulties mentioned above. In the work done by Charles (1978), he studied in his laboratory with a dial Brookfield viscometer (model LVT) which has scale readings (proportional to viscosity), the viscosity as a function of time at various speeds for a 1% (w/v) *Aspergillus niger* culture broth sample. The readings shown were erratic but tended to decrease with time (more so at higher speeds) and at first seemed to indicate thixotropic behavior. However, through visual observation, the author saw partial settling and also phase separation near the rotating spindle (Brookfield No. 1), which were responsible for the observed time effect. He also observed similar behavior with a yeast suspension having a biomass concentration of 4% (w/v), although to a much smaller extent. Elsewhere, Allen and Robinson (1987) discussed extensively the slip problems encountered during experimentation and their effect on the end results.

In order to overcome such difficulties, many have worked with alternate geometries. Bongenaar et al. (1973) and Roels et al. (1974) developed a modified viscometer (basic unit was a Haake Rotovisko; MK50) which employed a turbine impeller instead of the more conventional smooth, geometrically simple concentric cylinders. They claimed that this fixture provides two important advantages:

a) phase separation and settling are prevented, and
b) the shear rate is simply related to the impeller speed via the Metzner and Otto (1957) relationship:

$$\dot{\gamma} = k N \qquad 2.15$$

where N is the rotational speed of the impeller, and k a constant that may be taken as approximately 10 for turbine impellers, at least for many pseudoplastic non-Newtonian fluids. The value of k depends on impeller type and geometry, which can be obtained in the laboratory, by calibrating procedures described by Metzner and Otto (1957). However, an extensive compilation of k values for various impeller types and for dilatant and Bingham fluids can be found in literature.

The turbine impeller establishes a relatively complex flow pattern which does not allow straightforward calculation of shear rate and raises some questions regarding the significance of the calculated viscosity. In particular, the instrument does not seem to satisfy the requirements for measuring viscosity as defined formally and therefore it is not clear immediately that the calculated quantity is an intrinsic property of the fluid. Nevertheless, the instrument does eliminate operating problems associated with rotational viscometers used to study mycelial broths and appears to give internally consistent data. Furthermore, data analysis while not absolutely rigorous from a rheological point of view is based on well-proven and widely-accepted empirical correlations. Roels et al. (1974) have presented the following derivation. The generally-accepted empirical relationship between power number, N_P and Reynolds number, N_{Re}, in the laminar flow region ($Re < 10$) is:

$$N_P = \frac{64}{N_{\mathrm{Re}}} \qquad 2.16$$

$$N_{\mathrm{Re}} = \frac{d_i^{\,2} N \rho}{\mu} \qquad 2.17$$

where d_i is the impeller diameter, ρ is the fluid density and μ is the fluid viscosity. The power number is, by definition,

$$N_P = \frac{P}{\rho N^3 d_i^5} \tag{2.18}$$

where P is the power input. The power input is also related to the torque, M, exerted on the impeller:

$$P = 2\pi N M \tag{2.19}$$

Combining Equations 2.16 through 2.19, one obtains:

$$M = \frac{64 d_i^3}{2\pi} \mu \tag{2.20}$$

As stated previously, it has been shown experimentally that the shear rate at the tip of a turbine can be expressed conveniently and usefully as in Equation 2.15, where k is a constant. Combining Equation 2.15 with Equation 2.1 results in

$$\tau = \mu \dot{\gamma} = \mu k N \tag{2.21}$$

Finally, Equations 2.20 and 2.21 are combined to give

$$\tau = \frac{2\pi k}{64 d_i^3} M \tag{2.22}$$

$$\tau = C_i M \tag{2.23}$$

where C_i may be viewed as an instrument constant. Thus, one may determine viscosity as a function of shear rate by simply measuring torque at various rotational speeds, so long as Re < 10. More recently, Lopez et al. (2005) adapted the above equations to further improve measurement for a non-Newtonian fermentation broth. The equations they obtained are used to predict the shear rate and the shear stress, respectively, for a Power-Law fluid in laminar regime:

$$\dot{\gamma} = k_i \left(\frac{4n}{3n+1} \right)^{\frac{n}{n-1}} N \qquad 2.24$$

$$\tau = \frac{2\pi k_i \left(\frac{4n}{3n+1} \right)^{\frac{n}{n-1}}}{c d_i^3} M \qquad 2.25$$

where k_i and c are constants that are dependent on the geometry of the system, n is the flow index. The constants are obtained through a two-stage calibration of the instrument: first, with a Newtonian fluid with known viscosity and, second, with a non-Newtonian fluid with known profile. The advantage of this system is in the direct calculation of the Power-Law parameters (K, the consistency index and n, the flow index) from instruments which typically measure the torque (M) and the impeller rotation speed (N). The authors accomplished this by further developing the above equations to give:

$$M = \frac{K c d_i^3}{2\pi} \left(\frac{4n}{3n+1} \right)^n k_i^{n-1} N^n \qquad 2.26$$

While the methods do offer considerable promise for the study of mycelial broth rheology, it will definitely require further testing. In particular, comparisons should be made between viscosities of homogeneous non-Newtonian fluids determined by the new method and by conventional methods. Also, effects of gas bubbles and of various geometric parameters (e.g., impeller size and configuration, presence of baffles) should be investigated carefully. It is also suggested to possibly include the yield stress by modifying Equation 2.24-2.26 for a Hershel-Bulkley model.

2.5.1.4 Viscosity Measurement in-situ and on-line

In view of the importance of rheological properties as process variables, the use of an on-line or an in-situ rheometer would have significant advantages for continuous monitoring and control purposes of the rheology of fermentation process. Also, the measurement in-situ of the rheology avoids the extraction of samples to an ex-situ location, which can result in alterations to the sample due to the sensitivity of the fermentation broth. The effect of time on samples and ex-situ conditions can have detrimental effects, altering sample properties relative to those in the bioreactor (Metz et al., 1979). In the literature, there are few publications addressing the development of in-situ or on-line measurement of viscosity. This is probably due to the difficulty in the measurement of suspensions like fermentation broth, discussed above. Also, the importance of maintaining sterile conditions also restricts the use of many rheometers typically used in industry, a problem which is also encountered in the food industry, as discussed by Steffe (1996). The following two cases are among the few which attempt to address these problems.

Charles (1978) discusses the work done by Wang and Fewkes (1977). The latter have attempted to make an in-situ instrument, by using a technique similar to Bongenaar's method to measure the rheological properties of a *Streptomyces niveus* culture by using the reactor and the drive with a torque sensor as a rheometer. Charles (1978) describes that this can be accomplished by reducing the agitator speed to ensure "laminar" flow and then measuring power input as a function of agitator speed. He then suggest that the necessity for maintaining laminar flow when applying Bongenaar's method is clear since the calculations are based on the assumption of laminar flow. However, he then stated that the necessity for laminar flow in the present Wang and Fewkes case was not clear. While they

gave no details of the calculation, he suggested that it is probably safe to assume that their measurements were used in conjunction with the N_P vs. N_{Re} and the correlation of Metzner and Otto (1957) (Equation 2.15) for the shear rate at the impeller tip in view of obtaining the relationship between viscosity and shear rate. A similar approach was discussed by Skelland (1967). Charles (1978) describes the following procedure, as an example to Wang and Fewkes technique:

1. Calculate N_P (*see* Equation 2.18).
2. From the Metzner and Otto (1957) correlation obtain the corresponding N_{Re}
3. Calculate the apparent viscosity:

$$\mu = \frac{d_i^{\,2} N \rho}{N_{\mathrm{Re}}} \qquad 2.27$$

4. Calculate the shear rate at the impeller tip: $\dot{\gamma} = k N$

Charles (1978), noticed then, that both n and K appear to be functions of rotational speed for shear rate in the range of 25-75 s^{-1}. For such a narrow range, he suggested that one would expect the power law model to correlate the data reasonably well with only one value each for n and K. Elsewhere, he discussed that the fact that n and K do vary is possibly due to some deficiency in the method as used. He added that the conditions at which the measurements are done could cause significant deviations in the results due to the sensitivity related to viscosity calculations. As an example, he explained that the failure to shut off air flow during measurements would distort markedly the results.

Indeed, further research is required for this method to be applicable. As for in-situ instruments, it should be noted that at present there appears to be only one commercial viscometer suitable for use in agitated vessels. This is the Dynatrol® Viscosity

Measurement Probes (Automation Products, Inc.) which has been used for various process applications. However, no reports have been published of its successful use in fermenters.

As an alternative to in-situ, on-line measurements seem more promising. Although there are very few publications, the work done by Kemblowski et al. (1985) showed successful results. Figure 2.5 is a simplified version of the on-line rheometers that were designed. The advantage of this system is the capacity to use measuring geometries such as the vane impeller to avoid problems with settling and wall slip, discussed above. In addition, sterile conditions are maintained by designing a closed circuit. Kemblowski et al. (1985) perform measurements in fermentations with *Aureobasidium pullulans*. Olsvik and Kristiansen (1992), laboratory colleagues of the formers, also worked with the on-line rheometers constructed. They used successfully the instrument in a continuous fermentation of *Aspergillus niger*. The viscosity was a monitored process parameter and used as a reference to adjust the dilution rate to maintain low viscosity conditions, thus keeping higher mass transfer conditions.

Badino Jr. et al. (1997) constructed a similar instrument and compared two geometries: a ribbon impeller and a six-blade impeller. The system with one of the helical ribbon impellers was selected for on-line continuous rheological measurements due to its small dimensions and its wide measurement range. In addition, the performance of the proposed device, in terms of rheological measurements in *Aspergillus awamori* broths, was compared to that of a commercial bench rheometer. The comparison of on-line and off-line rheological measurements showed a good agreement between both measurement techniques. Furthermore, their results suggested that the on-line rheometer features higher sensitivity and easier operation than bench top rheometers.

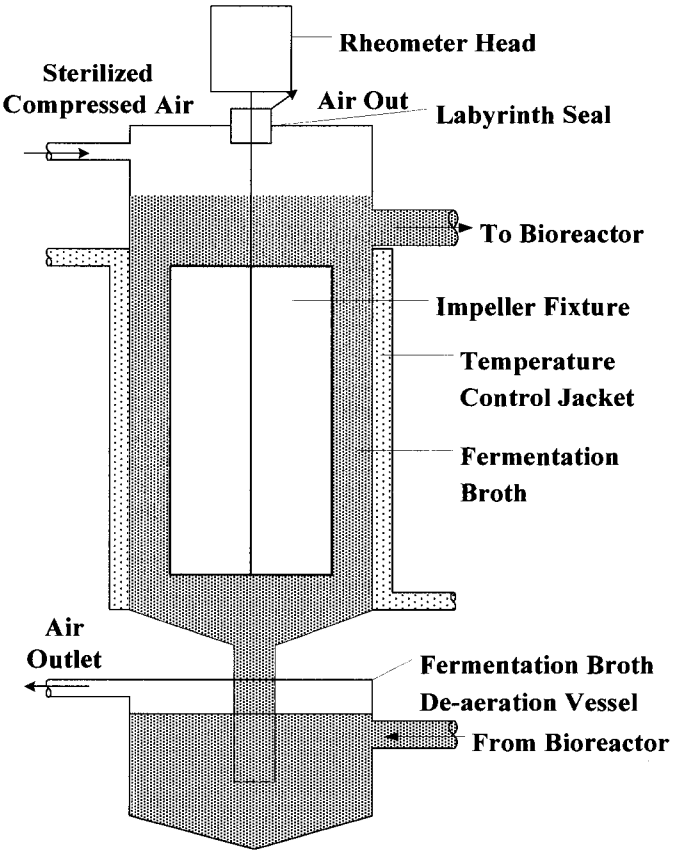

Figure 2.5 Online Rheometer Diagram

2.6 Factors to consider when choosing a rheometer and fixtures

The factors and conditions required for choosing both a rheometer and a measuring geometric fixture for rheological analysis are widely discussed in rheological textbooks. There are many textbooks that specialize in the measurements of polymers, foods, paints, and suspensions. For the case of fermentation broth rheology, very little information is available. Nevertheless, some principles found in those textbooks are general to the discipline of rheology and are applicable to fermentation broth, which is a suspension of microorganism cells. Elsewhere, publications by Bongenaar et al. (1973), Roels et al. (1974), Metz et al. (1979) and Allen and Robinson (1987 and 1990) are good sources of information on the measurement of fermentation broth rheology. They describe the

problems encountered with conventional instruments like the concentric cylinders and develop their own solutions to circumvent those problems. The common problems and their suggested solutions are:

1. The size of cells (or cell aggregates) has the same size as the annulus, resulting in the destruction of cells, and the obstruction of the free rotation of the cylinder.
2. Formation of less dense layers at the wall surface or wall slip
3. Biomass settling, resulting in a suspension that is inhomogeneous and phase separation

For the first problem, it is commonly suggested in literature to have an annulus 10 times the size of the particles (Brummer, 2006; Schatzmann et al., 2003). From the above, the mixer geometries are capable of overcoming the other two problems. So, for our purpose, priority was emphasized on the choice of a rheometer capable of using mixer geometries with annulus 10 times greater than *T. reesei* cell aggregates (clumps and dispersed morphologies are present - see Chapter 3 for more details).

During the selection of geometries, it is commonly known that the following list of boundary conditions or measurement constraints must be met to obtain adequate data in volume loaded geometry (Schramm, 1998):

- Laminar Flow
- Steady State Flow
- No slippage
- Samples must be homogeneous
- No chemical or physical changes in the sample during testing
- No elasticity

- End effects should be negligible
- Radial and axial flow velocity components should be zero (for cup geometries)

Figure 2.6 shows representative figures of five geometries tested in our laboratory that were attached to TA Instruments AR-G2 rheometer. Figure 2.7 shows the analysis of a fermentation broth sample using the geometries. In addition, three cones with different characteristics were tested: steel (to compare with lighter material), two acrylic with different cone angles (the angle results in different truncation; the lighter acrylic results in less inertia). It is clear from Figure 2.7, all the cone and plate geometries and the double concentric cylinders show values higher than the other geometries which results are in close agreement. The higher values are probably due to the particle size which obstructs the free movement of the geometry. Through visual observation, it is clear that biomass aggregates were forming, separating from the broth and rolling into filaments. A similar phenomenon was observed for analysis of Solka Floc by the acrylic cone and plate with an angle of 2°. Figures 2.8 and 2.9 are pictures of the Solka Floc, before and after a rheological measurement. From these results, two geometries were therefore selected for the examination of the fermentation samples for experimentation discussed in Chapter 3: the concentric cylinders and the vane. The concentric cylinders were used for the first two samples from fermentation runs. At the beginning, samples had low biomass concentration (below 5 g/L) and the broth rheology properties resembled those of water. Figure 2.10 shows the first sample of fermentation analyzed using the two geometries: the vane and the concentric cylinders. Clearly, the vane does not adequately measure properties of the sample, since the calculation of N_{Re} showed that for a large portion of the shear rate range, the flow was not laminar.

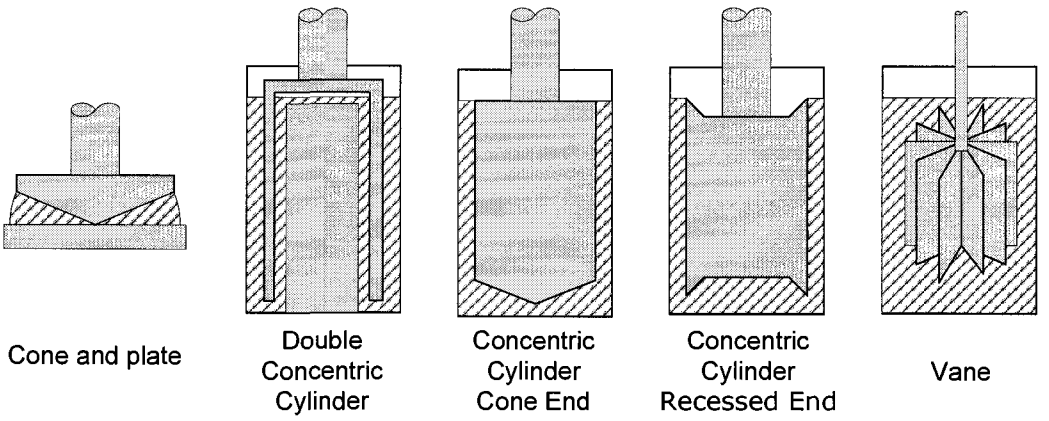

Figure 2.6 Different geometries tested in our laboratory.

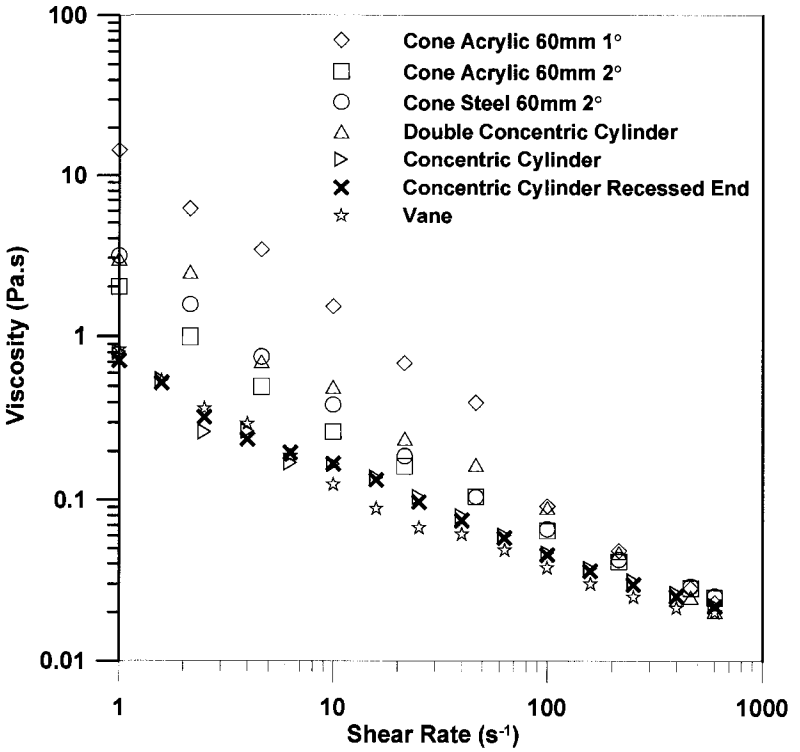

Figure 2. 7 Comparison of the rheological analysis of a fermentation broth sample using 5 different fixtures. The sample was taken from a run done at 0.5 Hz in a reciprocating plate bioreactor. The rheometer used was TA Instruments AR-G2.

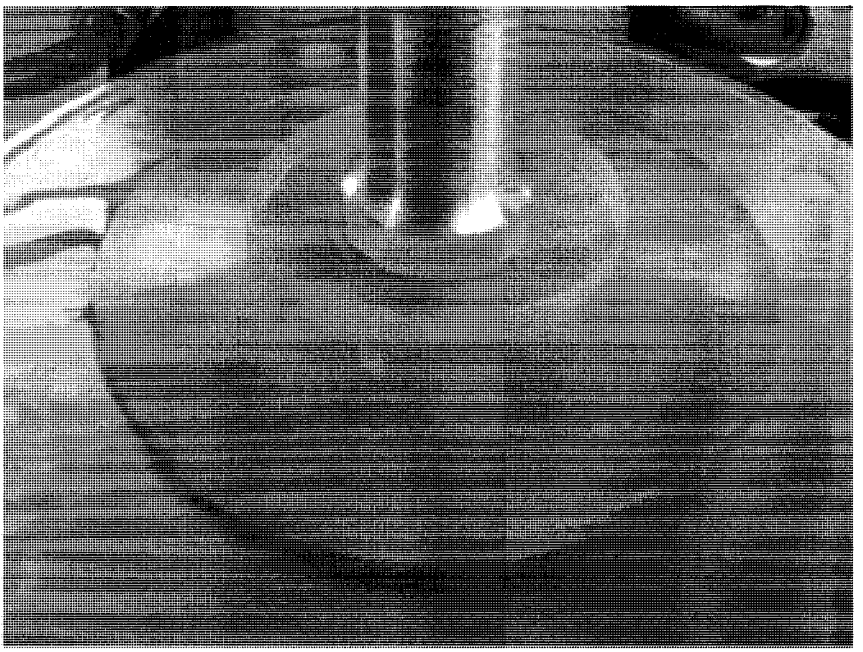

Figure 2. 8 Analysis of Solka Floc using an acrylic cone and plate fixture. The picture shows the sample at the beginning of the run, before the cone rotated. The sample looks homogeneous.

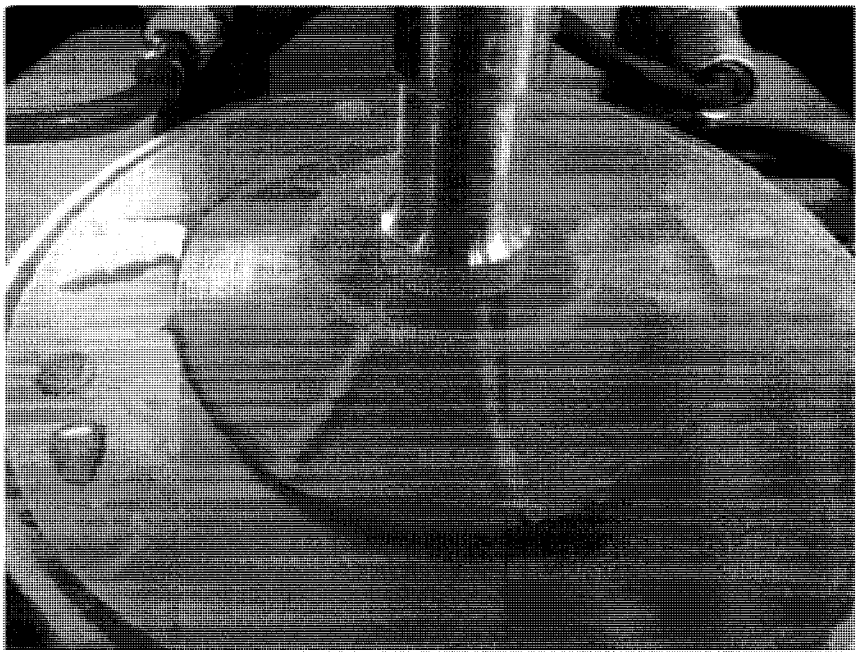

Figure 2. 9 Analysis of Solka Floc using an acrylic cone and plate fixture. The picture shows the sample at the after the end of run. The Solka Flow is clearly aggregated into filaments.

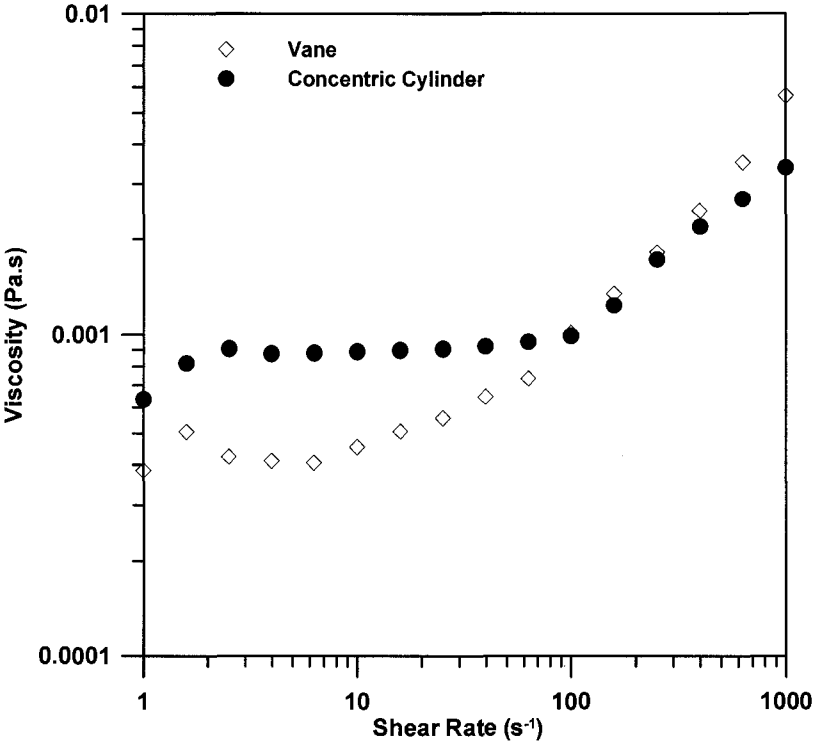

Figure 2.10 Comparison of rheological analysis of the first sample in a fermentation run using a vane and concentric cylinders.

Another important consideration to make while choosing a rheometer is to know the shear rate range required to perform the analysis. The shear rate range is determined by factors such as the shear conditions in the reactor and the stirring mechanism. Estimates of the shear rate are based on the Metzner and Otto (1957) relation discussed earlier. For more precise estimates, computational fluid dynamics is done on a specific system. In our case, the shear rate range is based on literature estimates for our reactors. The commonly used shear rates range from 1 to 1000 s^{-1}.

Rheometer drives and the torque sensor determine the capability to reproduce the shear rate range required. On the one hand, the lower the viscosity of the suspension, the more difficult is to measure the rheology at low shear rates. Therefore, the more sensitive the torque sensing mechanism, the lower the shear rate can be achieved and the less viscous suspensions can be analyzed. On the other hand, the higher the shear rate needed the more

power a drive must output. In addition, these factors as well as the level of sophistication impact directly on the cost of the rheometers. In this manner, our choice of a rheometer depends on the possibility of running tests for a shear rate range of 1 to 1000 s^{-1}, the use of the geometries discussed above and the cost. Finally, a last point to consider in the choice of a rheometer is the possibility of temperature control, due to the high dependency of the viscosity on temperature. In the following section, details are shown of the different rheometers considered.

2.7 Finding a Rheometer

Today, many different rotational rheometers are available on the market. Table 2.3 shows some of the rheometers considered for the purpose of measuring fermentation rheology and that fulfill the conditions discussed above. The make and the model name are shown as well with some important characteristics: the torque, the rotational speed, the shear stress, the shear rate, the viscosity and the estimated cost. The ranges of shear stress, shear rate and viscosity are dependent on the geometry used. The ranges shown are obtained by combining all geometries ranges available for the rheometers. The information given in the table is therefore for the widest possible shear stress, shear rate or viscosity ranges possible with corresponding rheometers. TA Instruments AR-G2 is capable of giving the required shear rate range for our analysis. However, this information was not in the documentation and was found through experimentation. Some instruments give the option to use custom-made geometries, which would give different ranges.

The rheometers shown in the Table 2.3 vary from the lowest end to the most sophisticated on the market. Haake, Bohlin and Brookfield Engineering rheometers use

mechanical bearing and a calibrated coil spring as a torque sensor, while the TA Instruments has magnetic bearing and a deflection mechanism for torque sensing. Haake Viscotester 7-L and Brookfield DVIII-LV function fundamentally the same way. There are several variations of these rheometers dependent on the viscosity range required, with the designations L and LV indicating the low viscosity versions. Unlike all other rheometers in the table, the Haake Viscotester 7-L does not have vane geometry available. In addition, both these rheometers and the Haake VT550 do not cover the entire range of shear rates (1-1000 s^{-1}) required. Despite the fact that Bohlin V88 covers the shear rate range, the minimal viscosity measurable is 5 mPa.s which can be a limitation when measuring viscosity associated with the first samples of a fermentation run. As discussed before, these samples have viscosities close to water viscosity (1 mPa.s). The remaining two rheometers are AntonPaar RheolabQC and TA Instruments AR-G2. The last one is without a doubt a more sophisticated rheometer than the former one. TA Instruments has the option to use many different geometries such as cone and plate, parallel plates, vanes, concentric cylinders, as well as others. Also, the temperature control system has the ability to bring samples to process temperature in a just a few minutes, thanks to their Peltier heating/cooling system. One major difference is the option to study structural properties of materials thanks to the oscillatory analysis mode and the ability to use streaming video to monitor analysis.

All mentioned rheometers would be useful to measure our sample rheology. However, the last two rheometers are able to run tests with shear rates close to the target range if not the entire range (this is dependent on geometry and not on these two rheometers because their drives and torque sensors are capable). The choice between one rheometer and the other would be the availability of the funding. In our case, funding was limited, thus the only option would be the RheolabQC. The possibility of using a high-end

rheometers has its advantages, with the possibility of using the equipment for rheology analysis other than the fermentation broth. Therefore, collaboration was considered as an option. At the start, collaboration was sought with other laboratories. Few were found with rheometers capable of measuring viscosities in our range. Professor Denis Rodrigue from Laval University (Quebec) accepted to collaborate and had a Rheometrics RDAIII. The geometry used was parallel plates with 6-cm diameter. Two problems were encountered during the test. For samples that had viscosities close to water viscosity, the instrument was unable to measure the viscosity. In this case, the torque was the limiting factor. The instrument was not sensitive enough to measure low viscosities. Second, the parallel plate geometry changed the morphology of the sample. The suspension was transformed into separate solid and liquid phases. The solid phase formed aggregates. At high shear rates, these aggregates were expelled out of the parallel plate gap, altering the solid concentration. From this test, it was concluded that both the geometry and the instrument were not useful for our rheology measurements. The other option was to contact directly both TA Instruments and AntonPaar companies for establishing collaborations. AntonPaar gave us the possibility to test their equipment for a month, while TA Instruments let us use the instrument for all the duration of our experimentation. The following section shows some results from the analysis using both instruments.

2.8 Comparing TA Instruments and AntonPaar

Both instruments were provided with a large set of geometries. All the geometries were tested for measurement of fermentation broth, as well as, water solutions, carboxymethyl cellulose (CMC), and suspensions (paper pulp and Solka Floc). These solutions and suspensions have properties close to that of the fermentation broth. Figure

2.7, discussed before, shows the result of fermentation broth analyses with the different geometries provided by TA Instruments. Since we had the instruments at different times, a different sample of fermentation broth was analyzed using AntonPaar RheolabQC. Figure 2.11 shows the results of a rheology analysis using all the provided fixtures from AntonPaar. For the same sample biomass concentration, the double gap concentric cylinders and both concentric cylinders were used to measure the viscosity. However, the fixtures have different shear rate ranges. In the case of the provided vane, the measurements are not correct. This was expected since the operating range for this fixture found in the documentation was no suitable for our samples.

Figures 2.12 and 2.13 show that both instruments are capable of measuring the rheology of water and CMC with the provided fixtures. However, the shear rate ranges at which the analysis was done differs between both instruments for all the fluids analyzed. The torque sensitivity of the instruments diverges significantly. TA Instruments AR-G2 minimum torque is 83333 times lower than the AntonPaar RheolabQC, therefore making TA Instruments operate at wider shear rate ranges.

Figures 2.14 and 2.15 are measurements of paper pulp suspensions at 1 and 10 g/L, respectively, using both instruments. However, the results should be examined with caution, since the gap size condition was not satisfied. This was visible in Figure 2.14, the measured rheology differs greatly between both instruments. The difference is not due to the instrument, but to the fixture. A double gap concentric cylinder fixture was used in the AntonPaar instrument, where the gap size was close to the size of the particles. This obstructed the free movement of the cylinder, thus showing a more viscous curve, than the vane geometry in TA Instruments. Unfortunately, none of the fixtures provided for the

Table 2.3 List of rheometers considered for rheological analysis of our fermentation broth samples.

Make	Model	Torque N.cm	Speed Range RPM	Shear Rate s^{-1}	Shear Stress Pa	Viscosity mPa.s	Cost[a] CAD
Haake	Viscotester 7 - L	N/A (1 - 100%)	0.1 - 200	-	-	$3 - 6\times10^{6}$	4883
Haake	VT550	0.01 - 3 0.01 - 2	0.5 to 400 rpm 0.5 to 800 rpm	-	-	$1 - 10^{6}$	14500[b]
Bohlin	V88	0 - 1	0 - 1000	$0 - 2\times10^{4}$	$0 - 10^{4}$	$5 - 10^{7}$	23481
Anton Paar	RheolabQC	0.025-7.5	0.01 - 1500	0.01 - 4000	$0.5 - 3\times10^{4}$	$1 - 10^{9}$	32215
Brookfield	DVIII - LV	$6.74\times10^{-5} - 0.00674$	0.01 - 250	0 - 330	-	$1 - 6\times10^{6}$	12504
TA Instruments	AR - G2	$3\times10^{-7} - 20$	$1.334\times10^{-8} - 2865$	-	-	-	73327

[a]The cost is the total value of the rheometer and the accessories necessary to analyze rheology of fermentation broth with the exception of Haake Viscotester 7 – L which does not have temperature control nor vane geometries. Costs are from quotes obtained directly from the companies.
[b]The cost is in US Dollars. There is no quote and the cost was given through e-mail communication.

RheolabQC were suitable for this measurement. In this case, the vane geometry (TA Instruments) results seem more credible. In Figure 2.15, the results seem to concord. A different geometry was used with AntonPaar instrument. The viscosity of the paper pulp was higher, so the CC27 concentric cylinder geometry was used (this geometry did not have the gap size problem). Once more, the shear rate ranges at which the instruments operate differ due the reasons mentioned above. Also, a higher paper pulp concentration of 20 g/L was attempted. However, both fixtures provided with the instruments were obstructed and gave highly unstable results.

In addition, measurements were attempted on Solka Floc fiber suspensions. This suspension had the tendency to precipitate quickly. Then, AntonPaar fixtures were unable to keep the fibers suspended, thus measurements obtained were unstable.

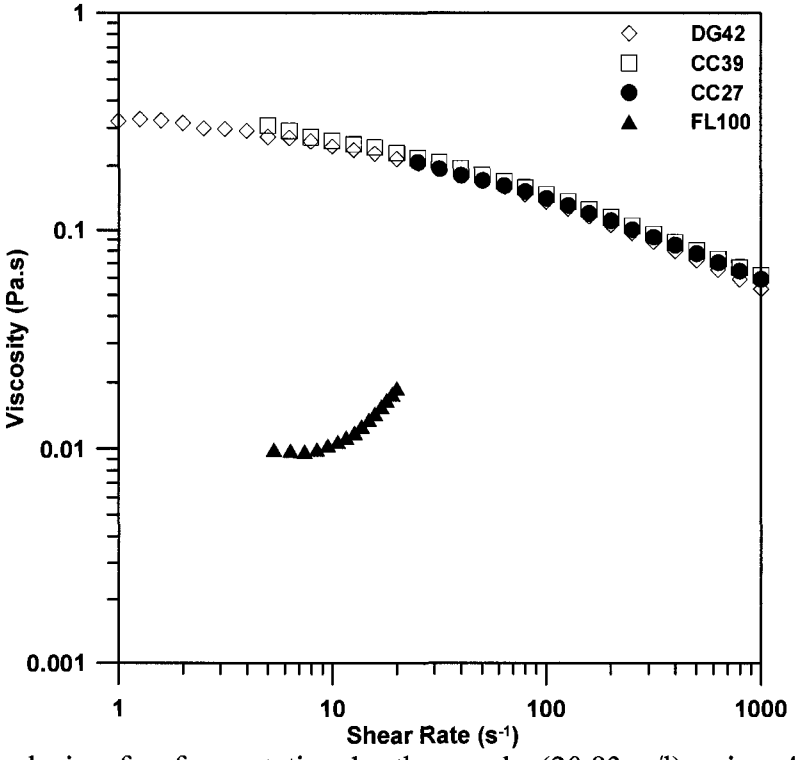

Figure 2.11 Analysis of a fermentation broth sample (20.93 g/l) using 4 fixtures with RheolabQC rheometer. The fixtures are: DG42 (double gap concentric cylinder); CC39 (concentric cylinder); CC27 (concentric cylinder); FL100 (6 bladed vane).

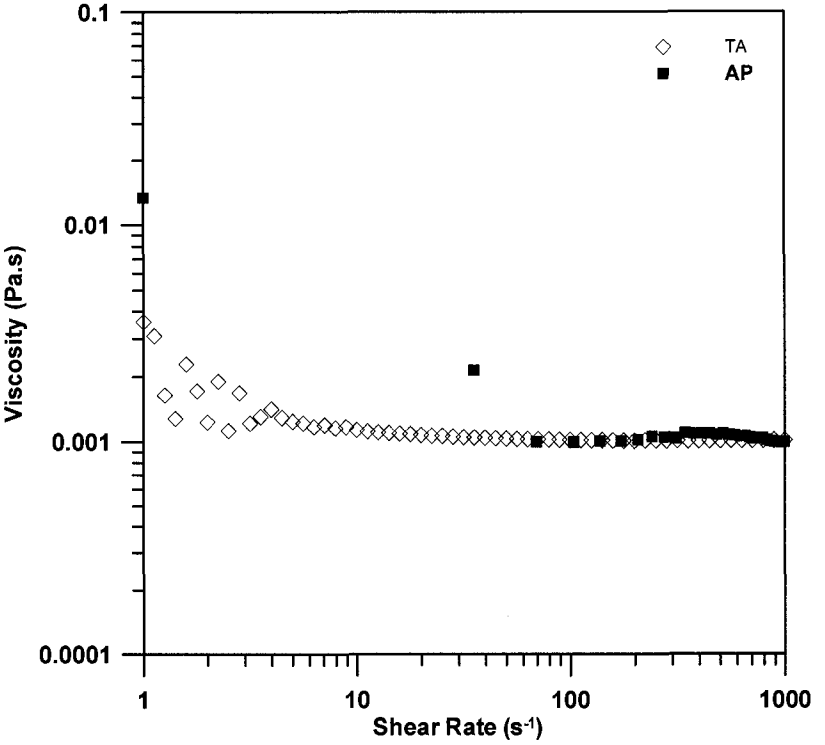

Figure 2.12 Water viscosity measured by TA Instruments AR-G2 (double gap concentric cylinder fixture) compared to AntonPaar RheolabQC (fixture DG42).

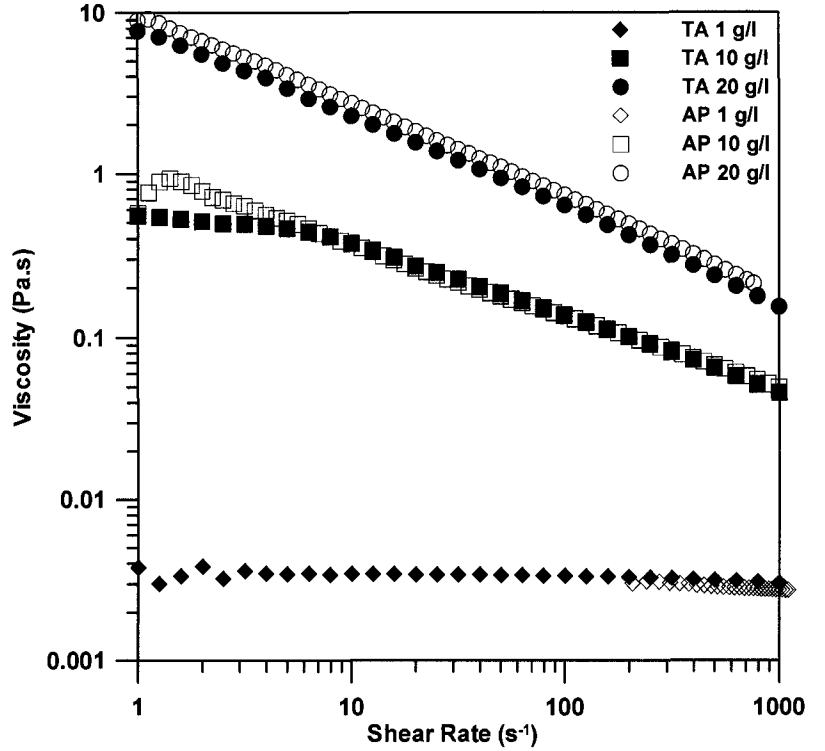

Figure 2. 13 Three CMC concentrations were analyzed for their rheology using TA Instruments AR-G2 (double gap concentric cylinder fixture) compared to AntonPaar RheolabQC (fixture DG42).

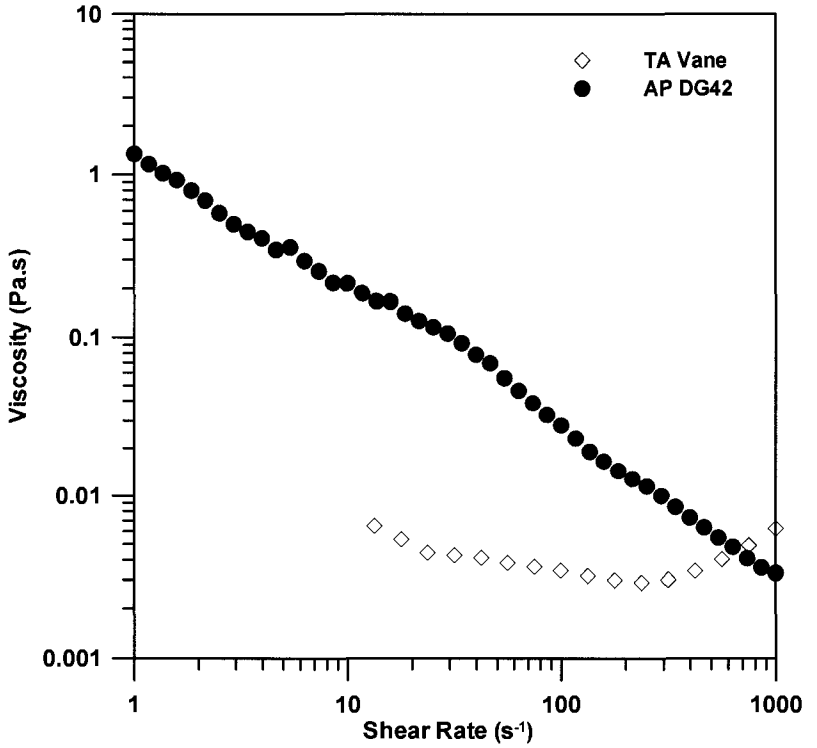

Figure 2. 14 Rheology analysis of paper pulp at a concentration of 1 g/L was done using two rheometers: TA: TA Instruments AR-G2 (vane fixture) and AP: AntonPaar RheolabQC (fixture double gap concentric cylinder DG42).

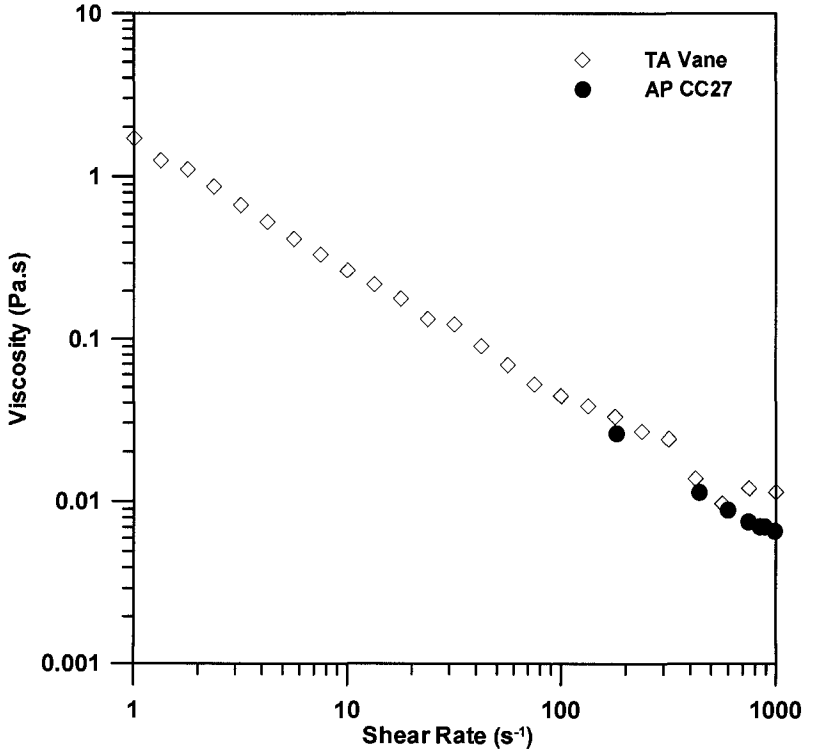

Figure 2. 15 Rheology analysis of paper pulp at a concentration of 10 g/L was done using two rheometers: TA: TA Instruments AR-G2 (vane fixture) and AP: AntonPaar RheolabQC (fixture concentric cylinder CC27).

2.9 Rheology Measurement System and Procedure

Background:

The TA Instruments AR-G2 rheometer is a stress-controlled/strain-controlled rotational instrument. It is a versatile rheometer, suited to determine the rheological properties of a wide range of types in fluids and soft matters. A few characteristics are real-time raw data capture: easy to use, many geometries to choose from and reliable measurements.

Apparatus:

Figure 2.16 shows a picture of the AR-G2 rheometer. The drive head and the torque sensor height can be adjusted thanks to a motorized system. To the rod, geometries are connected. Figure 2.17 shows the Peltier Smart Swap Jacket (for temperature control), the sample cup (which goes in the jacket) and the two geometries used to analyze rheology during fermentation runs. General details are presented here; for more information, extensive descriptions can be found in instrument manuals as well as in brochures.

Figure 2.18 shows the components of typical AR series rheometers:

1. Drag Cup Motor
2. Thrust Bearing
3. Radial Air Bearings
4. Optical Encoder
5. Normal Force Transducer
6. Rigid One-Piece Aluminum Casting and Linear Ball Slide

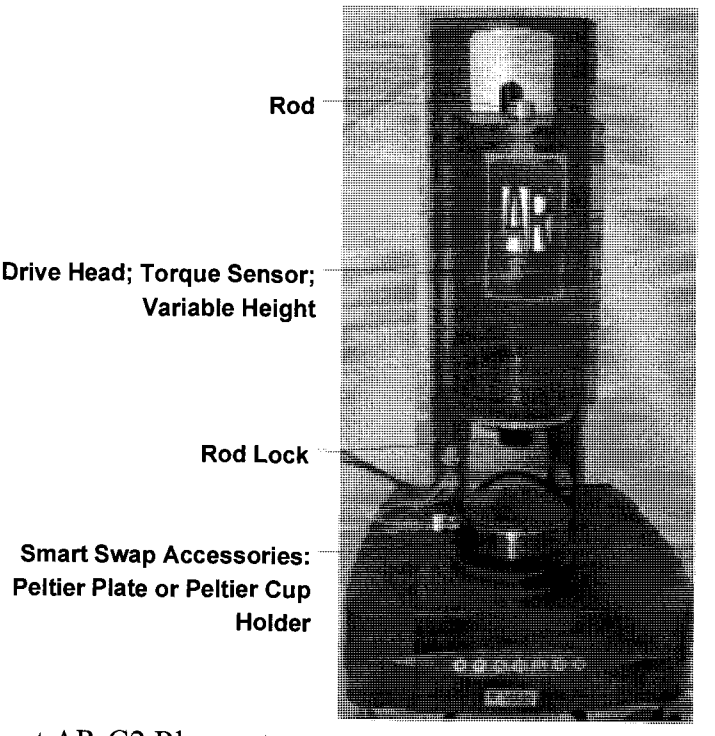

Figure 2.16 TA Instrument AR-G2 Rheometer.

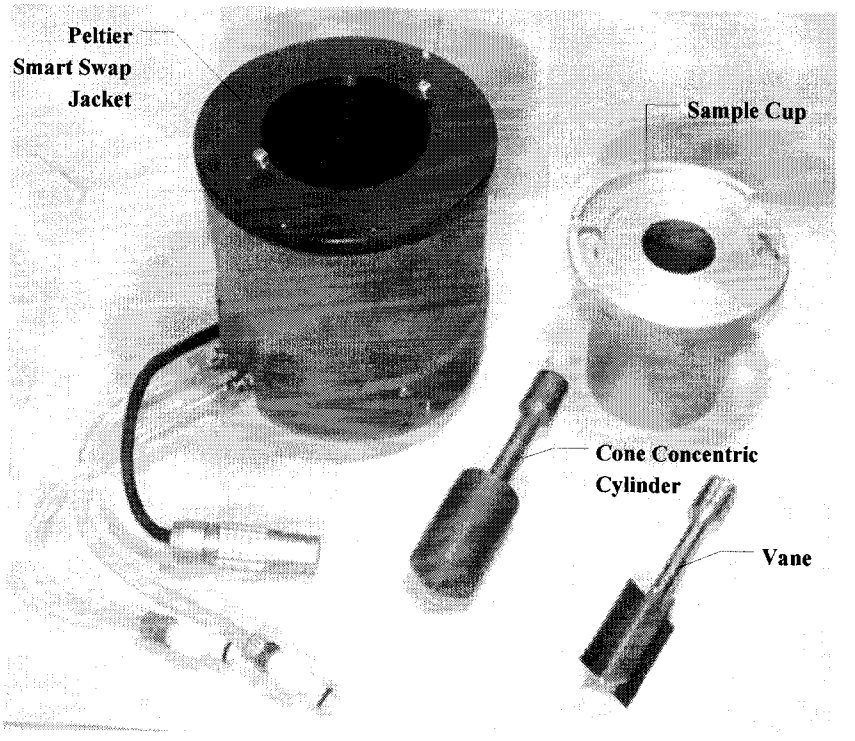

Figure 2.17 TA Instrument accessories used for fermentation broth analysis: Peltier temperature control system, the sample cup, the cone concentric cylinder, the 4-blade vane.

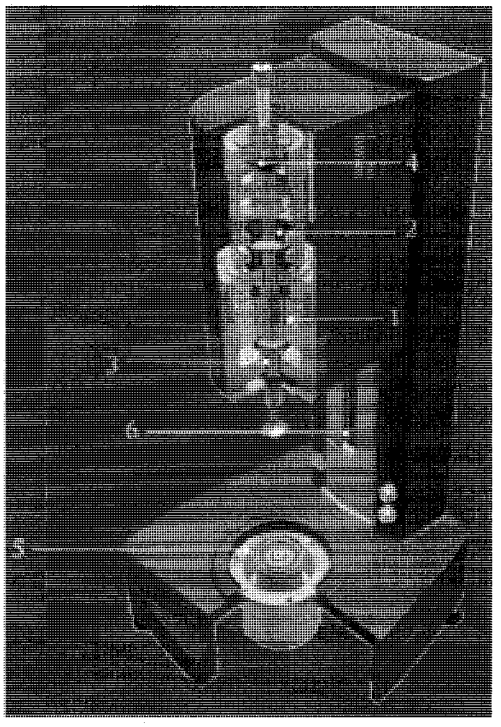

Figure 2.18 TA Instruments AR-G2 mechanical components

Figure 2.19 is a close up of the technology behind the head of an AR-G2 rheometer:

1. Magnetic Thrust Bearing
2. Patented Drag Cup Motor
3. Radial Air Bearing

Equipment Needed:

AR-G2 Rheometer (Instrument specification can be found in Appendix A)

Geometries: Vane; Concentric Cylinder Cone End; Cup

Sample container

Sample

Computer for control

Setup:

TA Instrument provided a general instructions guide for operation of AR rheometers. The guide can be found in instrument documentations under "Introductory guide to using an AR series rheometer using Rheology Advantage software". The following summary was instructed by TA Instruments technicians:

Turning on the AR-G2 must be done in this order:

1. Turn on the air supply and adjust to 30 psi using regulator.
2. Turn on the water pump for the Peltier Temperature Control System.
3. Unlock the draw rod.
4. Turn on the computer controller to turn on the rheometer electronics.
5. Check the apparatus for proper working order and no visible problems. No error codes displayed.
6. Ensure all parts are clean and dry.

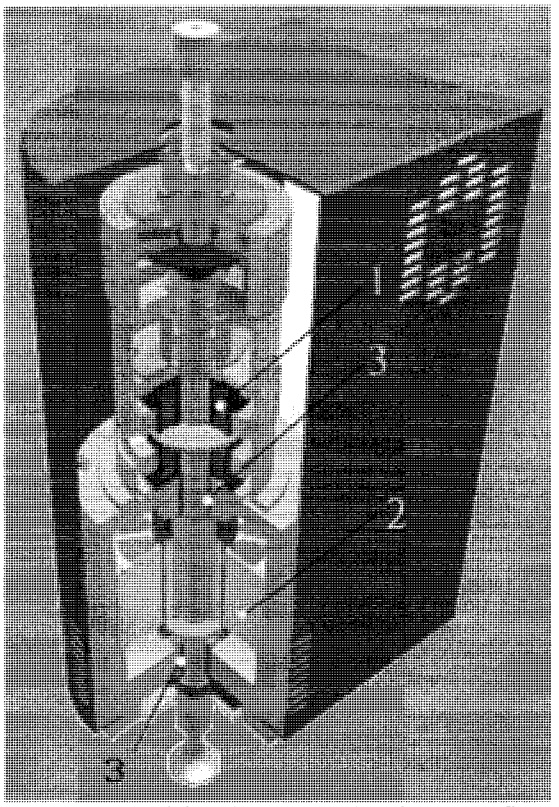

Figure 2.19 TA Instruments AR-G2 drive head mechanical configuration

Operation:

7. Calibrate for instrument inertia, geometry inertia and bearing friction.
8. Install geometries.
9. Pre-set operating temperature.
10. Map instrument.
11. Zero geometry gap.
12. Set analysis procedure.
13. Load sample according to suggested volume.
14. Close geometry to preset position.
15. Run Test.

Resetting the Device and Cleanup:

16. Raise geometry.
17. Remove geometry and sample cup.
18. Remove the sample and dispose of properly.
19. Wash gently and thoroughly geometry and sample cup with hand soap (to prevent damage to materials).
20. Dry and wipe geometry and sample cup.
21. Ensure all portions of the instrument are clean and clear of sample.
22. Follow steps 7 to 15 for further sample testing.

Turning off the AR-G2 must be done in this order:

23. Turn off the computer controller to turn off the rheometer electronics.
24. Lock the draw rod finger tight.
25. Turn off the water pump for the Peltier Temperature Control System.
26. Turn off air pressure.

Precautions:

- It is critical to have the appropriate air pressure before unlocking the draw rod. Failure to have correct conditions could cause severe damage to bearing system.
- Correct gap zeroing is important. Incorrect gap closure can result in the geometry hitting the cup base and permanently damaging normal force sensor.

2.10 Nomenclature

C_f	Torque correction factor (-)
C_i	Instrument constant (-)
d_i	Impeller diameter (m)
k	Constant (-)
K_C	Casson consistency index (Pa.s$^{0.5}$)
K_{HB}	HB consistency index (Pa.s^n)
k_i	Constant (-)
K_{PL}	Power-Law consistency index (Pa.s^n)
L	Cylinder height (m)
M	Torque (N.m)
n	Flow index (-)
N	Rotational speed (min^{-1})
N_P	Power number (-)
N_{Re}	Reynolds number (-)
P	Power input (kg.m/s)
r	Radius between inner and outer cylinders (m)
R_i	Radius of inner cylinder (m)
R_o	Radius of outer cylinder (m)

Greek letters

α	Cone angle (rad)
$\dot{\gamma}$	Shear rate (s^{-1})
$\dot{\gamma}_i$	Shear rate at inner cylinder (s^{-1})
$\dot{\gamma}_r$	Shear rate at radius r (s^{-1})
μ	Viscosity (Pa.s)
ρ	Fluid Density (kg/m^3)
τ	Shear stress (Pa)
τ_i	Shear stress at inner cylinder (s^{-1})
τ_o	Shear stress at outer cylinder (s^{-1})

τ_r	Shear stress at radius r (s^{-1})
τ_{y_B}	Bingham yield stress (Pa)
τ_{y_C}	Casson yield stress ($Pa^{0.5}$)
$\tau_{y_{HB}}$	Herschel-Bulkley yield stress (Pa)
Ω	Angular velocity (rad/s)

Subscripts

B	Bingham model
C	Casson model
HB	Herschel-Bulkley model
i	Inner cylinder
P	Power
PL	Power Law model
o	Outer cylinder
r	Radius between inner and outer cylinder
Re	Reynolds
y	Yield Stress

2.11 References

Akroyd T.J. and Nguyen Q.D. 2003. Continuous on-line rheological measurements for rapid settling slurries. Minerals Engineering, 16, pp.731-738.

Allen D.G. and Robinson C.W. 1987. The Influence of slip on rheological measurements on a mycelial broth of *Aspergillus niger*. Annals of the New York Academy of Sciences, 506, pp.589-599.

Allen D.G. and Robinson C.W. 1990. Measurement of rheological properties of filamentous fermentation broths. Chemical Engineering Science, 45, pp.37-48.

Allen D.G. and Robinson C.W. 1991. The prediction of transport parameters in filamentous fermentation broths based on results obtained in pseudoplastic polymer solutions. Canadian Journal of Chemical Engineering, 69, pp.498-505.

Badino Jr. A.C., Facciotti M.C.R. and Schmidell W. 1997. Construction and operation of an impeller rheometers for on-line rheological characterization of non-Newtonian fermentation broths. Brazilian Journal of Chemical Engineering, 14, pp.359-365.

Badino Jr. A.C., Facciotti M.C.R. and Schmidell W. 1999. Estimation of the rheology of glucoamylase fermentation broth from the biomass concentration and shear conditions. Biotechnology Techniques, 13, pp.723-726.

Barnes H.A. 1999. The yield stress - a review or 'παντα ρει' - everything flows? Journal of Non-Newtonian Fluid Mechanics, 81, pp.133-178.

Barnes H.A. and Bell D. 2003. Controlled-stress rotational rheometry: An historical review. Korea-Australia Rheology Journal, 15, pp.187-196.

Benchapattarapong N., Anderson W.A., Bai F. and Moo-Young M. 2005. Rheology and hydrodynamic properties of *Tolypocladium inflatum* fermentation broth and its simulation. Bioprocess and Biosystems Engineering, 27, pp.239-247.

Bhargava S., Nandakumar M.P., Roy A., Wenger K.S. and Marten M.R. 2003. Pulsed feeding during fed-batch fungal fermentation leads to reduced viscosity without detrimentally affecting protein expression. Biotechnology and Bioengineering, 81, pp.341-347.

Blanch H.W. and Bhavaraju S.M. 1976. Non-Newtonian fermentation broths: rheology and mass transfer. Biotechnology and Bioengineering, 18, pp.745-790.

Bongenaar J.J., Kossen N.W.F., Metz B. and Meijboom F.W. 1973. Method for characterizing rheological properties of viscous fermentation broths. Biotechnology and Bioengineering, 15, pp.201-206.

Brar S.K., Verma M., Tyagi R.D., Valero J.R. and Surampalli R.Y. 2007. *Bacillus thuringiensis* fermentation of hydrolyzed sludge - Rheology and formulation studies. Chemosphere, 67, pp.674-683.

Brummer R. 2006. Rheology essentials of cosmetic and food emulsions. Verlag Berlin Heidelberg: Springer. 180 p.

Bueno S.M. and Garcia-Cruz C.H. 2001. The influence of fermentation time and the presence of salts in the rheology of the fermentation broth of a polysaccharide-producing bacteria free of soil. Journal of Food Engineering, 50, pp.41-46.

Casas J.A., Santos V.E. and Ochoa F. 2000. Xanthan gum production under several operational conditions: Molecular structure and rheological properties. Enzyme and Microbial Technology, 26, pp.282-291.

Charles M. 1978. Technical aspects of the rheological properties of microbial cultures. Advances in Biochemical Engineering/Biotechnology, 8, pp.1-62.

Chavarria-Hernandez N., Rodriguez-Hernandez A.I., Perez-Guevara F. and de la Torre M. 2003. Evolution of culture broth rheological properties during propagation of the entomopathogenic nematode *Steinernema carpocapsae*, in submerged monoxenic culture. Biotechnology Progress, 19, pp.405-409.

Chavez-Parga M.C., Gonzalez-Ortega O., Negrete-Rodriguez M.L.X., Medina-Torres L. and Silva E.M.E. 2007. Hydrodynamics, mass transfer and rheological studies of gibberellic acid production in an airlift bioreactor. World Journal of Microbiology & Biotechnology, 23, pp.615-623.

Chen F., Chen H. and Gong X.D. 1997. Mixotrophic and heterotrophic growth of *Haematococcus lacustris* and rheological behaviour of the cell suspensions. Bioresource Technology, 62, pp.19-24.

Cho Y.J., Hwang H.J., Kim S.W., Song C.H. and Yun J.W. 2002. Effect of carbon source and aeration rate on broth rheology and fungal morphology during red pigment production by *Paecilomyces sinclairii* in a batch bioreactor. Journal of Biotechnology, 95, pp.13-23.

Deindoerfer F.H. and West J.M. 1960. Rheological examination of some fermentation broths. Journal of Biochemical and Microbiological Technology and Engineering, 2, pp.165-175.

Fatile I.A. 1985. Rheological characteristics of suspensions of *Aspergillus niger* - Correlation of rheological parameters with microbial concentration and shape of the mycelial aggregate. Applied Microbiology and Biotechnology, 21, pp.60-64.

Gehrig I., Bart H.J., Anke T. and Germerdonk R. 1998. Influence of morphology and rheology on the production characteristics of the basidiomycete *Cyathus striatus*. Biotechnology and Bioengineering, 59, pp.525-533.

Ghildyal N.P., Thakur M.S., Srikanta S., Jaleel S.A., Prapulla S.G., Prasad M.S., Devi P.N. and Lonsane B.K. 1987. Rheological studies on *Streptomyces fradiae* ScF-5 in submerged fermentation. Journal of Chemical Technology and Biotechnology, 38, pp.221-234.

Gibbs P.A., Seviour R.J. and Schmid F. 2000. Growth of filamentous fungi in submerged culture: Problems and possible solutions. Critical Reviews in Biotechnology, 20, pp.17-48.

Goudar C.T., Strevett K.A. and Shah S.N. 1999. Influence of microbial concentration on the rheology of non-Newtonian fermentation broths. Applied Microbiology and Biotechnology, 51, pp.310-315.

Gouveia E.R., Baptista-Neto A., Hokka C.O. and Badino J. 2000. Studies on the rheology and oxygen mass transfer in the clavulanic acid production by *Streptomyces clavuligerus*. Brazilian Journal of Chemical Engineering, 17, pp.827-834.

Hernandez-Penaranda A.M., Salazar-Montoya J.A., Rodriguez-Vazquez R. and Ramos-Ramirez E.G. 2001. Rheological behavior of *Phanerochaete chrysosporium* broth during lignin degradation. Journal of Environmental Science and Health Part A-Toxic/Hazardous Substances & Environmental Engineering, 36, pp.1983-1996.

Hwang H.J., Kim S.W., Xu C.P., Choi J.W. and Yun J.W. 2004. Morphological and rheological properties of the three different species of basidiomycetes Phellinus in submerged cultures. Journal of Applied Microbiology, 96, pp.1296-1305.

Ju L.K., Ho C.S. and Shanahan J.F. 1991. Effects of carbon-dioxide on the rheological behavior and oxygen-transfer in submerged penicillin fermentations. Biotechnology and Bioengineering, 38, pp.1223-1232.

Kemblowski Z., Kristiansen B. and Ajayi O. 1985. Online rheometer for fermentation liquids. Biotechnology Letters, 7, pp.803-808.

Kim S.W., Hwang H.J., Xu C.P., Choi J.W. and Yun J.W. 2003. Effect of aeration and agitation on the production of mycelial biomass and exopolysaccharides in an enthomopathogenic fungus *Paecilomyces sinclairii*. Letters in Applied Microbiology, 36, pp.321-326.

Leduy A., Marsan A.A. and Coupal B. 1974. Study of rheological properties of a non-Newtonian fermentation broth. Biotechnology and Bioengineering, 16, pp.61-76.

Leong-Poi L. and Allen D.G. 1992. Direct measurement of the yield stress of filamentous fermentation broths with the rotating vane technique. Biotechnology and Bioengineering, 40, pp.403-412.

Li G.Q., Qiu H.W., Zheng Z.M., Cai Z.L. and Yang S.Z. 1995. Effect of fluid rheological properties on mass transfer in a bioreactor. Journal of Chemical Technology and Biotechnology, 62, pp.385-391.

Lim J.S., Lee J.H., Kim J.M., Park S.W. and Kim S.W. 2006. Effects of morphology and rheology on neo-fructosyltransferase production by *Penicillium citrinum*. Biotechnology and Bioprocess Engineering, 11, pp.100-104.

Lopez J.L.C., Perez J.A.S., Sevilla J.M.F., Porcel E.M.R. and Chisti Y. 2005. Pellet morphology, culture rheology and lovastatin production in cultures of *Aspergillus terreus*. Journal of Biotechnology, 116, pp.61-77.

Marten M.R., Velkovska S., Khan S.A. and Ollis D.F. 1996. Rheological, mass transfer, and mixing characterization of cellulase producing *Trichoderma reesei* suspensions. Biotechnology Progress, 12, pp.602-611.

Metz B., Kossen N.W.F. and Van Suijdam J.C. 1979. The rheology of mould suspensions. Advances in Biochemical Engineering/Biotechnology, 11, pp.103-156.

Metzner A.B. and Otto R.E. 1957. Agitation of non-Newtonian fluids. Aiche Journal, 3, pp.3-10.

Mishra P., Srivastava P. and Kundu S. 2005. A comparative evaluation of oxygen mass transfer and broth viscosity using Cephalosporin-C production as a case strategy. World Journal of Microbiology & Biotechnology, 21, pp.525-530.

Mohseni M. and Allen D.G. 1995. The effect of particle morphology and concentration on the directly measured yield stress in filamentous suspensions. Biotechnology and Bioengineering, 48, pp.257-265.

Mohseni M., Kautola H. and Allen D.G. 1997. The viscoelastic nature of filamentous fermentation broths and its influence on the directly measured yield stress. Journal of Fermentation and Bioengineering, 83, pp.281-286.

Moo-Young M., Halard B., Allen D.G., Burrell R. and Kawase Y. 1987. Oxygen-transfer to mycelial fermentation broths in an airlift fermenter. Biotechnology and Bioengineering, 30, pp.746-753.

Moo-Young M., Hirose T. and Geiger K.H. 1969. The rheological effects of substrate-additives on fermentation yields. Biotechnology and Bioengineering, 11, pp.725-730.

Muller C., Hansen K., Szabo P. and Nielsen J. 2003. Effect of deletion of chitin synthase genes on mycelial morphology and culture viscosity in *Aspergillus oryzae*. Biotechnology and Bioengineering, 81, pp.525-534.

O'Cleirigh C., Casey J.T., Walsh P.K. and O'Shea D.G. 2005. Morphological engineering of *Streptomyces hygroscopicus var. geldanus*: regulation of pellet morphology through manipulation of broth viscosity. Applied Microbiology and Biotechnology, 68, pp.305-310.

Olsvik E. and Kristiansen B. 1992. Influence of oxygen-tension, biomass concentration, and specific growth-rate on the rheological properties of a filamentous fermentation broth. Biotechnology and Bioengineering, 40, pp.1293-1299.

Olsvik E. and Kristiansen B. 1992. On-line rheological measurements and control in fungal fermentations. Biotechnology and Bioengineering, 40, pp.375-387.

Olsvik E. and Kristiansen B. 1994. Rheology of filamentous fermentations. Biotechnology Advances, 12, pp.1-39.

Olsvik E., Tucker K.G., Thomas C.R. and Kristiansen B. 1993. Correlation of *Aspergillus niger* broth rheological properties with biomass concentration and the shape of mycelial aggregates. Biotechnology and Bioengineering, 42, pp.1046-1052.

Oncul S., Tari C. and Unluturk S. 2007. Effect of various process parameters on morphology, rheology, and polygalacturonase production by *Aspergillus sojae* in a batch bioreactor. Biotechnology Progress, 23, pp.836-845.

Pamboukian C.R.D. and Facciotti M.C.R. 2005. Rheological and morphological characterization of *Streptomyces olindensis* growing in batch and fed-batch fermentations. Brazilian Journal of Chemical Engineering, 22, pp.31-40.

Pedersen A.G., Bundgaard-Nielsen M., Nielsen J., Villadsen J. and Hassager O. 1993. Rheological characterization of media containing *Penicillium chrysogenum*. Biotechnology and Bioengineering, 41, pp.162-164.

Pollard D.J., Hunt G., Kirschner T.K. and Salmon P.M. 2002. Rheological characterization of a fungal fermentation for the production of pneumocandins. Bioprocess and Biosystems Engineering, 24, pp.373-383.

Queiroz M.C.R., Facciotti M.C.R. and Schmidell W. 1997. Rheological changes of *Aspergillus awamori* broth during amyloglucosidase production. Biotechnology Letters, 19, pp.167-170.

Reuss M., Debus D. and Zoll G. 1982. Rheological properties of fermentation fluids. Chemical Engineer, pp.233-236.

Richard A. and Margaritis A. 2003. Rheology, oxygen transfer, and molecular weight characteristics of poly(glutamic acid) fermentation by *Bacillus subtilis*. Biotechnology and Bioengineering, 82, pp.299-305.

Riley G.L., Tucker K.G., Paul G.C. and Thomas C.R. 2000. Effect of biomass concentration and mycelial morphology on fermentation broth rheology. Biotechnology and Bioengineering, 68, pp.160-172.

Roels J.A., Vandenbe J. and Voncken R.M. 1974. Rheology of mycelial broths. Biotechnology and Bioengineering, 16, pp.181-208.

Roukas T. and Mantzouridou F. 2001. Effect of the aeration rate on pullulan production and fermentation broth theological properties in an airlift reactor. Journal of Chemical Technology and Biotechnology, 76, pp.371-376.

Schatzmann M., Fischer P. and Bezzola G.R. 2003. Rheological behavior of fine and large particle suspensions. Journal of Hydraulic Engineering-Asce, 129, pp.796-803.

Schramm G. 1998. A practical approach to rheology and rheometry. Karlsruhe: Gebrueder HAAKE GmbH. 291 p.

Schügerl K. 1981. Oxygen transfer into highly viscous media. Advances in Biochemical Engineering/Biotechnology, 19, pp.71-174.

Scott Blair G.W. 1966. The success of Casson's equation. Rheologica Acta, 5, pp.184-187.

Shi Y., Ryu D.D.Y. and Ballica R. 1993. Rheological properties of mammalian cell culture suspensions: Hybridoma and HeLa cell lines. Biotechnology and Bioengineering, 41, pp.745-754.

Sinha J., Tae Bae J., Pil Park J., Hyun Song C. and Won Yun J. 2001. Effect of substrate concentration on broth rheology and fungal morphology during exo-biopolymer production by *Paecilomyces japonica* in a batch bioreactor. Enzyme and Microbial Technology, 29, pp.392-399.

Skelland A.H.P. 1967. Non-Newtonian flow and heat transfer. New York: John Wiley & Sons Inc. 469 p.

Steel R. and Maxon W.D. 1962. Some effects of turbine size on Novobiocin fermentations. Biotechnology and Bioengineering, 4, pp.231-240.

Steffe J.R. 1996. Rheological methods in food processing engineering. East Lansing: Freeman Press. 428 p.

Stoupis T., Stewart G.G. and Stafford R.A. 2002. Mechanical agitation and rheological considerations of ale yeast slurry. Journal of the American Society of Brewing Chemists, 60, pp.58-62.

Tanner R.I. 2000. Engineering rheology. New York: Oxford University Press. 559 p.

Thorne L., Mikolajczak M.J., Armentrout R.W. and Pollock T.J. 2000. Increasing the yield and viscosity of exopolysaccharides secreted by *Sphingomonas* by augmentation of chromosomal genes with multiple copies of cloned biosynthetic genes. Journal of Industrial Microbiology and Biotechnology, 25, pp.49-57.

Toda K., Furuse H., Amari T. and Wei X. 1998. Cell concentration dependence of dynamic viscoelasticity of *Escherichia coli* culture suspensions. Journal of Fermentation and Bioengineering, 85, pp.410-415.

Verma M., Brar S.K., Tyagi R.D., Surampalli R.Y. and Valero J.R. 2006. Dissolved oxygen as principal parameter for conidia production of biocontrol fungi *Trichoderma viride* in non-Newtonian wastewater. Journal of Industrial Microbiology & Biotechnology, 33, pp.941-952.

Chapter 3

Relationship between Morphology and Rheology during *Trichoderma reesei* RUT-30 Fermentation

Philippe Malouf[1], Nilesh Patel[1], Denis Rodrigue[2] and Jules Thibault[1*]

[1]Department of Chemical and Biological Engineering
University of Ottawa
Ottawa, Ontario, Canada K1N 6N5

[2]Department of Chemical Engineering
Laval University
Quebec City, Quebec, Canada G1K 7P4

*Corresponding author: Tel.: 613-562-5800 x6094; Email: Jules.Thibault@uottawa.ca

3.1 Abstract

Bioethanol can be produced from a wide variety of feed stocks; however, it appears that using cellulosic residues such as corn stovers, straws and wood chips is a more viable solution even though cellulase hydrolysis remains a challenging step in the bioethanol production process. Cellulase can be produced by the filamentous fungus *Trichoderma reesei*. Due to the morphological complexity of this fungus, the fermentation broth during the process reaches high viscosities limiting nutrient and oxygen transfer to the cells, thus affecting enzyme productivity.

In the present study, the relationship between biomass concentration, morphology and broth rheology was characterized under two different modes of agitation: a stirred tank bioreactor operated at 200, 300, 400 and 500 RPM and a reciprocating plate bioreactor agitated at 0.25, 0.50, 0.75 and 1.00 Hz. The rheology was best described by the Herschel-

Bulkley model. Both the biomass concentration (X) and the consistency index (K) showed strong dependence on agitation. The morphological factor (K/X^{α}) varied during the course of the fermentation, underlying the importance of including a morphological parameter in the prediction of K. Through biomass reconstitution experiments, the biomass exponent α was shown to remain constant during fermentation runs performed under different agitation conditions.

Fermentation broth morphology was assessed by image analysis. Both morphological classes, clumps and the dispersed forms were shown to vary during fermentation. Morphological parameters were averaged over all morphological classes and correlated to K/X^{α}. Roundness was found to have the strongest correlation when data from the batch and the fed-batch phases were considered separately. A linear and a power-law mathematical model were suggested to characterize the correlations for the batch and the fed-batch phases, respectively. Data separation in both phases improved the capacity to predict the experimental values of K.

3.2 Introduction

Global warming due to greenhouse gas emissions continues to be a growing concern for its impact on the planet's weather pattern and the potential rise of the sea level. Fossil fuel is the main contributor of greenhouse gases and it is necessary to seek new energy sources that are renewable and sustainable. From a fuel perspective, bioethanol and biodiesel are the fuel sources that can provide, in the immediate future, a reduction in the net CO_2 gas emission.

Bioethanol is produced from simple carbohydrates (sugars) through a fermentation process. There exist mainly three feed stocks of fermentable sugars to produce bioethanol: sugar cane giving sucrose (one glucose and one fructose), corn (as glucose dimer), or cellulosic fibers (mixture of carbohydrate polymers when hydrolyzed gives mainly glucose and xylose). Sugars from sugar cane and corn are more easily obtained. However, they are both food sources and corn is a staple food in some countries, which can affect supplies and prices to low income families. On the other hand, cellulosic materials are widely abundant in nature. They can be found in the form of agriculture waste such as corn stover, straw, or waste from the lumber industry. Although cellulosic material is widely abundant, cellulose, a glucose polymer, requires intensive processing for the extraction of the fermentable sugar. Different methods are used to hydrolyze cellulose into glucose such as using sulfuric acid. However, the latter is toxic and gives secondary products (Mohaghehi et al., 1988). A more environmentally-safe method to process the cellulose part of the biomass is using cellulase enzymes. Cellulase hydrolyzes cellulose to give only glucose as a product and has the advantage to be biodegradable. Although, the price contribution of these enzymes to the bioethanol cost has drastically dropped in recent years in large part to strain and genetic improvement of the microorganisms, further research is required to decrease production costs by the optimization of the production process of cellulase enzymes (Philippidis, 1994; Philippidis and Hatzis, 1997; Schell et al., 2001; Aden et al., 2002; Novozymes, 2003, 2007).

Cellulase is a mixture of enzymes which hydrolyze completely cellulose fibers. Although many microbes produce cellulase enzymes, few are capable of producing the enzyme complex which completely hydrolyzes cellulose fibers. From literature, the filamentous fungus *Trichoderma reesei* is reported to be the most efficient natural producer

of cellulase and is widely used in industry for providing all the cellulase enzymes (Maras et al., 1999; Tolan and Foody, 1999; Nidetzky et al., 1994; Merino and Cherry, 2007). Akin to many other fungi, of which some are listed in Table 3.1, it is well established that the filamentous nature gives the microorganism a complex morphology responsible along with the contribution of the biomass concentration for a highly viscous and non-Newtonian fermentation broth. Variation of these properties during fermentation influences the bioreactor momentum, thus affecting mass and heat transfer. These transport properties have a strong influence on the efficiency and cellulase productivity in a bioreactor. Figure 3.1 shows a summary of the relationship between the process variables. To improve cellulase production, this study aims at characterizing the relationships between rheology, morphology and biomass concentration in an attempt to improve reactor performance (Schügerl et al., 1998).

Table 3.1 List of some industrially-relevant filamentous microorganisms.

Microorganism	Authors	Year
Aspergillus niger, Penicillium chrysogenum and *Streptomyces levoris*	Allen and Robinson	1990
Aspergillus niger	Leong-Poi and Allen	1992
Penicillium chrysogenum	Pedersen et al.	1993
Aspergillus niger and *Streptomyces levoris*	Mohseni et al.	1997
Aspergillus oryzae	Marten and Wenger	1997
Aspergillus awamori	Badino Jr. et al.	1999
Penicillium chrysogenum	Goudar et al.	1999
Aspergillus oryzae	Li et al.	2000
Penicillium chrysogenum	Riley et al.	2000
Aspergillus awamori	Badino Jr. et al.	2001
Paecilomyces sinclairii	Cho et al.	2002
Aspergillus oryzae	Bhargava et al.	2003
Aspergillus oryzae	Müller et al.	2003
Streptomyces olindensis	Pamboukian and Facciotti	2005
Tolypocladium inflatum	Benchapattarapong et al.	2005
Aspergillus terreus	Lopez et al.	2005
Aspergillus sojae	Oncul et al.	2007
Aspergillus terreus	Gupta et al.	2007

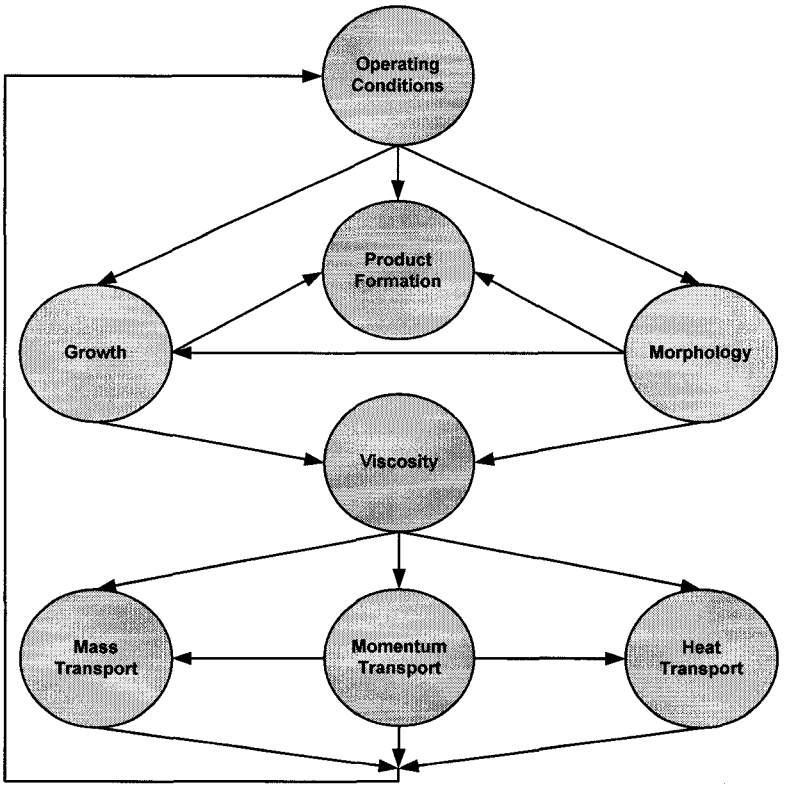

Figure 3.1 Schematic representation of the interrelations between processes in viscous fermentation. Adapted from Metz et al. (1979).

In order to examine the influence of morphology on rheology, different categorizations were done to describe the filamentous fungi complex growth forms. There are two main growth forms: pellet and dispersed (Lecault et al., 2007; Paul and Thomas, 1996). Although pellet morphology is less viscous (Gbewonyo et al. 1992), the dispersed form is favoured for cellulase production in *T. reesei* (Domingues et al., 2000). The dispersed form has been classified into 4 categories: unbranched, branched, entangled and clumped. Clumps represent more than 80% of the morphology for some filamentous fungi fermentation (Paul and Thomas, 1998) and its morphological properties are used to build models correlating to viscosity (Tucker and Thomas, 1993; Tucker, 1994; Olsvik et al., 1993; Olsvik and Kristiansen, 1994; Pamboukian and Facciotti, 2005). Nonetheless, it has

been shown that clump morphology level dropped in favor of the other three morphologies during the course of filamentous fermentations (Riley et al., 2000). In such fermentations, the morphological property used to correlate with viscosity was the weighted average of all the dispersed classes. On the other hand, rheology of fermentation broth has been studied extensively (Goudar et al., 1999; Gupta et al., 2007; Mohseni and Allen., 1995; Lopez et al., 2005; Pamboukian and Facciotti, 2005; Müller et al., 2003). Fungal broth is typically non-Newtonian pseudo-plastic and is commonly described by the Power-Law (Ostwald-de Waele) model. However, for some filamentous fungi, yield stress properties become important and need to be considered. The yield stress is more adequately described by either the Casson or the Herschel-Bulkley model (Marten et al., 1996; Pamboukian and Facciotti, 2005; Lopez et al., 2005; Cho et al., 2002, Badino Jr. et al., 1999; Allen and Robinson, 1990).

In order to examine the influence of morphology on rheology, different categorizations were done to describe the filamentous fungi complex growth forms. There are two main growth forms: pellet and dispersed (Lecault et al., 2007; Paul and Thomas, 1996). Although pellet morphology is less viscous (Gbewonyo et al. 1992), the dispersed form is favoured for cellulase production in *T. reesei* (Domingues et al., 2000). The dispersed form has been classified into 4 categories: unbranched, branched, entangled and clumped. Clumps represent more than 80% of the morphology for some filamentous fungi fermentation (Paul and Thomas, 1998) and its morphological properties are used to build models correlating to viscosity (Tucker and Thomas, 1993; Tucker, 1994; Olsvik et al., 1993; Olsvik and Kristiansen, 1994; Pamboukian and Facciotti, 2005). Nonetheless, it has been shown that clump morphology level dropped in favor of the other three morphologies during the course of filamentous fermentations (Riley et al., 2000). In such fermentations,

the morphological property used to correlate with viscosity was the weighted average of all the dispersed classes. On the other hand, rheology of fermentation broth has been studied extensively (Goudar et al., 1999; Gupta et al., 2007; Mohseni and Allen., 1995; Lopez et al., 2005; Pamboukian and Facciotti, 2005; Müller et al., 2003). Fungal broth is typically non-Newtonian pseudo-plastic and is commonly described by the Power-Law (Ostwald-de Waele) model. However, for some filamentous fungi, yield stress properties become important and need to be considered. The yield stress is more adequately described by either the Casson or the Herschel-Bulkley model (Marten et al., 1996; Pamboukian and Facciotti, 2005; Lopez et al., 2005; Cho et al., 2002, Badino Jr. et al., 1999; Allen and Robinson, 1990).

In the literature, many studies have suggested relating the biomass concentration (X) and the consistency index (K) of the Power-Law rheological model, in order to develop correlations for process control or design purposes (Queiroz et al., 1997; Badino Jr. et al., 1999). Since morphology of the filamentous fungi was seen to influence the fermentation broth viscosity, some authors suggested the addition of a morphological parameter in the correlation (Tucker, 1994; Olsvik and Kristiansen, 1994; Riley et al., 2000; Pamboukian and Facciotti, 2005). Some morphological parameters used to predict the consistency index are summarized in Table 3.2 (Metz et al., 1979; Olsvik et al., 1993; Mohseni and Allen, 1995; Riley et al., 2000; Pamboukian and Facciotti, 2005). The parameters chosen are dimensional properties of the filamentous fungi or one of the growth forms, mostly clumps, that parallel principles discussed in suspension rheology (Macosko, 1994). When the parameters are introduced in the prediction of the consistency index, the models obtained are generally expressed in the following form (Riley et al., 2000; Pamboukian and Facciotti, 2005):

$$K = a \times X^{\alpha} \times f(MP) \qquad 3.1$$

where a is a constant, X is the biomass concentration, α is the biomass concentration exponent, and $f(MP)$ a function of morphological parameters. Few authors have also discussed the reliability of the model. Riley et al. (2000) made a thorough analysis of every parameter in the model and studied the prediction of K. In order to study the effect of biomass, the morphological parameters as described previously by Tucker (1994) were kept constant. The biomass concentration exponent was found to be relatively constant during a fermentation run but was found to vary significantly in the range of 0.3 to 3.3 for different microorganisms (Tucker, 1994; Riley et al., 2000; Gupta et al., 2007; Badino Jr. et al., 1999; Li et al., 1995; Queiroz et al., 1997).

Table 3.2 List of morphological parameters deemed important in this study.

Morphological Parameters	Definitions
L_d	Mean hyphal diameter
L_e	Effective mean length or the mean length of the main hyphae
L_{hgu}	Mean length of the hyphal growth unit or total mean length per number of growth tips
L_t	Total length of the hyphae
L_e^*	Dimensionless length (ratio of effective length over diameter)
F	Compactness (ratio of the projected area of the hyphae in a clump to the projected convex area of that clump)
D	Mean maximum dimension (ratio of the projected area of the hyphae in a clump to the projected convex area of that clump)
R	Roughness or roundness (perimeter^2/ 4π area)
A	Mean area

Previous investigations have studied *T. reesei* for its ability to produce cellulase (Mohagheghi et al., 1990, Nidetzky et al., 1994; Maras et al., 1999; Tolan and Foody, 1999). As well, some studies describe the rheology (Marten et al., 1996) and the morphology (Lecault et al., 2007) of this microorganism. However, there were no attempts to correlate the rheology to the biomass concentration and the morphology for *T. reesei.*

This study aims at characterizing the relationship of these morphological parameters for *T. reesei* under two agitation mechanisms (stirred tank bioreactor and reciprocating plate bioreactor) at 4 agitation rates each.

3.3 Materials and Methods

3.3.1 Microorganism Stocks

The cellulase producing filamentous fungi *Trichoderma reesei* Rut C30 (ATCC 56765) was used to carry out the fermentation runs. The strain was obtained from both Iogen Corporation (Ottawa) and ATCC. Glycerol stocks were made according to ATCC protocol and maintained at -80°C. Spores from glycerol stocks were transferred to potato dextrose agar plates and maintained at 28°C for 4 days, until a thick spore lawn was obtained. The plates were stored, thereafter, in a refrigerator at 4°C, for one month. Then, the process was repeated to obtain a fresh set of plates.

3.3.2 Culture Conditions

The growth medium was prepared using the concentrations shown in Table 3.3 for an operating volume of 10 L. The pH was adjusted to 5.5 with 10 N NaOH and 3 mL of antifoam 204 (Sigma) was added. The corn steep floccules were grinded using a blender and autoclaved at 130°C for 60 minutes, then mixed with the rest of the medium components. The bioreactors with medium were sterilized for 30 minutes at 121°C. Feed solution composed solely of 150 g/L of lactose was autoclaved in a separate container at 121°C for 20 minutes. 500 mL of inoculum was prepared in 1 L Erlenmeyer flask with

three baffles using the same medium composition as in Table 3.3 and seeded with spores at a concentration of approximately 5×10^3 spores/mL. The spores were previously collected from plates and diluted in sterile water, after which spore concentration was calculated using a Petroff Hausser counting chamber (Hausser Scientific, Horsham, PA). The flasks were incubated at 28°C for a period of 55 h shaking at 200 RPM in an orbital shaker (Model 3535CC Incubator shaker, Lab-Line Instrument Inc., Melrose Park, IL).

Table 3.3 Culture medium composition.

	Medium composition[1] (g/L)
Glucose	13.0
$(NH_4)_2SO_4$	1.40
KH_2PO_4	2.00
$MgSO_4\cdot7H_2O$	0.60
$CaCl_2\cdot7H_2O$	0.30
Corn Steep	6.0
$FeSO_4\cdot7H_2O$	0.0050
$MnSO_4\cdot H_2O$	0.0016
$ZnSO_4\cdot7H_2O$	0.0014
$CoCl_2\cdot6H_2O$	0.0020

[1] Chemicals were ACS reagent grade and purchased from Sigma-Aldrich.

3.3.3 Bioreactor Operating Conditions

Table 3.4 provides the physical characteristics of the two bioreactors as well as the operating conditions. Batch phase was initiated by inoculating the seed culture into the bioreactor. The fed-batch phase was started when the initial glucose was consumed. The feed solution was fed in the bioreactor to keep the dissolved oxygen (DO) level in the vicinity of 30% of saturation. A feed strategy was adopted in order to accomplish this control, such that every 20 s, the DO level was measured and the lactose feed flow rate was manipulated appropriately. When the DO level was above 30% of saturation, a predetermined amount of lactose solution was fed into the bioreactor, while no solution was

fed when the level was below 30% of saturation. The amount of lactose solution fed was manually adjusted throughout the fed-batch phase of the fermentation run. In the same way, a one-sided pH control was performed by the addition of NH_4OH (15% v/v) to maintain pH at 4.5.

Eight fed-batch experiments were carried out in two bioreactors having different agitation mechanism. Four runs were performed in a stirred tank bioreactor (STB) with three identical Rushton turbines, mounted on a central shaft and located at 54, 132 and 210 mm when measured from the bottom of the column. The turbines have 6 blades (25 mm long, 15 mm high and 1.5 mm thick) each mounted on the periphery of a 50 mm diameter disk. Four additional runs were performed in a reciprocating plate bioreactor (RPB) with six stainless steel perforated plates (221 mm diameter and 1.25 mm thickness) spaced 50 mm apart from one another. Each plate has perforations 19 mm in diameter which are distributed on an equilateral triangular pitch. The schematic diagram of both bioreactors is shown in Figure 3.2 (Gagnon et al., 1998).

3.3.4 Sampling and Analysis

60 mL samples of the fermentation broth were withdrawn at regular intervals of 4-6 h during batch phase and of 12 h during fed-batch. Each sample was divided into portions for analysis as follows: 15 mL for biomass concentration, 35 mL for rheology, and 1 mL for image analysis. The biomass concentration was determined by dry weight analysis. Each sample was filtered through a pre-dried and pre-weighted glass fiber (grade A/E, Gelman Sciences, MI) and washed with twice the sample volume of deionized distilled water. The sample was then dried for 24 h at 95°C and incubated in a desiccator for 24 h after which the weight was measured.

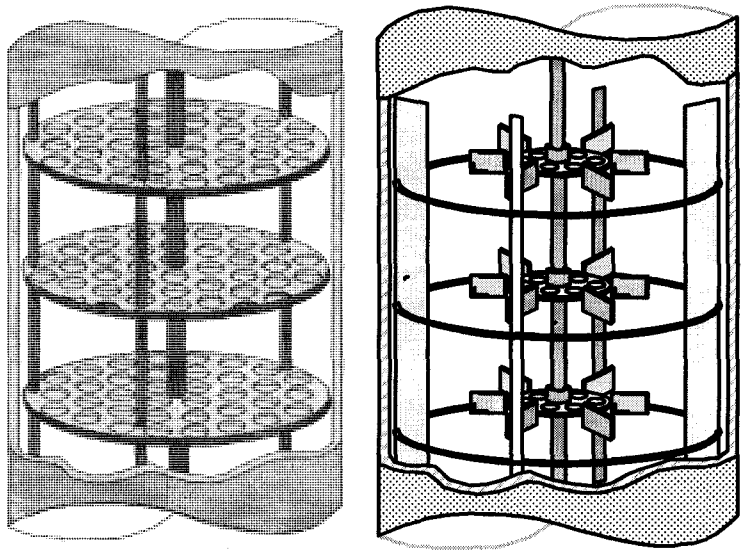

(a) (b)

Figure 3.2 Schematic diagrams of the bioreactors used: (a) RPB and (b) STB

Table 3.4 Bioreactor Operating Conditions and Dimensions.

Reactor	Stirred Tank Bioreactor	Reciprocating Plate Bioreactor
Agitation Rate	200, 300, 400, 500 (RPM)	0.25, 0.50, 0.75, 1.00 (Hz)
Temperature (°C)	28	28
Aeration Rate (L/min)	10	10
Initial Volume (L)	10	10
Inoculum Size (mL)	500	500
pH controlled[1]	4.5	4.5
DO controlled[2] (%)	30	30
Total Reactor Volume (L)	22.5	22.5
Operating Volume (L)	17	17
Inner Diameter (mm)	228	228
Column Height (mm)	550	550
4-Baffles (mm)	375(H) × 16(W) × 1(T)	-
Agitation Mechanism	Rushton Turbines	Reciprocating Plates

[1] The pH was measured *in-situ* by a pH FermProbe (Broadley-James Corporation, Irvine, CA).

[2] Dissolved oxygen (DO) was monitored in-situ by a DO sensor (Broadley-James Corporation, Irvine, CA).

3.3.5 Image Analysis

Image analysis was done using a monochrome camera (CoolSnap ES, Roper Scientific, Tucson, AZ) mounted on an Olympus IX81 microscope (Olympus, Melville, NY), with an automated stage controlled by the Image-Pro® Plus software (Image-Pro® Plus version 5.1, Media Cybernetics, Silver Spring, MD). For every sample, several morphological parameters were measured as described by Lecault et al. (2007) and Choy (2008) after classification of the morphology into the 4 growth forms of *T. reesei*: unbranched (U), branched (B), entangled (E), and clump (C). The parameters most relevant to this work are: count, area, box/area ratio, aspect ratio, perimeter, convex perimeter, perimeter ratio, roundness, dendritic length, viable area, mean diameter, percent viability, and density (Lecault et al., 2007). The relative amount of morphological types was calculated by dividing the area of a specific type by the total area for a sample. The measurement of the viability was done by staining *T. reesei* cells with FDA (fluorescein diacetate) solution. Under fluorescence microscopy, the FDA solution reveals active mycelia by fluorescing while dead mycelia remain dark.

For modeling, the weighted average of the measured parameters (*MP*) was calculated for every sample as follows:

$$MP = u \times MP(U) + b \times MP(B) + e \times MP(E) + c \times MP(C) \qquad 3.2$$

where *u, b, e and* c are the percentage values of the growth forms, and *MP(U)*, *MP(B)*, *MP(E)* and *MP(C)* are the morphological parameter values associated to each growth form.

3.3.6 Rheological Measurements

Rheological characterization of the fermentation broth was performed offline using a rotational rheometer AR G2 (TA Instruments, New Castle, Delaware, United States). The rheometer was connected to a computer running the AR Instrument Control and Data Analysis software. The advantage of using this high end rheometer is for its ability to measure low viscosity fluids (< 1 Pa.s) over a wide range of shear rates (0.1 - 10000 s^{-1}) as well as for the possibility to use different measuring fixtures that are factory calibrated. In the literature, the geometries typically used to measure viscosity for fermentation broth of filamentous microorganism are either a vane or a concentric cylinder in a cup (Bhargava et al., 2003; Hwang et al., 2004; Riley et al, 2000; Lopez et al., 2005; Barnes and Nguyen, 2001; Marten et al., 1996; Goudar et al., 1999; Müller et al., 2003; Benchapattarapong et al., 2005). However, these fixtures require a relatively large sample volume which could limit the number of samples for small volume bioreactors (0.5 – 20 L). Other classes of fixtures, which require from 10 to 100 times less sample volume than the previously-mentioned fixtures, are the cone/plate or parallel/plate configurations. They were tested in this investigation to compare their performance for fermentation broths of filamentous microorganisms *T. reesei*. The latter two fixtures are rarely used for fermentation filamentous broth (Mohseni et al., 1997; O'Cleirigh et al., 2005; Metz et al., 1979). The geometries used in this investigation are listed in Table 3.5 with their respective characteristics and physical dimensions.

Table 3.5 Description of the geometries used for the rheological characterizations.

Rotor	Stator	Materials	Dimensions	Sample Volume (mL)
Concentric Cylinder (545012.001)	Cup	Hard Anodized Aluminum	14 mm inside diameter 15 mm outside diameter 42 mm in height	19.6
Vane Rotor (545025.001)	Cup	Stainless Steel	14 mm inside diameter 15 mm outside diameter 42 mm in height	28.72
Cone (516606.901)	Plate	Acrylic	60 mm diameter 2° cone angle 69 μm gap	1.98
Parallel Plate (516600.901)	Plate	Acrylic	60 mm diameter 2 mm gap	3.01

The different geometries presented in Table 3.5 were tested for their ability to measure fermentation broth rheology of *T. reesei*. In suspension rheology, the gap between the rotating head and the stationary side should be at least 10 times larger than the maximum particle diameter (Brummer, 2006; Schatzmann et al., 2003). Cone and plate geometry has the advantage of subjecting the sample with a uniform shear rate. However, typical truncation values for commercially available cone are less than 50 μm, which is not sufficient to provide clearance for fungi cells of *T. reesei* of approximately 100 μm. For the parallel plate geometry, the gap can be easily adjusted to 10 times the particle size. However, visual observations have highlighted two problems. First, the sample morphology was altered. As the transparent acrylic parallel plate rotated, the fungi suspension aggregated and formed thread-like structure. Second, for shear rates higher than 150 s^{-1}, the microorganisms were ejected outside the sample enclosure leaving only the liquid portion of the broth, thus changing sample properties. For these reasons, the use of this category of geometry was discarded for further rheological measurements on *T. reesei* fermentation broth, further confirming results by Metz et al. (1979).

A standard protocol was developed to ensure that reproducible results could be obtained using the concentric cylinder and vane and cup geometries. The concentric cylinder was favoured over the vane to assess the rheology of the first two to three samples of the fermentation runs, i.e. when the broth still had properties close to water. As biomass concentration increased with time, the vane and cup was favoured for measuring viscosity because this geometry prevented sedimentation and wall slip, while preserving the sample morphology. All samples used for rheological analysis were maintained at the bioreactor operating temperature of 28°C. Each sample was pre-sheared for 30 s at 20 s^{-1} to erase any structural history due to fixture insertion, after which an equilibration was done for 6 minutes. Rheological measurements were performed under controlled shear rate conditions in the range 1-1000 s^{-1}. Although each sample was tested on the whole shear rate range, the data used to fit the rheological models were taken only within the valid range. In this investigation, the valid range corresponds to data having Reynolds numbers less than 10, the upper limit for laminar flow in the system (Riley et al., 2000).

3.4 Results and Discussion

3.4.1 Rheological Models

Three models are commonly used to fit data of fermentation broth rheology:

Power Law (PL) $$\tau = K_{PL}\dot{\gamma}^{n} \quad (3.3)$$

Casson: $$\sqrt{\tau} = \sqrt{\tau_{y_c}} + K_c\sqrt{\dot{\gamma}} \quad (3.4)$$

Hershel-Bulkley (HB) $$\tau = \tau_{y_{HB}} + K_{HB}\dot{\gamma}^{n} \quad (3.5)$$

where τ is the shear stress, $\dot{\gamma}$ the shear rate, n the flow index, K_{PL} the power law consistency index, K_c the Casson consistency index, τ_{y_c} the Casson yield stress, K the Herschel-Bulkley consistency index, and τ_y the Herschel-Bulkley yield stress.

Figure 3.3 shows the fit of the three models to a typical sample from a fermentation run. Even though the power-law model is the most widely used model to describe the shear thinning behaviour of a fluid, it does not provide an adequate fit for the fermentation broth of *T. reesei*. In contrast, when a yield stress term is included in the model, as in Herschel-Bulkley and Casson, the models show a better fit with the first model having the best fit. This is in agreement with the work of Marten et al. (1996). These authors favoured the Casson model to characterize rheology of their fermentation because it is a two-parameter model: the Casson viscosity and the Casson yield stress. In the Casson model, the flow index is fixed at 0.5 and, as a result, this model cannot predict adequately the rheological behaviour at the beginning of the fermentation run where the broth rheology resembles the one of water and the flow index is close to unity. On the other hand, the HB model has three parameters: the consistency index, the flow index, and the yield stress. In this model, the variation in flow properties is taken into account with the flow index. Thus, the use of HB is favoured in this investigation because the flow properties of the fermentation change with time.

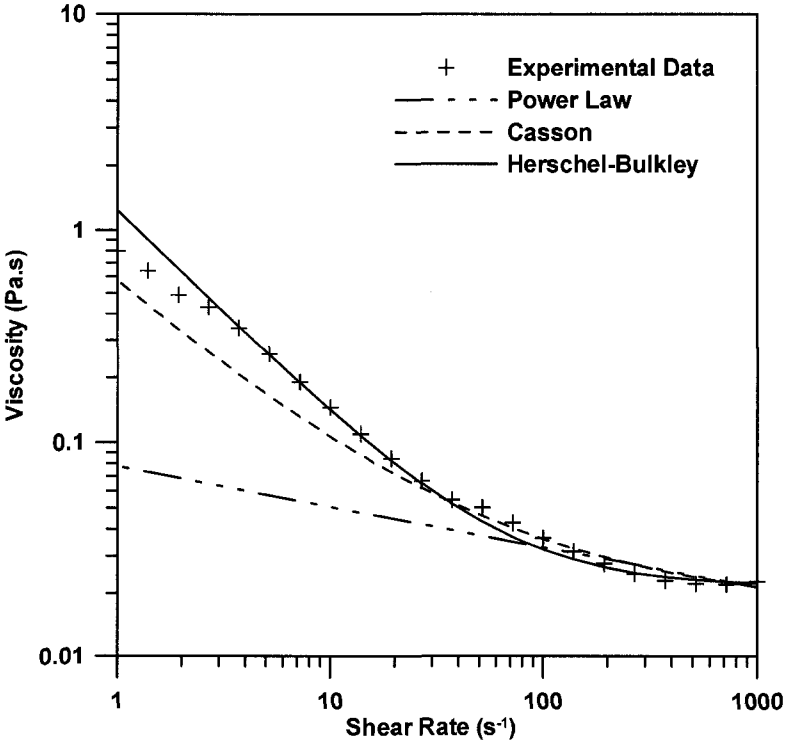

Figure 3.3 Fermentation sample from Stirred Tank Bioreactor at 500 RPM with a biomass concentration of 20.7 g/L. Measured viscosity versus the shear rate varying from 1 - 1000 s^{-1} fitted with three rheological models: Power-Law, Casson and Herschel- Bulkley.

3.4.2 Biomass of all Fermentation Runs

Fed-batch fermentations of the filamentous fungi *T. reesei* were done in two bioreactors to compare different agitation mechanisms and different agitation rates. All fermentations were started with the same initial conditions. DO level was monitored and dropped to 0% during the batch phase for most fermentations. When the initial glucose substrate was depleted, DO level increased and was maintained at 30% by feeding in lactose substrate every time DO went above this set point. In the case of 500 RPM, the DO level never dropped low enough to reach the 30% level. In this case, lactose was overfed to lower the DO level, resulting in a secondary batch phase. Figures 3.4 and 3.5 show the biomass concentration for two agitation mechanisms at different agitation rates. It can be clearly observed that the rate of production of biomass is essentially the same in the batch

phase for all agitations in both bioreactors, except at 200 RPM in the STB. Also, higher biomass concentrations are achieved when the agitation rate is increased. The higher oxygen mass transfer obtained at higher agitation rates led to a greater utilization of the substrate.

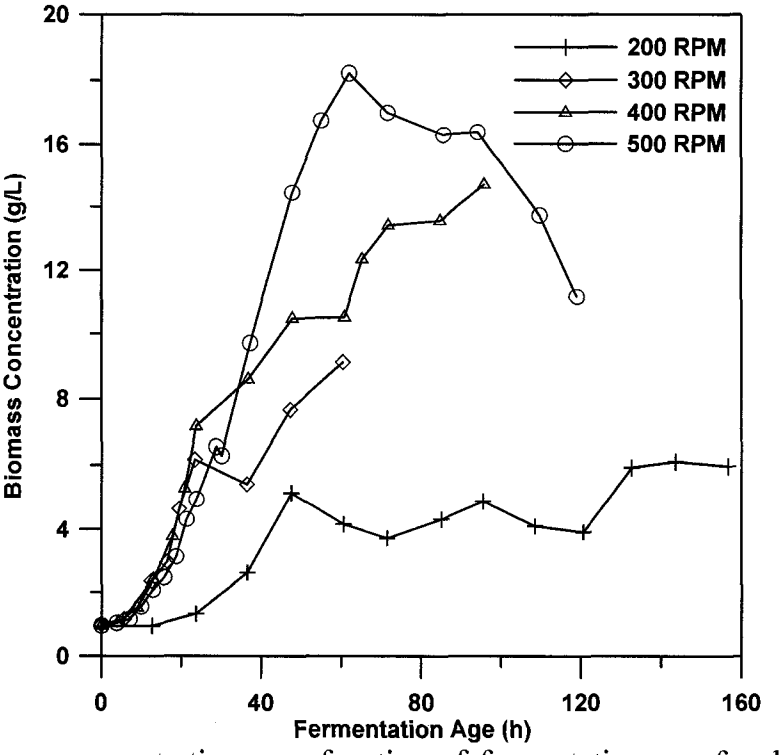

Figure 3.4 Biomass concentration as a function of fermentation age for different stirred tank bioreactor speeds: 200, 300, 400 and 500 RPM.

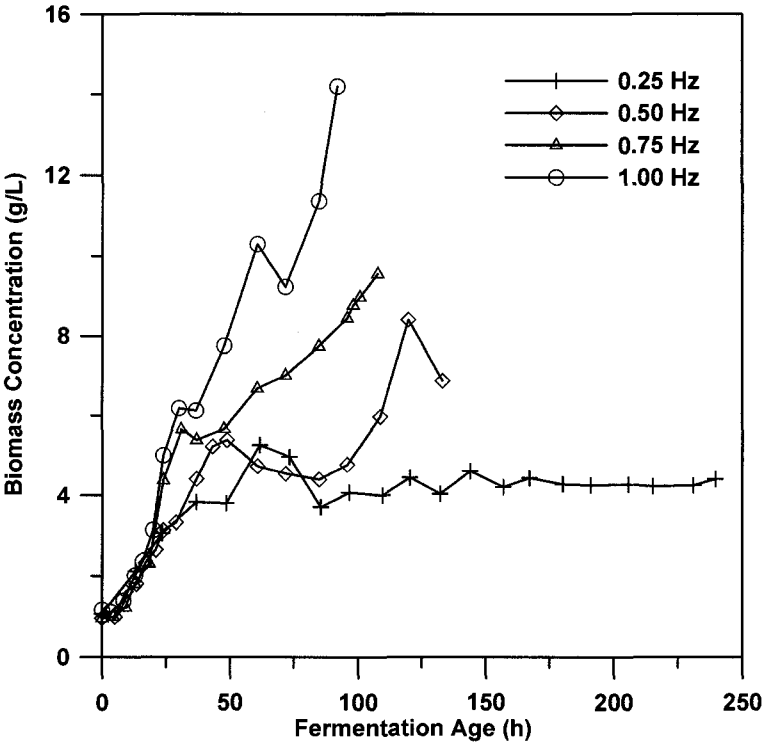

Figure 3.5 Biomass concentration as a function of fermentation age for different reciprocating plate bioreactor frequencies: 0.25, 0.50, 0.75 and 1.00 Hz.

3.4.3 Trends in the consistency index for all runs

For all samples taken throughout all experiments, a complete rheological analysis has been performed. Figures 3.6 and 3.7 show the trends of the Herschel-Bulkley consistency index parameter K at different agitation rates for the STB and the RPB, respectively. Akin to the biomass results, the consistency index is visibly dependent on the agitation rate under which the fermentation was conducted. A similar observation was made for *T. reesei* by Marten et al. (1996). This is indicative of a relationship between biomass and rheology. Also, Badino Jr. et al. (1999) related the agitation rate to the consistency index. For both types of agitation systems, the consistency index maximum peaks occur at earlier times as the agitation rate is increased, which is in accordance with

the earlier observation on biomass. In the STB at 500 RPM, there are visibly three peaks, which the second and the third are due to the secondary batch phase discussed earlier.

The values of the Herschel-Bulkley consistency index for both agitation systems reached a maximum with an approximate value of 0.3 $Pa.s^n$. The Casson viscosities observed in Marten et al. (1996) for *T. reesei* peaked at 0.14 $Pa.s^{1/2}$ at biomass concentration of 24 g/L. For other fungi, such as *Streptomyces olindensis* (Pamboukian and Facciotti, 2005), the Power-Law consistency index reached maximum values of 0.7 and 1.8 $Pa.s^n$ for batch and fed-batch, respectively, at biomass concentrations remaining below 8 g/L. In Riley et al. (2000), the Power-Law consistency index for *Penicillium chrysogenum* goes up to 4 $Pa.s^n$ at biomass concentrations around 25 g/L. The observed differences in the reported viscosity for similar biomass concentrations could be the result of differences in morphologies of various fungi. Moreover, the use of different models and instrumentation to obtain the viscosity may also contribute to the differences observed.

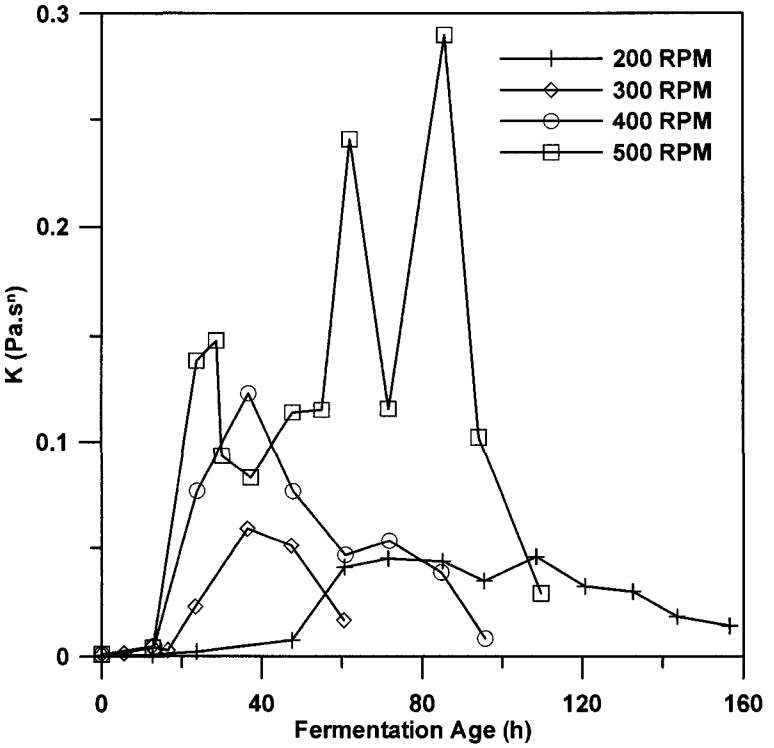

Figure 3.6 The Herschel-Bulkley consistency index as a function of fermentation age for different stirred tank bioreactor fermentations speeds: 200, 300, 400 and 500 RPM.

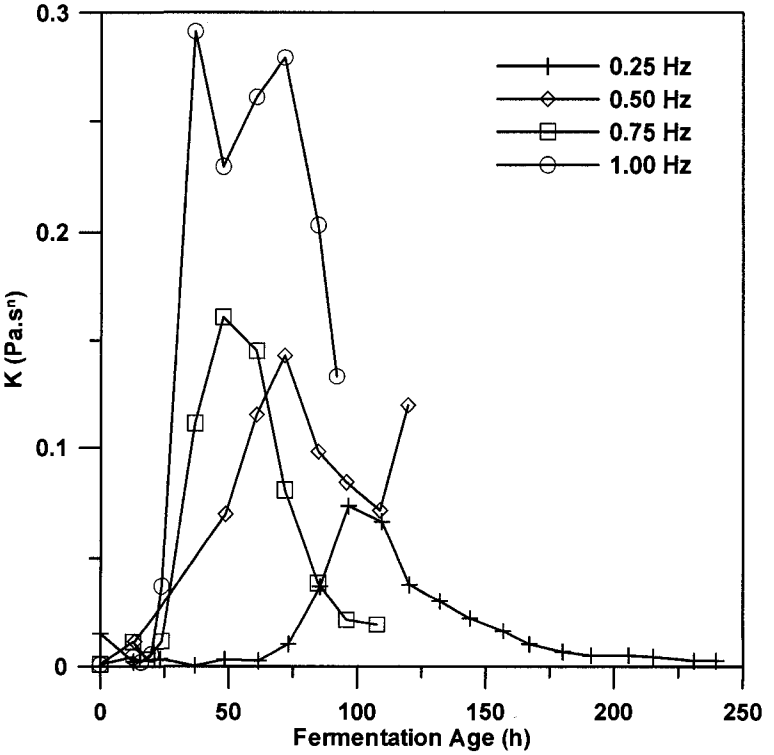

Figure 3.7 The Herschel-Bulkley consistency index profiles as a function of fermentation age for different reciprocating plate bioreactor frequencies: 0.25, 0.50, 0.75 and 1.00 Hz.

3.4.4 Trends of *X, K, n* and Yield Stress for one run

Figure 3.8 shows the three parameters of the Herschel-Bulkley model (K, n and τ_y) as a function of fermentation age performed in the STB at 400 RPM. The trends in this fermentation run are representative of the trends seen in all the other fermentations that were performed in both bioreactors. The variations of the rheological parameters are typical of filamentous fungi. At the beginning of the fermentation run where the broth mainly consists of the original fermentation medium solution with properties close to that of water, the broth has Newtonian properties with n values close to 1. As the fermentation progresses and the biomass concentration increases, the fermentation broth becomes non-Newtonian with shear-thinning ($n < 1$) and yield stress properties. Both the yield stress and the consistency index increase and reach a maximum at the end of the batch phase and during the initial 24 h of the fed-batch phase, respectively. Although biomass continues to increase, both the yield stress and the consistency index decrease beyond the observed maximum. Similar results were also reported in the literature for *T. reesei*, as well for other fungi (Marten et al., 1996; Riley et al., 2000; Gupta et al., 2007; Pamboukian and Facciotti, 2005; Pamboukian and Facciotti., 1998; Queiroz et al., 1997; Li et al., 1995). These parameters are thus dependent on other properties of filamentous fungi such as morphology. Effectively, near the end of the fermentation run, the filamentous fungi partly change to spores. The spores have a spherical morphology and display lower viscous flow properties than the filamentous aggregates thus causing a drop in the consistency index and the yield stress. In addition, the drop could be due to a structural change in the cells, which makes them less resistant to shear. This structural change can be the result of a deficiency in some nutrient essential to a component in its structure. Müller et al. (2003) modified

genetically the ability of the fungi *Aspergillus oryzae* of building a structural component resulting in the decrease of the broth viscosity. As well, yield stress and consistency index reach a maximum at different times, indicative that these parameters are partly independent. The yield stress is possibly dependent on the availability of carbon, while the consistency index on nutrients that are exhausted during the fed-batch. In an experimental run performed at 400 RPM (not shown here), nutrients were added when the growth rate decreased. The Herschel-Bulkley consistency index was observed to increase with biomass even after the batch phase, while the yield stress peaked at the end of the batch phase and dropped drastically thereafter.

Moreover, it is important to note that the Herschel-Bulkley consistency index follows the biomass concentration and increase during the batch phase and the initial portion of the fed-batch phase. This is indicative that the biomass concentration is initially the main contributor to the Herschel-Bulkley consistency index. As the biomass concentration increases, the particle to particle interaction increases, which cause the Herschel-Bulkley consistency index to increase. Following the maximum observed in the Herschel-Bulkley consistency index, the consistency index decreases even though the biomass concentration continues to increase. Figure 3.9 shows the value of K as a function of the biomass concentration. It is clear that there are different values of K for a same biomass concentration. This is an indication that, in addition to biomass, other factors affect the broth consistency index. It is believed that morphology plays a major role.

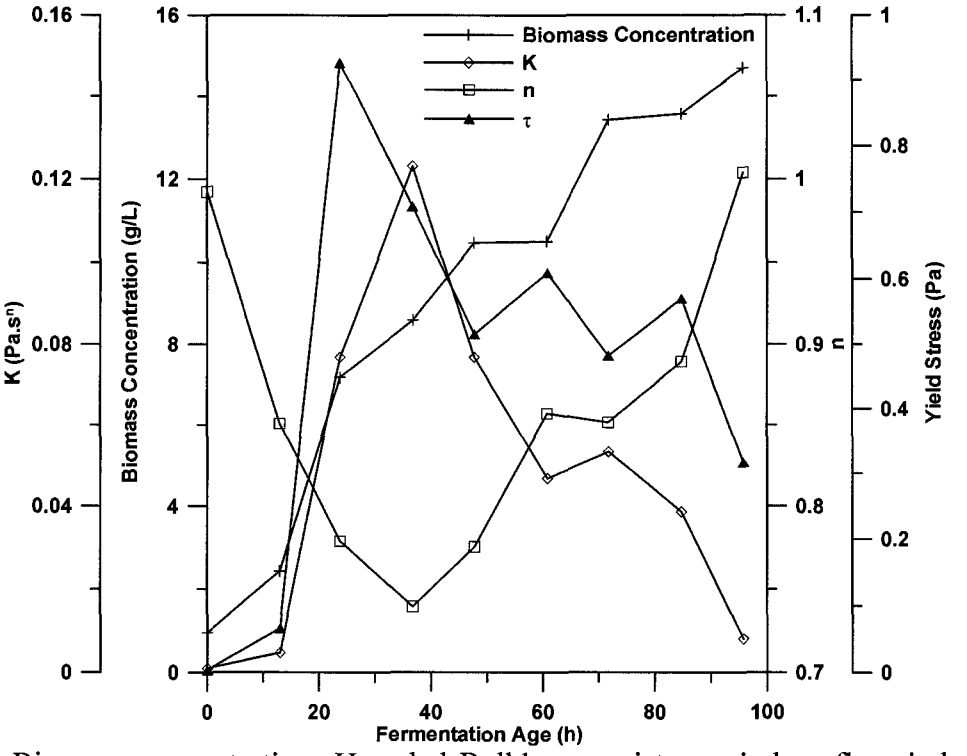

Figure 3.8 Biomass concentration, Herschel-Bulkley consistency index, flow index and yield stress profiles versus fermentation age in the stirred tank bioreactor at 400 RPM.

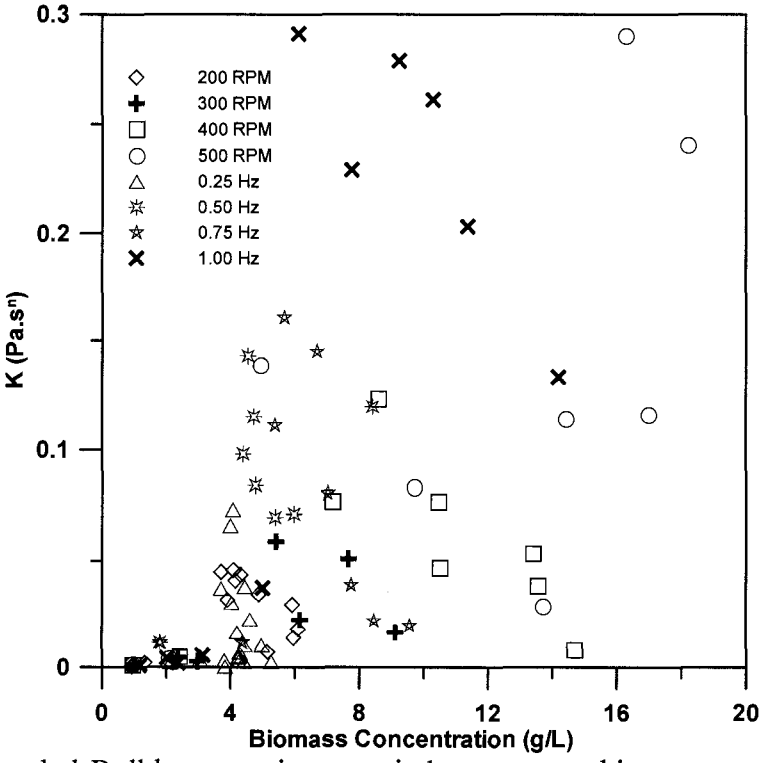

Figure 3.9 Herschel-Bulkley consistency index versus biomass concentration for fermentations runs performed in STB (200, 300, 400 and 500 RPM) and RPB (0.25, 0.50, 0.75 and 1.00 Hz).

The results of Figure 3.9 also show that both K and X are related to agitation. Indeed, both K and X increase as the agitation increases. For lower agitation rates (200 RPM and 0.25 Hz), the consistency index and the biomass concentration are clustered in the range of 0-0.1 Pa.s^n and 0-6 g/L. For intermediate agitation rates (300 RPM, 0.5 Hz and 0.75 Hz), the ranges increase to 0-0.2 Pa.s^n and 0-10 g/L. The ranges expand even further for higher agitation rates (400 RPM, 500 RPM and 1.00 Hz) to 0-0.3 Pa.s^n and 0-20 g/L. In addition, since different consistency indices have the same biomass concentration, it is obvious that correlations for predicting K solely based on X would be limited (Riley et al., 2000; Pamboukian and Facciotti, 2005; Gupta et al., 2007). In addition, Figure 3.9 shows that the data of the RPB is somewhat separate from the STB data. At high RPB agitation, lower biomass concentrations give higher consistency index. This confirms again that the consistency index is also dependent on morphology for *T. reesei*. The morphology is in turn influenced by the agitation mechanism and agitation rate (Badino Jr. et al., 1999). Previous works have shown that the consistency index/biomass relation is strongly influenced by the specific growth rate, DO tension, and mixing time (Olsvik and Kristiansen, 1994). It can be noted that, for all the fermentations included in this investigation, all three parameters varied.

3.4.5 Correlation of *K*, morphology and *X* parameters

In previous investigations, the relationship between rheology, morphology and biomass concentration was studied for different fungi (Riley et al., 2000; Pamboukian and Facciotti, 2005). The Power-Law consistency index K_{PL} was mainly correlated to some morphological parameters (MP) and the biomass concentration (X). In the present work, the Herschel-Bulkley consistency index was used in the general equation:

$$K = X^{\alpha} \times f(MP) \qquad 3.6$$

where α is the biomass concentration exponent and $f(MP)$ is a function of a morphological parameter. Tucker (1994) found that the exponent α was generally constant throughout a fermentation run. Similar results were found by Riley et al. (2000) and Gupta et al. (2007).

3.4.5.1 Influence of Biomass on rheology parameter

The influence of biomass concentration on the consistency index was studied when identical morphology prevailed such that the term $f(MP)$ in Equation 3.6 remains constant. This was done by extracting a large volume of the fermentation broth at a specific fermentation time which was then used to create broth samples, via centrifugation and dilution, having a wide range of biomass concentration. Different methods were suggested in the literature to reconstitute biomass (Mohseni and Allen, 1995). In this investigation, the biomass was concentrated by centrifugation to give a biomass cake and a supernatant phase. The cake was diluted to specific biomass concentrations using the supernatant. Image analysis of the original sample and samples generated by reconstitution was performed to confirm that the experimental procedure did not alter the morphology and that it remained constant from sample to sample.

Figure 3.10 shows an example of the consistency index K as a function of the reconstituted biomass concentration ranging from 0 to 20 g/L. Figure 3.10 is representative of the remaining tests performed for samples obtained from different fermentation runs and fermentation times shown in Table 3.6. The relationship between the consistency index and the biomass concentration corresponds to power-law behaviour. Thus, this confirms that the

form of the biomass concentration to the power α in Equation 3.6, defined in previous work (Riley et al., 2000), is also applicable for *T. reesei*.

The evaluation of α was done for three fermentation runs, two in STB and one in RPB, and the results are shown in Table 3.6. For one of the STB runs, the samples were taken at different fermentation ages, two in the batch phase and three during fed-batch, to examine the influence of the fermentation age on exponent α. The average value of α for the biomass concentration experiments was 2.9 with a standard deviation of 0.4 (14%). Effectively, there are two levels of calculations on the raw data to obtain α. First, the raw data is measured by the rheometer. The HB model is then fitted to the raw data to find the HB consistency index K. Second, α is obtained by fitting K-X data to Equation 3.6, where the function of the morphology parameter is constant.

Replicate rheological tests performed on three samples gave a standard deviation of 1.4% for the estimation of K. In addition, from analysis done on the method for biomass concentration measurement used in our laboratory, biomass concentrations 1 g/L or less, 1 to 6 g/L, 6 to 15 g/L, 15 g/L and above, gave approximate errors of 10%, 7%, 5%, 3%, respectively. To examine the impact that the precision on K and X has on the precision in the determination of α, a Monte Carlo simulation of 100 tests was performed whereby K and X were corrupted by conservative random Gaussian errors of ±2% and ±15%, respectively and α was evaluated for each test. The resulting standard deviation on α was approximately 27%, whereas the one determined experimentally was 14%. It is clear from these tests that the measurement of rheological parameters is moderately sensitive to error. Nevertheless, it is important to measure as accurately as possible rheological parameters and the biomass concentration.

Exponent α lies at the higher end of the range of 0.3 to 3.3 found in studies where biomass concentrations of the fermentation run were correlated directly to the consistency index K (Tucker, 1994; Riley et al., 2000; Gupta et al., 2007; Badino Jr. et al., 1999; Li et al., 1995; Queiroz et al., 1997). Exponent α is higher than the value of 2.0 obtained in similar studies on the influence of biomass under similar morphology by Riley et al. (2000) and Gupta et al. (2007). However, the average percentage deviation of α, approximately 14%, obtained in this study was the same as the one obtained by Riley et al. (2000). Although it was suggested that the influence of biomass is constant, the high standard deviation can be due to the different conditions at which the exponent was evaluated. In this investigation, it varied from 2.5 to 3.4. Another source of error was the generation of the range of biomass concentrations. Measurements were taken to examine the rheology for the range of biomass concentrations as quickly as possible after the sample was taken from the bioreactor. In order to achieve this objective, the biomass cake obtained by centrifugation was estimated to have approximately 5% dry solid and 95% water. This approximation was determined from preliminary laboratory testing and used to dilute the biomass cake to achieve a targeted biomass concentration range from 0 to 20 g/L which is representative of biomass concentrations obtained in the fermentation runs of this investigation. The actual dry weight of reconstructed biomass samples was determined afterwards. Samples taken during the batch phase had less biomass to recreate the above concentration range. As a result, for those samples, the biomass concentration range was decreased due to the limited sample volume. The volume of sample withdrawn was limited in order to minimize alteration of fermentation conditions, which was particularly important for samples collected during the batch phase. Another source of variability on α,

as suggested in the literature, is the potential biomass degradation that can alter filamentous aggregate interactions and hyphal rigidity (Olsvik and Kristiansen, 1994; Riley et al., 2000; Gupta et al., 2007).

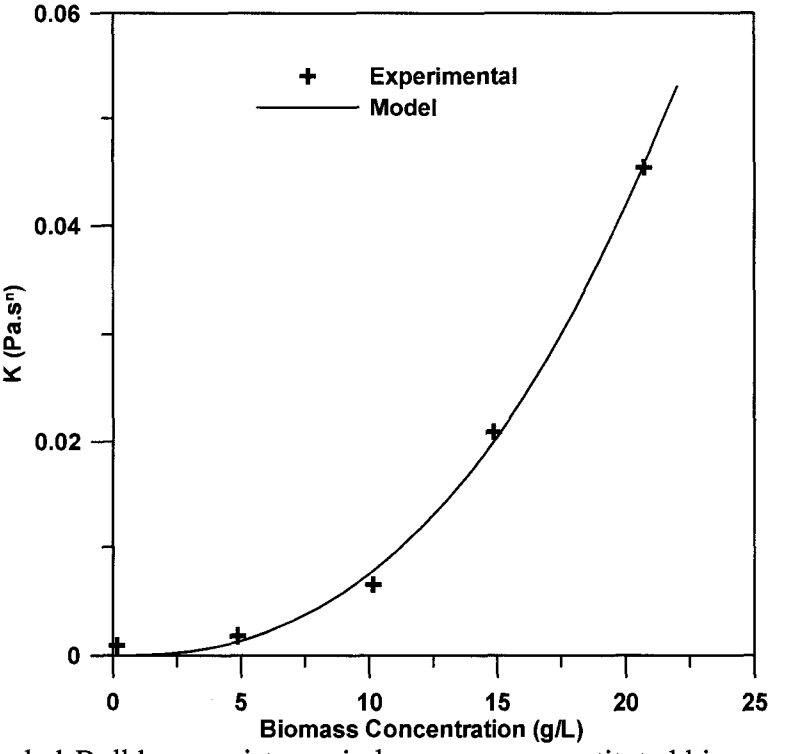

Figure 3.10 Herschel-Bulkley consistency index versus reconstituted biomass concentration from a sample obtained in STB run at 500 RPM and at 63.7 h.

Table 3.6 Values of exponent α obtained from biomass concentration reconstitution tests. Two runs were done in STB at two agitations rates and one in RPB. Samples were taken at different fermentation times for the run at 400 RPM in STB.

Reactor	Agitation Rate	Fermentation Time (h)	α
STB	500 RPM	63.73	2.486
RPB	0.75 Hz	84.47	3.021
STB	400 RPM	15.19	2.558
STB	400 RPM	19.48	3.000
STB	400 RPM	47.74	3.400
STB	400 RPM	60.69	2.485
STB	400 RPM	65.46	3.416
		Average	2.909
		Standard Deviation	0.408

Figure 3.11 shows the plot of K/X^{α} as a function of fermentation age. In the literature, the ratio K/X^{α} is called the "morphological factor" or "morphological index" (Roels et al., 1974; Metz et al., 1979; Olsvik and Kristiansen, 1992). The morphological factor was found to decline as the fermentation progressed. When the data were analyzed as a function of the agitation rate, the decline showed a dependence on agitation. For agitation rates of 300 RPM, 400 RPM, 500 RPM and 1.00 Hz, the plot shows a steep decline at the beginning of the fermentation. This initial rapidly declining phase is followed by a moderately constant or slowly declining morphological factor. The trends are similar to those observed in previous works (Riley et al., 2000; Mishra et al., 2005; Gupta et al., 2007). However, for the other three agitation rates in RPB (0.25, 0.50 and 0.75 Hz) and the lowest agitation in STB (200 RPM), a slower decline throughout the fermentation run was observed. For RPB, the morphological factor shows a dependence on the agitation rate. The STB run at 200 RPM is the only run noticeably different from the other STB agitations. This suggests that the morphological factor does not only depend on the agitation rate, but also, seems to be influenced by the type of mixing mechanism. Additionally, this plot shows that the morphological factor is not constant and changes throughout the fermentation run. This explains why relationships based purely on biomass concentration correlate poorly with the consistency index. Thus, it is crucial to develop a correlation between a morphological parameter and K/X^{α}.

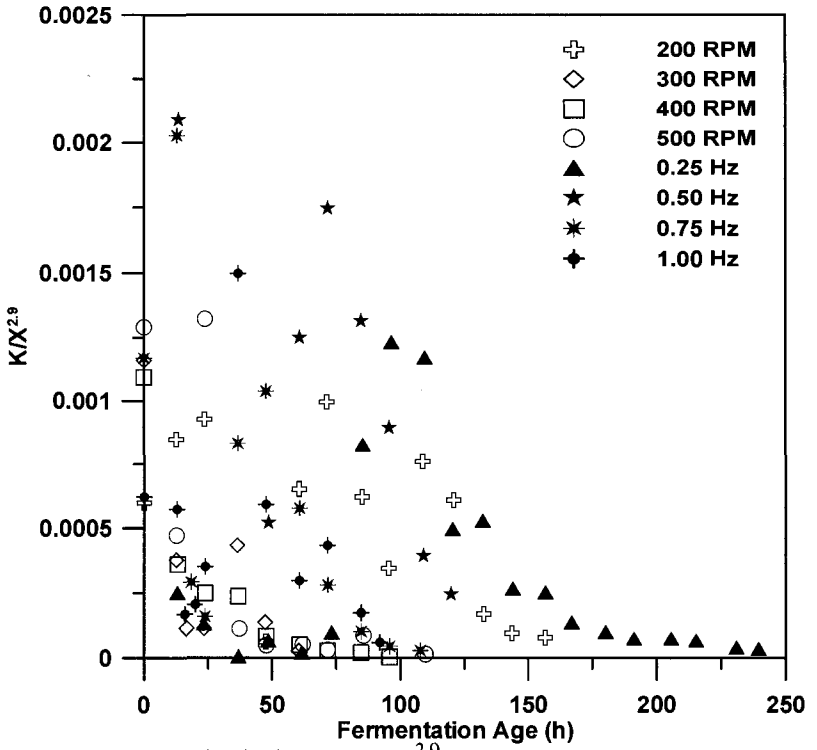

Figure 3.11 The morphological factor $K/X^{2.9}$ as a function of fermentation age for fermentations performed in STB (200, 300, 400 and 500 RPM) and RPB (0.25, 0.50, 0.75 and 1.00 Hz).

3.4.5.2 Selection of the morphological parameter

The morphological classes are found to vary throughout the fermentation runs. Figure 3.12 presents the percentages of unbranched, branched, entangled and clumped morphological states, based on the projected area, during the fermentation run at 400 RPM in STB. Similar profiles were obtained in other runs at different agitation speeds in STB and RPB. Unlike previous work involving other fungi where the clump percentage remained around 80-90% during the fermentation runs, the clump percentage drops drastically until clumps completely disappear from the fermentation broth while the freely dispersed forms increases (Olsvik et al., 1993; Pamboukian and Facciotti, 2005). This observation is similar to fed-batch fermentation of *Penicillium chrysogenum* performed by

Riley et al. (2000). Accordingly, morphological parameters for correlation analysis are averaged on all morphological classes, as characterized by Equation 3.2.

The morphological parameters required for the correlation of rheology and morphology corresponds to dimensional properties of the morphological classes of the fungi. In total, 14, 27, 26 and 26 parameters were used in this investigation to characterize the unbranched, branched, entangled and clumped morphological forms, respectively. These parameters were measured according to a standardized protocol as described previously by Lecault et al. (2007). In order to average the effect of the classes on the morphological parameters as represented by Equation 3.2, the parameters common to all morphological forms were selected. Twelve parameters were found common to all morphological forms. A cross-correlation analysis of these twelve parameters showed that seven are strongly correlated to the following five parameters: Area, Convex Perimeter, Roundness, Dendritic Length and Viable Area. These five parameters were therefore retained to try to establish a correlation to the morphology factor K/X^{α}. The roundness (R) was found to have the highest correlation to the morphological factor. This finding agrees with previous works done on filamentous fungi (Olsvik et al., 1993; Tucker and Thomas, 1993). However, the roundness in those studies was only measured for clumps with the exception of Riley et al. (2000). In their work, the roundness (termed roughness) was measured on all morphological classes but was not found to have the highest correlation with the morphological factor. In their case, the maximum dimension and the mean area were the factors with the highest correlation.

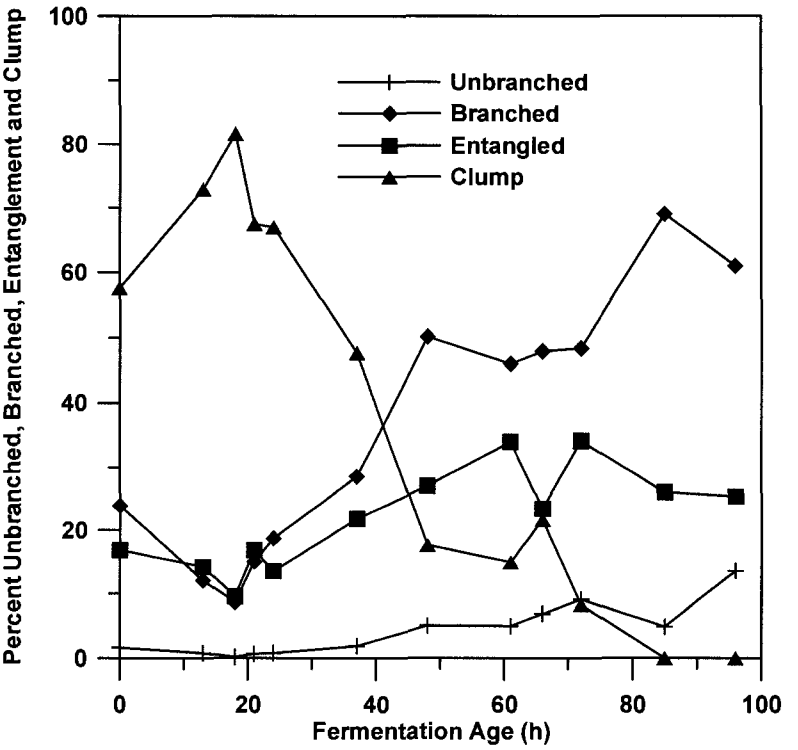

Figure 3.12 Percentages of the four morphological classes of *T. reesei* (Unbranched, Branched, Entangled and Clumped) versus fermentation age for the experiment in STB performed at 400 RPM.

3.4.5.3 Relationship of K/X^{α} and R

Figure 3.13 shows the mean roundness (R) as a function of fermentation age. The profiles of the curves in STB at 300, 400 and 500 RPM, and in RPB at 0.75 and 1.00 Hz show an initial steep decline in the first hours of the fermentation followed by a slower decline during the rest of the fermentation. The profiles at lower agitations exhibit a slower decline during the fermentation runs. The trends observed are similar to the trends for the K/X^{α} plot suggesting that a good correlation may exist between these two variables. Table 3.7 shows the parameters of two possible correlations between K/X^{α} and R. Equation 3.7 is a linear relationship that was suggested previously in the literature (Olsvik et al., 1993; Riley et al., 2000), while Equation 3.8 is a power law relation that was used by Tucker and Thomas (1993).

$$\frac{K}{X^{\alpha}} = b \times R + a \qquad 3.7$$

$$\frac{K}{X^{\alpha}} = a \times (R)^{b} \qquad 3.8$$

where a and b are two model parameters. The linear regression based on all STB and RPB data have very low r^2 values despite R had the highest correlation between K/X^{α} and all morphological parameters. This value is statistically too low to be considered as a significant relationship and a more refined analysis is required. However, Figure 3.14 shows that when batch and fed-batch data points are distinguished on a K/X^{α}-R plot, data clusters can be clearly observed. For the batch phase, the roundness ranges from 12.5 - 37.5, while the range is 12.5 - 22.5 for the fed-batch phase. This suggests that the change in culture conditions between the batch phase and the fed-batch phase is reflected in morphological changes that are well characterized by the clusters in the data.

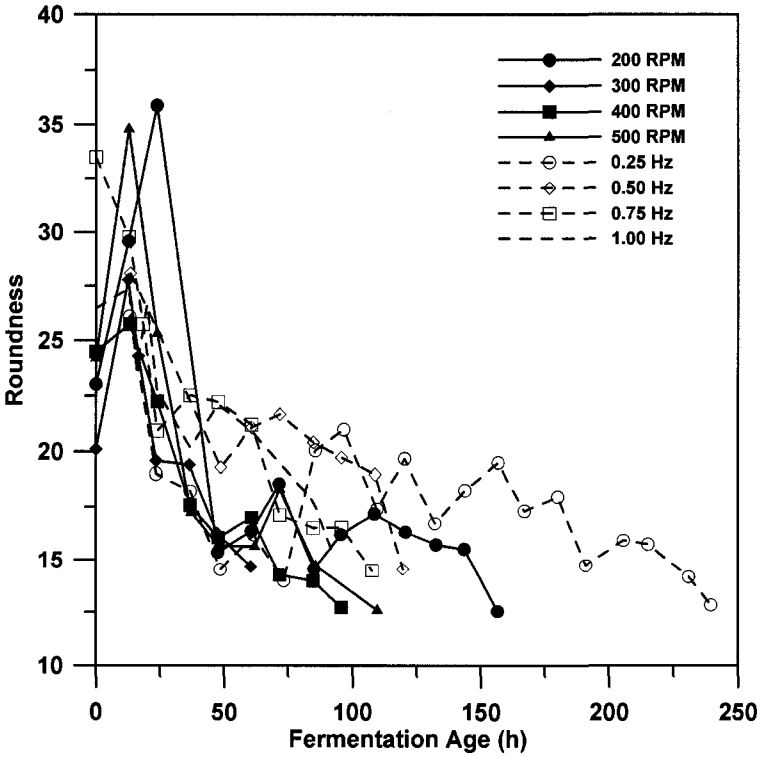

Figure 3.13 Mean roundness versus fermentation age for fermentations performed in STB (200, 300, 400 and 500 RPM) and RPB (0.25, 0.50, 0.75 and 1.00 Hz).

Table 3.7 Model parameters of the corresponding equations and the associated r^2 values for different combinations of experimental data.

Experimental Data	Model	*a*	*b*	r^2
All Runs	Eq. 3.7	-5.70×10^{-4}	5.24×10^{-5}	0.294
STB (200, 300, 400, 500 RPM)	Eq. 3.7	-3.44×10^{-4}	3.79×10^{-5}	0.300
RPB (0.25, 0.50, 0.75, 1.00 Hz)	Eq. 3.7	-8.70×10^{-4}	6.96×10^{-5}	0.325
Batch	Eq. 3.7	-7.38×10^{-4}	5.33×10^{-5}	0.292
Batch without first points	Eq. 3.7	-5.07×10^{-4}	3.49×10^{-5}	0.628
Fed-batch	Eq. 3.7	-15.6×10^{-4}	11.4×10^{-5}	0.489
Fed-batch	Eq. 3.8	5.08×10^{-13}	6.96	0.594
Fed-batch without 200 RPM run	Eq. 3.8	1.16×10^{-14}	8.22	0.827

The batch phase is plotted separately in Figure 3.15, which gives an r^2 of 0.292 when a linear regression is considered. Points corresponding to the first sample at time zero of fermentation runs at the different agitations tested have been plotted with an encircled symbol. At this point, the amount of biomass and insoluble substrate (CSL) is approximately 1 g/L for all runs. This concentration results in a very low phase volume at constant density, which undoubtedly produces very low particle-to-particle interaction. At such low interaction, the shape of the fungi, thus the roundness, has a very low influence on the rheological properties of the fluids. In fact, the rheology of those samples exhibited similar properties as water. In addition, at this sampling time the measurement of morphological characteristics were prone to higher error due to the presence of corn steep solids. More importantly, the sample morphology was dictated by the shake flask shear conditions used to inoculate the culture rather than conditions prevailing within the bioreactor. In addition, the low concentration of fungi contributes to a larger error in the results. Thus, it is justifiable to eliminate these points from the regression of the rest of the batch data, thus giving an r^2 value of 0.628 (Table 3.7). In this case, the slope is 3.49×10^{-5} with an intercept close to zero (-5.07×10^{-4}).

Similarly, Figure 3.16 shows the plot of K/X^{α} versus R for the fed-batch data separately. A linear regression on the data gives an r^2 value of 0.489 (Table 3.7). However, through visual examination of the data, the power-law model is suggested to characterize the relationship between K/X^{α} and R for the fed-batch phase, and r^2 increases to 0.594. Further examination of the data reveals that the encircled data points in Figure 3.16 correspond to the STB at 200 RPM run. As observed above, data at 200 RPM follows a separate trend than all the other runs. Results of Figure 3.16 further confirm this effect, thus suggesting the separation of the data from the rest of the runs. The power-law model fit on the data without the STB at 200 RPM increases the r^2 to 0.827. The power-law exponent is 8.22 indicating a very strong influence of the roundness during the fed-batch phase as opposed to the batch phase. In the case of Olsvik et al. (1993), they used a linear relationship for a continuous culture of *Aspergillus niger*, where clump morphology predominated throughout fermentation. However, Tucker and Thomas (1993) used a power-law model where the exponent on the roundness was 0.7 for *Penicillium chrysogenum* batch fermentation. The differences might be due to both the strains and the culture conditions which influence the fungi morphology differently, resulting in the difference in roundness relationship with K/X^{α}.

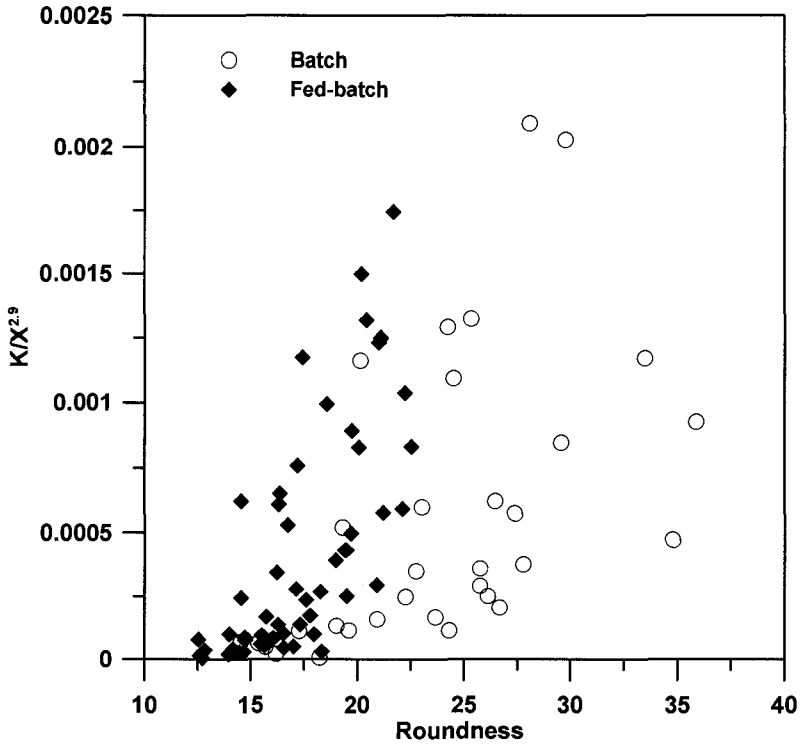

Figure 3.14 Morphological factor K/X^{α} versus mean roundness for fermentations in STB (200, 300, 400 and 500 RPM) and RPB (0.25, 0.50, 0.75 and 1.00 Hz).

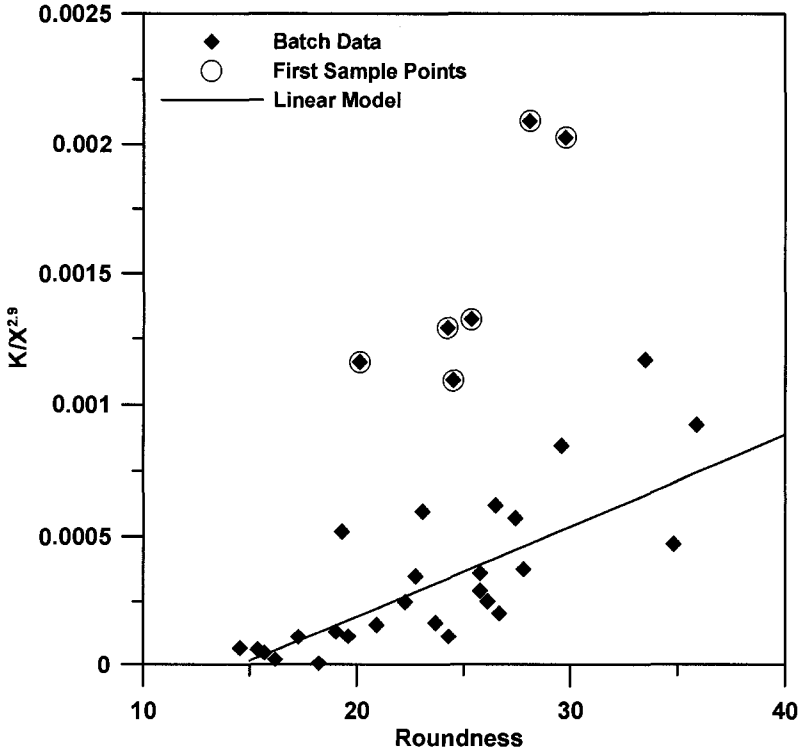

Figure 3.15 Morphological factor K/X^{α} versus mean roundness for fermentations in batch phase performed in STB (200, 300, 400 and 500 RPM) and RPB (0.25, 0.50, 0.75 and 1.00 Hz). The encircled data points correspond to samples taken at time 0 h. The first samples from runs at 0.25 and 0.50 are not presented.

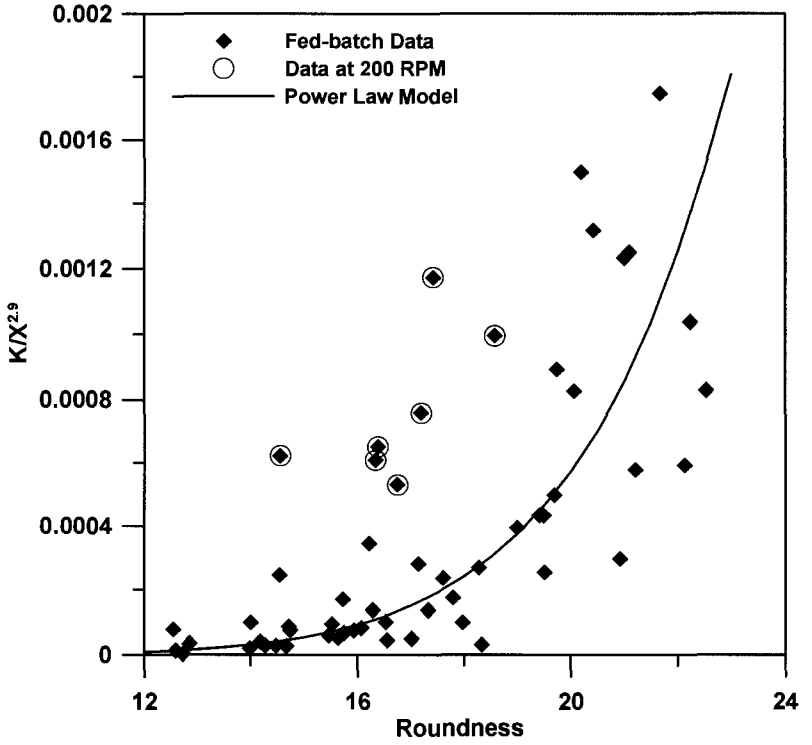

Figure 3.16 Morphological factor K/X^{α} versus mean roundness for T. reesei fermentations fed-batch phase data in STB (200, 300, 400 and 500 RPM) and RPB (0.25, 0.50, 0.75 and 1.00 Hz). The encircled data points correspond to samples from fermentation in STB at 200 RPM.

3.4.5.4 Comparison of experimental and predicted *K*

Figures 3.17 and 3.18 show the parity plots of the predicted K with the values of K determined from rheological analysis for the batch and fed-batch phases, respectively. It can be observed that in the batch phase, data scatter is heterogeneous and clustered at the lower right end of the plot. Examination of the scattered points at the higher and left end of the plot reveals that they correspond to the last points from the batch phase from runs at 300 RPM, 400 RPM, 500 RPM, 0.5 Hz, 0.75 Hz and 1 Hz. The heterogeneous scatter of the data can be due to the fast changing conditions occurring in the batch phase of the fermentation runs. Thus, the linear model to predict K in the batch phase should be used with caution. In the case of the fed-batch phase, the data is more homogenously scattered

and is moderately centralized on the diagonal of the plot. Thus, the power-law model in the fed-batch phase is better able to predict these data. This confirms previous result where a reasonably high regression coefficient between K/X^{α} and R was obtained for the fed-batch. The limitations of the predicted consistency index for the batch phase ranges from agitations at 200-500 RPM in STB and 0.25-1.00 Hz in RPB while excluding samples at time zero. In the case of the fed-batch phase, the prediction limitation ranges from 300-500 RPM in STB and 0.25-1.00 Hz in RPB.

In a previous study done on *Streptomyces olindensis* by Pamboukian and Facciotti (2005), the experimental power-law consistency index was successfully predicted for both batch and fed-batch runs. The morphological parameter related to the morphological factor was the average clump dimension. A biomass exponent α was not used and the data was directly related to the biomass concentration runs. The correlation of the consistency index, the biomass concentration and the average clump dimension had an r^2 of 0.94 for which the parity plot of the predicted vs. the experimental K gave an r^2 of 0.78. Although this value is close to our predictions, the model has a smaller range of applicability since only one agitation rate and one agitation mechanism was evaluated.

In Riley et al. (2000), data from both batch and fed-batch fermentations of *Penicillium chrysogenum* at variable agitation rates in two bioreactors were used to develop correlations. A biomass exponent of 2.0 and a standard deviation 0.3 were calculated and used to obtain the morphological factor. Although, the exponent value was different than the one calculated in this work, the percent standard deviation values are close. The morphological factor was related to the maximum dimension and the mean area with r^2 values of 0.73 and 0.50, respectively. In their case, the ability of K to predict the

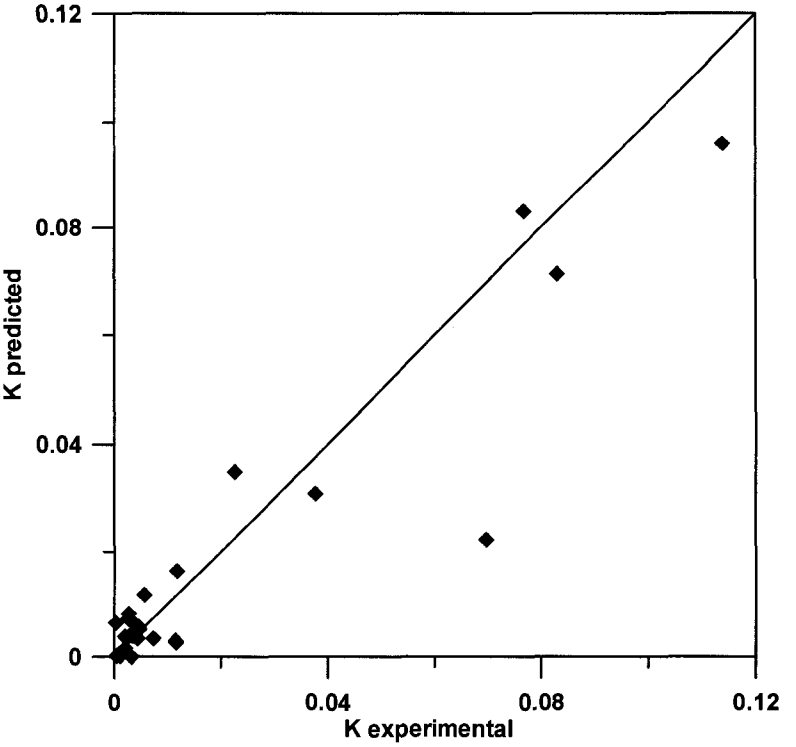

Figure 3.17 Parity plot of the Herschel-Bulkley consistency index K prediction vs K experimental for *T. reesei* fermentations in the batch phase in STB (200, 300, 400 and 500 RPM) and RPB (0.25, 0.50, 0.75 and 1.00 Hz).

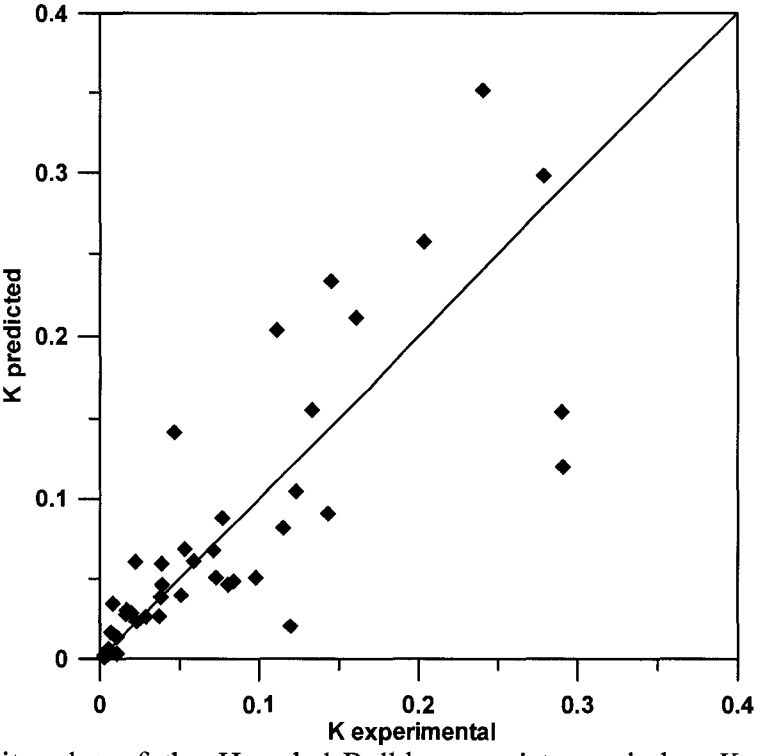

Figure 3.18 Parity plot of the Herschel-Bulkley consistency index K prediction vs K experimental of *T. reesei* fermentations in the fed-batch phase in STB (300, 400 and 500 RPM) and RPB (0.25, 0.50, 0.75 and 1.00 Hz).

experimental results was not adequate, whereas showed a good prediction in this work. Possibly, this is due to the use of a different organism and, here, data was separated between batch and fed-batch.

3.5 Conclusion

The fermentation broth of *T. reesei* was cultured under different agitation rates in a stirred tank bioreactor and in a reciprocating plate bioreactor. The rheological behaviour was characterized by using the Herschel-Bulkley rheology model. The consistency index, the flow index and the yield stress were shown to vary during the course of the fermentation runs.

Both the biomass concentration and the Herschel-Bulkley consistency index were shown to be dependent on the agitation rate. When the agitation rate increased, both the biomass concentration and the consistency index increased. The influence of biomass concentration and morphology on rheology was studied independently. The effect of biomass concentration was measured independently of morphology by reconstituting biomass from selected fermentations into samples of different concentrations. As done in previous work, the relationship between the biomass concentration and the consistency index was shown to be a power-law function with a biomass exponent α relatively constant. An average biomass exponent of 2.9 and a standard deviation of 0.41 were determined. The use of the average exponent for all the fermentation runs enabled the independent examination of the influence of the morphology. The plot of the morphological factor K/X^{α} was shown to vary during the course of the fermentation runs. This shows that the use of correlations to predict the consistency index based exclusively on biomass concentration would have inconsistence results.

Similar to the work of Riley et al. (2000), close examination of the morphological classes showed that the clump and the dispersed morphologies varied during the course of the fermentation runs. Therefore, the morphological parameters were based on all the morphological classes. Several parameters were found to correlate with K/X^{α} and the roundness was found to have the strongest correlation. Plotting K/X^{α} against roundness showed that the batch and fed-batch phases were clustered, leading to the development of two separate correlations for each phase. The relationship for the batch phase was based on a linear relationship, while the one for the fed-batch was a power-law. Restriction of the applicability of the models produced better results. The model during the batch phase was applicable to all agitations in both reactors without the initial sample. However, the fed-batch model was not applicable to agitation in STB at 200 rpm. Analysis of the parity plots of the predicted and the experimental K showed good fit for the models. Considering the difficulties in measuring mycelial broth rheology, and that an empirical model (i.e., power-law) has been fitted to highly scattered experimental data, the quality of predictions using Equations 3.7 and 3.8 is good and we recommended them for estimating the rheological properties of *Trichoderma reesei* fermentation broths. These data are useful for design purposes and production control.

3.6 Nomenclature

a	Constant
b	Constant/ Percentage of branched
B	Branched morphology class
c	Percentage of clump
C	Clump morphology class
e	Percentage of entangled
E	Entangled morphology class
$f(MP)$	Function of a morphological parameter
HB	Herschel-Bulkley
K_C	Casson consistency index ($Pa.s^{0.5}$)
K_{HB}	HB consistency index ($Pa.s^n$)
K_{PL}	Power-Law consistency index ($Pa.s^n$)
MP	Morphological parameter
$MP(B)$	Branched morphological parameter
$MP(C)$	Clump morphological parameter
$MP(E)$	Entangled morphological parameter
$MP(U)$	Unbranched morphological parameter
n	Flow index (-)
R	Roundness
u	Percentage of unbranched
U	Unbranched morphology class
X	Biomass concentration (g/L)

Greek letters

α	Biomass concentration exponent (-)
τ	Shear stress (Pa)
τ_{y_C}	Casson yield stress ($Pa^{0.5}$)
$\tau_{y_{HB}}$	Herschel-Bulkley yield stress (Pa)
$\dot{\gamma}$	Shear rate (s^{-1})

Subscripts

C	Casson
HB	Herschel-Bulkley
PL	Power Law
y	Yield Stress

Symbols

$\cdot$	Rate
$f(\ )$	Function

3.7 References

Aden, A., Ruth, M., Ibsen, K., Jechura, J., Neeves, K., Sheehan, J., Wallace, B., Montague, L., Slayton, A., and Lukas, J. 2002. Lignocellulosic biomass to ethanol process design and economics utilizing co-current dilute acid prehydrolysis and enzymatic hydrolysis for corn stover. National Renewable Energy Lab., Golden, CO. (US). Report TP-510-32438.

Allen D.G. and Robinson C.W. 1990. Measurement of rheological properties of filamentous fermentation broths. Chemical Engineering Science, 45, pp.37-48.

Badino Jr. A.C., Facciotti M.C.R. and Schmidell W. 1999. Estimation of the rheology of glucoamylase fermentation broth from the biomass concentration and shear conditions. Biotechnology Techniques, 13, pp.723-726.

Badino Jr. A.C., Facciotti M.C.R. and Schmidell W. 2001. Volumetric oxygen transfer coefficients (k_La) in batch cultivation involving non-Newtonian broths. Biochemical Engineering Journal, 8, pp.111-119.

Barnes H.A. and Nguyen Q.D. 2001. Rotating vane rheometry-a review. Journal of Non-Newtonian Fluid Mechanics, 98, pp.1-14.

Benchapattarapong N., Anderson W.A., Bai F. and Moo-Young M. 2005. Rheology and hydrodynamic properties of *Tolypocladium inflatum* fermentation broth and its simulation. Bioprocess and Biosystems Engineering, 27, pp.239-247.

Bhargava S., Nandakumar M.P., Roy A., Wenger K.S. and Marten M.R. 2003. Pulsed feeding during fed-batch fungal fermentation leads to reduced viscosity without detrimentally affecting protein expression. Biotechnology and Bioengineering, 81, pp.341-347.

Brummer R. 2006. Rheology essentials of cosmetic and food emulsions. Verlag Berlin Heidelberg: Springer. 180 p.

Cho Y.J., Hwang H.J., Kim S.W., Song C.H. and Yun J.W. 2002. Effect of carbon source and aeration rate on broth rheology and fungal morphology during red pigment production by *Paecilomyces sinclairii* in a batch bioreactor. Journal of Biotechnology, 95, pp.13-23.

Choy, V. 2008. Influence of agitation on the morphology of *Trichoderma reesei* and its correlation with the protein production. MASc thesis, University of Ottawa, Ottawa, Canada.

Domingues F.C., Queiroz J.A., Cabral J.M.S. and Fonseca L.P. 2000. The influence of culture conditions on mycelial structure and cellulase production by *Trichoderma reesei Rut C-30*. Enzyme and Microbial Technology, 26, pp.394-401.

Gagnon H., Lounes M. and Thibault J. 1998. Power consumption and mass transfer in agitated gas-liquid columns: A comparative study. Canadian Journal of Chemical Engineering, 76, pp.379-389.

Gbewonyo K., Hunt G. and Buckland B. 1992. Interactions of cell morphology and transport processes in the lovastatin fermentation. Bioprocess Engineering, 8, pp.1-7.

Goudar C.T., Strevett K.A. and Shah S.N. 1999. Influence of microbial concentration on the rheology of non-Newtonian fermentation broths. Applied Microbiology and Biotechnology, 51, pp.310-315.

Gupta K., Mishra P.K. and Srivastava P. 2007. A correlative evaluation of morphology and rheology of *Aspergillus terreus* during lovastatin fermentation. Biotechnology and Bioprocess Engineering, 12, pp.140-146.

Hwang H.J., Kim S.W., Xu C.P., Choi J.W. and Yun J.W. 2004. Morphological and rheological properties of the three different species of basidiomycetes *Phellinus in* submerged cultures. Journal of Applied Microbiology, 96, pp.1296-1305.

Lecault V., Patel N. and Thibault J. 2007. Morphological characterization and viability assessment of *Trichoderma reesei* by image analysis. Biotechnology Progress, 23, pp.734-740.

Leong-Poi L. and Allen D.G. 1992. Direct measurement of the yield stress of filamentous fermentation broths with the rotating vane technique. Biotechnology and Bioengineering, 40, pp.403-412.

Li G.Q., Qiu H.W., Zheng Z.M., Cai Z.L. and Yang S.Z. 1995. Effect of fluid rheological properties on mass transfer in a bioreactor. Journal of Chemical Technology and Biotechnology, 62, pp.385-391.

Li Z.J., Shukla V., Fordyce A.P., Pedersen A.G., Wenger K.S. and Marten M.R. 2000. Fungal morphology and fragmentation behavior in a fed-batch *Aspergillus oryzae* fermentation at the production scale. Biotechnology and Bioengineering, 70, pp.300-312.

Lopez J.L.C., Perez J.A.S., Sevilla J.M.F., Porcel E.M.R. and Chisti Y. 2005. Pellet morphology, culture rheology and lovastatin production in cultures of *Aspergillus terreus.* Journal of Biotechnology, 116, pp.61-77.

Macosko C.W. 1994. Rheology: Principles, Measurements, and Applications. New York: Wiley-VCH. 550 p.

Maras M., van Die I., Contreras R. and Van den Hondel C.A.M.J. 1999. Filamentous fungi as production organisms for glycoproteins of bio-medical interest. Glycoconjugate Journal, 16, pp.99-107.

Marten M.R., Velkovska S., Khan S.A. and Ollis D.F. 1996. Rheological, mass transfer, and mixing characterization of cellulase producing *Trichoderma reesei* suspensions. Biotechnology Progress, 12, pp.602-611.

Marten M.R. and Wenger K.S. 1997. Rheology, mixing time, and regime analysis for a production-scale *Aspergillus oryzae* fermentation. Bioreactor and Bioprocess Fluid Dynamics, A.W. Nienow (ed.), BHRGroup, Cranfield, UK.

Martinez-Padilla L.P. and Rivera-Vargas C. 2006. Flow behavior of Mexican sauces using a vane-in-a-large cup rheometer. Journal of Food Engineering, 72, pp.189-196.

Merino S.T. and Cherry J. 2007. Progress and challenges in enzyme development for biomass utilization. Biofuels, 108, pp.95-120.

Metz, B., Kossen, N., and van Suijdam, J. 1979. The rheology of mould suspensions. Advances in Biochemical Engineering/Biotechnology, 11, pp.103-156.

Mishra P., Srivastava P. and Kundu S. 2005. A comparative evaluation of oxygen mass transfer and broth viscosity using Cephalosporin-C production as a case strategy. World Journal of Microbiology & Biotechnology, 21, pp.525-530.

Mohagheghi A., Grohmann K. and Wyman C.E. 1988. Production of cellulase on mixtures of xylose and cellulose. Applied Biochemistry and Biotechnology, 17, pp.263-277.

Mohagheghi A., Grohmann K. and Wyman C.E. 1990. Production of cellulase on mixtures of xylose and cellulose in a fed-batch process. Biotechnology and Bioengineering, 35, pp.211-216.

Mohseni M. and Allen D.G. 1995. The effect of particle morphology and concentration on the directly measured yield stress in filamentous suspensions. Biotechnology and Bioengineering, 48, pp.257-265.

Mohseni M., Kautola H. and Allen D.G. 1997. The viscoelastic nature of filamentous fermentation broths and its influence on the directly measured yield stress. Journal of Fermentation and Bioengineering, 83, pp.281-286.

Moo-Young M., Hirose T. and Geiger K.H. 1969. The rheological effects of substrate-additives on fermentation yields. Biotechnology and Bioengineering, 11, pp.725-730.

Muller C., Hansen K., Szabo P. and Nielsen J. 2003. Effect of deletion of chitin synthase genes on mycelial morphology and culture viscosity in *Aspergillus oryzae*. Biotechnology and Bioengineering, 81, pp.525-534.

Nidetzky B., Steiner W., Hayn M. and Claeyssens M. 1994. Cellulose hydrolysis by the cellulases from *Trichoderma reesei* - A new model for synergistic interaction. Biochemical Journal, 298, pp.705-710.

Novozymes and Cherry, J. R. 2003. Enzyme sugar platform project review : Cellulase Cost Reduction. www.novozymes.com. Consulted November 2007.

Novozymes and Petiot, E. 2007. Novozymes: Advancing Cellulosic Ethanol - Presentation for World Biofuels Markets Brussels. www.novozymes.com. Consulted November 2007.

O'Cleirigh C., Casey J.T., Walsh P.K. and O'Shea D.G. 2005. Morphological engineering of *Streptomyces hygroscopicus var. geldanus*: regulation of pellet morphology through manipulation of broth viscosity. Applied Microbiology and Biotechnology, 68, pp.305-310.

Olsvik E. and Kristiansen B. 1992. Influence of oxygen tension, biomass concentration, and specific growth rate on the rheological properties of a filamentous fermentation broth. Biotechnology and Bioengineering, 40, pp.1293-1299.

Olsvik E. and Kristiansen B. 1994. Rheology of filamentous fermentations. Biotechnology Advances, 12, pp.1-39.

Olsvik E., Tucker K.G., Thomas C.R. and Kristiansen B. 1993. Correlation of *Aspergillus niger* broth rheological properties with biomass concentration and the shape of mycelial aggregates. Biotechnology and Bioengineering, 42, pp.1046-1052.

Oncul S., Tari C. and Unluturk S. 2007. Effect of various process parameters on morphology, rheology, and polygalacturonase production by *Aspergillus sojae* in a batch bioreactor. Biotechnology Progress, 23, pp.836-845.

Pamboukian C.R.D. and Facciotti M.C.R. 1998. Correlation between pellet size and glucoamylase production in submerged cultures of *Aspergillus awamori*. Revista de Microbiologia, 29, pp.23-26.

Pamboukian C.R.D. and Facciotti M.C.R. 2005. Rheological and morphological characterization of *Streptomyces olindensis* growing in batch and fed-batch fermentations. Brazilian Journal of Chemical Engineering, 22, pp.31-40.

Paul G.C. and Thomas C.R. 1996. A structured model for hyphal differentiation and penicillin production using *Penicillium chrysogenum*. Biotechnology and Bioengineering, 51, pp.558-572.

Paul G.C. and Thomas C.R. 1998. Characterisation of mycelial morphology using image analysis. Advances in Biochemical Engineering/Biotechnology, 60, pp.1-59.

Pedersen A.G., Bundgaard-Nielsen M., Nielsen J., Villadsen J. and Hassager O. 1993. Rheological characterization of media containing *Penicillium chrysogenum*. Biotechnology and Bioengineering, 41, pp.162-164.

Philippidis G.P. 1994. Cellulase production technology - evaluation of current status. Enzymatic Conversion of Biomass for Fuels Production, 566, pp.188-217.

Philippidis G.P. and Hatzis C. 1997. Biochemical engineering analysis of critical process factors in the biomass-to-ethanol technology. Biotechnology Progress, 13, pp.222-231.

Queiroz M.C.R., Facciotti M.C.R. and Schmidell W. 1997. Rheological changes of *Aspergillus awamori* broth during amyloglucosidase production. Biotechnology Letters, 19, pp.167-170.

Riley G.L., Tucker K.G., Paul G.C. and Thomas C.R. 2000. Effect of biomass concentration and mycelial morphology on fermentation broth rheology. Biotechnology and Bioengineering, 68, pp.160-172.

Roels J.A., Vandenbe J. and Voncken R.M. 1974. Rheology of mycelial broths. Biotechnology and Bioengineering, 16, pp.181-208.

Schatzmann M., Fischer P. and Bezzola G.R. 2003. Rheological behavior of fine and large particle suspensions. Journal of Hydraulic Engineering-ASCE, 129, pp.796-803.

Schell D.J., Farmer J., Hamilton J., Lyons B., McMillan J.D., Saez J.C. and Tholudar A. 2001. Influence of operating conditions and vessel size on oxygen transfer during cellulase production. Applied Biochemistry and Biotechnology, 91-93, pp.627-642.

Schügerl K., Gerlach S.R. and Siedenberg D. 1998. Influence of the process parameters on the morphology and enzyme production of *Aspergilli*. Advances in Biochemical Engineering/Biotechnology, 60, pp.195-266.

Tolan, Jeffrey and Foody, Brian. 1999. Cellulase from submerged fermentation. Advances in Biochemical Engineering/Biotechnology, 65, pp.41-67.

Tucker, K. G. 1994. Relationship between mycelial morphology biomass concentration and broth rheology in submerged fermentations. PhD thesis, University of Birmingham, Birmingham, UK.

Tucker K.G. and Thomas C.R. 1993. Effect of biomass concentration and morphology on the rheological parameters of *Penicillium chrysogenum* fermentation broths. Food and Bioproducts Processing, 71, pp.111-117.

Chapter 4

Summary and Conclusion

Rheological equipment was carefully selected for the rheology characterization of *T. reesei* fermentation broth. Shear rate in bioreactor typically ranges between 1 to 1000 s^{-1}. Both instrument and measuring fixtures were chosen such as the shear rate range was replicated during measurement conditions. Two rotational rheological instruments were tested in our laboratory: AntonPaar RheolabQC and TA Instruments AR-G2. A series of fixtures, which are provided with the instruments, were compared for preventing sedimentation, wall slip, and having a gap size 10 × the fungi cell aggregates. Owing to the technological advantages, the TA Instruments AR-G2 outperformed RheolabQC, with the available fixtures. In addition, cone and plate geometries, which require small sample volumes, were tested for measuring fermentation broth. However, the fermentation broth morphology and homogeneity was altered during analysis. Concentric cylinder and vane fixtures were found to be the most suitable to measure fermentation broth.

Elsewhere, eight fed-batch fermentations runs of *T. reesei* were cultured in a stirred tank bioreactor and in a reciprocating plate bioreactor, at agitation rates of 200, 300, 400, 500 RPM and 0.25, 0.50, 0.75, 1.00 Hz, respectively. Rheology, biomass concentration and morphology were analyzed for all the fermentation experiments in order to describe the relationship between them. The Herschel-Bulkley (HB) model had the best fit of the rheological data. The HB consistency index K_{HB}, flow index and yield stress, as well as biomass concentration and morphology were shown to vary during the course of the

fermentation runs. K_{HB} increased with agitation rate, as was seen by Marten et al. (1996) in *T. reesei* fermentations. Also, in all runs, K_{HB} had typically increased during the batch phase and into the mid fed-batch phase, after which, it decreased although biomass concentration increased. Similar observations were discussed for other filamentous fungi. It was suggested that both morphological and biomass concentration changes due to the experimental conditions influenced K_{HB}.

The relationship between K_{HB}, morphology and biomass concentration (X) was modeled. The influence of biomass concentration and morphology on rheology was studied independently. This was done by reconstitution of biomass into samples with concentrations ranging between 1 to 30 g/L. For these samples, morphology was constant. K_{HB} against X was shown to be a power-law function with a biomass exponent α relatively constant. The biomass exponent was found to average 2.9 and standard deviation of 0.41. The use of the average exponent for all the fermentation runs enabled the independent study of the influence of the morphology. A plot of the morphological factor K/X^{α} varied during the course of the fermentation runs, thus showing that the use of correlations to predict K_{HB} based exclusively on X would have inconsistence results. Similar results were obtained by Riley et al. (2000).

The morphological classes varied during the course of the fermentation runs. The clump decreased while the dispersed morphologies increased. Thus the average of all classes was taken to calculate morphological parameters. Roundness was found to have the strongest correlation with K/X^{α}. Plotting K/X^{α} against roundness showed that the batch and fed-batch phases were isolated in separate clusters. Therefore, separate relationships for each phase were found to enhance correlations with K/X^{α}. A linear model described the

batch phase, while a power-law model described the fed-batch phase. However, the linear model was limited to batch data excluding sample at time zero. In the case of the power-law model, fed-batch data from run at 200 RPM was equally excluded. Parity plots of the predicted and the experimental K_{HB} showed reasonable fit for the models. Although data was highly scattered, considering the difficulties in measuring mycelial broth rheology, the predictions are recommended for estimating the rheological properties of *Trichoderma reesei* fermentation broths necessary in bioreactor design optimization and production control.

4.1 Recommendations

On-line rheological analysis was shown to the work for filamentous fungi fermentations (Badino Jr et al., 1997). Their statistical analysis showed a decrease in measurement variability relative to off-line analysis. Samples are immediately analyzed thus preventing any error due to changes caused by environment outside of the bioreactor. Also, the advantage of using an on-line rheometer over off-line instruments is in having more frequent measurements with no sample size limitations. Thus, a better description of the fermentation broth rheology can be obtained during the course of a fermentation run.

In order to increase the statistical significance of the correlation models, replicates of the fermentations runs are highly suggested. With additional data, further analysis of each agitation runs should be done separately to understand the dynamics of the three correlated parameters.

4.2 References

Badino J.R., Facciotti M.C.R. and Schmidell W. 1997. Construction and operation of an impeller rheometers for on-line rheological characterization of non-Newtonian fermentation broths. Brazilian Journal of Chemical Engineering, 14, pp. 359-365.

Marten M.R., Velkovska S., Khan S.A. and Ollis D.F. 1996. Rheological, mass transfer, and mixing characterization of cellulase- producing *Trichoderma reesei* suspensions. Biotechnology Progress, 12, pp. 602-611.

Riley G.L., Tucker K.G., Paul G.C. and Thomas C.R. 2000. Effect of biomass concentration and mycelial morphology on fermentation broth rheology. Biotechnology and Bioengineering, 68, pp. 160-172.

Appendix

A. Rheometer Specifications

Table A.1 TA Instruments AR-G2 rheometer specifications

Minimum Torque Oscillation Controlled Rate (μN.m)	0.003
Minimum Torque Oscillation Controlled Stress (μN.m)	0.003
Minimum Torque Steady Controlled Rate (μN.m)	0.01
Torque Range Steady Shear Controlled Stress (μN.m)	0.01
Maximum Torque (mN.m)	200
Torque Resolution (nN.m)	0.1
Motor Inertia (μN.m.s)	18
Angular Velocity Range Controlled Stress (rad/s)	0 to 300
Angular Velocity Range Controlled Rate (rad/s)	1.4×10^{-9} to 300
Frequency Range (rad/s)	7.5×10^{-9} to 628
Displacement Resolution (nrad)	25
Step change in velocity (ms)	7
Step change in strain (ms)	30
Direct Strain Control	Standard
Thrust Bearing	Magnetic Bearing
Normal/Axial Force Range (N)	0.005 to 50
Smart Swap™	Standard
Smart Swap Geometry	Standard
Peltier Plate (°C)	- 40 to 200
Environmental Test Chamber (°C)	- 160 to 600
ETC Camera Viewer	Optional
Concentric Cylinder Peltier Control (°C)	- 20 to 150
Upper Heated Plate (°C)	- 30 to 150
Camera Option with Streaming Video and Image Capture	Optional

B. Fermentation Runs Rheology Parameters and Biomass Concentration Data

B.1 Stirred Tank Bioreactor Data

Table A.2 Experiment Details: STB12 (200 RPM) 14 March 2007

Sample #	Time (h)	Concentration (g/l)	Shear Rate Range (s^{-1})	Herschel-Bulkley Model			Standard Error of Fit	$K/X^{2.91}$
				K ($Pa.s^n$)	n	Yield Stress (Pa)		
1	0.00	0.927	6-20	4.797E-04	1.043	0.000	9.619	5.987E-04
2	12.64	0.947	6-20	7.220E-04	1.000	0.000	269.0	8.468E-04
3	23.69	1.321	10-100	2.080E-03	1.000	0.154	140.1	9.264E-04
5	47.57	5.144	1-1000	7.315E-03	1.000	1.024	71.52	6.236E-05
6	60.61	4.154	1-500	4.101E-02	0.829	0.871	6.555	6.514E-04
7	71.51	3.707	1-500	4.500E-02	0.804	0.472	10.23	9.950E-04
8	85.09	4.314	1-500	4.369E-02	0.804	0.324	9.248	6.215E-04
9	95.53	4.878	1-500	3.459E-02	0.827	0.294	8.859	3.442E-04
10	108.58	4.094	1-500	4.583E-02	0.787	0.298	9.642	7.592E-04
11	120.66	3.906	1-500	3.204E-02	0.820	0.273	10.38	6.087E-04
12	132.61	5.918	1-500	2.964E-02	0.838	0.284	10.52	1.681E-04
13	143.58	6.100	1-300	1.816E-02	0.875	0.245	17.38	9.432E-05
14	156.63	5.962	1-300	1.393E-02	0.892	0.220	17.08	7.733E-05

Table A.3 Experiment Details: STB13 (300 RPM) 27 March 2007

Sample #	Time (h)	Concentration (g/l)	Shear Rate Range (s^{-1})	Herschel-Bulkley Model			Standard Error of Fit	$K/X^{2.91}$
				K ($Pa.s^n$)	n	Yield Stress (Pa)		
1	0.00	0.987	3.5-35	1.117E-03	0.981	0.003	7.115	1.161E-03
2	5.55	1.153	3.5-40	1.482E-03	1.000	0.014	86.077	9.790E-04
3	12.49	2.359	5-200	4.573E-03	0.747	0.145	45.39	3.764E-04
4	16.46	2.968	3-200	2.703E-03	1.000	0.686	143.77	1.141E-04
6	23.39	6.159	1-600	2.263E-02	0.806	1.492	6.385	1.143E-04
7	36.43	5.414	1-800	5.894E-02	0.724	1.197	8.100	4.332E-04
8	47.35	7.671	1-600	5.108E-02	0.880	0.443	9.057	1.362E-04
9	60.46	9.123	1-400	1.645E-02	1.000	0.373	9.393	2.649E-05

Table A.4 Experiment Details: STB16 (500 RPM) 13 April 2007

Sample #	Time (h)	Concentration (g/l)	Shear Rate Range (s^{-1})	Herschel-Bulkley Model			Standard Error of Fit	$K/X^{2.91}$
				K ($Pa.s^n$)	n	Yield Stress (Pa)		
1	0.00	0.952	3.5-35	1.120E-03	0.981	0.003	9.040	1.291E-03
5	12.75	2.081	3-150	3.990E-03	1.000	0.090	32.650	4.734E-04
9	23.78	4.947	1-700	1.384E-01	0.708	1.366	5.255	1.322E-03
10	28.72	6.552	1-700	1.478E-01	0.705	0.770	8.580	6.236E-04
11	30.09	6.278	1-700	9.355E-02	0.747	0.608	8.617	4.469E-04
12	37.25	9.713	1-700	8.305E-02	0.780	0.703	12.460	1.114E-04
13	47.77	14.453	1-800	1.139E-01	0.782	1.167	13.720	4.811E-05
14	55.07	16.756	1-800	1.152E-01	0.799	1.430	12.510	3.165E-05
15	62.00	18.211	1-1000	2.405E-01	0.702	1.349	12.190	5.186E-05
16	71.67	17.002	1-1000	1.157E-01	0.811	1.689	13.590	3.047E-05
17	85.67	16.303	1-1000	2.900E-01	0.697	1.163	11.700	8.628E-05
18	94.24	16.385	1-1000	1.021E-01	0.824	1.467	17.410	2.993E-05
19	109.76	13.730	1-600	2.878E-02	0.901	0.835	13.580	1.411E-05

Table A.5 Experiment Details: STB17 (400 RPM) 05 May 2007

Sample #	Time (h)	Concentration (g/l)	Shear Rate Range (s^{-1})	Herschel-Bulkley Model			Standard Error of Fit	$K/X^{2.91}$
				K ($Pa.s^n$)	n	Yield Stress (Pa)		
1	0.00	0.960	1-30	9.705E-04	0.992	0.004	6.95	1.093E-03
4	13.04	2.424	1-100	4.727E-03	0.851	0.067	38.37	3.596E-04
7	23.81	7.172	1-700	7.677E-02	0.779	0.927	6.649	2.489E-04
8	36.78	8.600	1-800	1.231E-01	0.739	0.709	11.09	2.354E-04
9	47.78	10.467	1-600	7.672E-02	0.775	0.516	10.75	8.285E-05
10	60.81	10.500	1-700	4.672E-02	0.857	0.609	10.38	4.999E-05
12	71.76	13.420	1-700	5.330E-02	0.851	0.482	10.69	2.793E-05
13	84.76	13.565	1-700	3.856E-02	0.889	0.570	7.414	1.958E-05
14	95.76	14.704	1-300	8.143E-03	1.004	0.317	10.41	3.271E-06

Table A.6 Experiment Details: STB18 (400 RPM) 21 May 2007

Sample #	Time (h)	Concentration (g/l)	Shear Rate Range (s^{-1})	Herschel-Bulkley Model			Standard Error of Fit	$K/X^{2.91}$
				K ($Pa.s^n$)	n	Yield Stress (Pa)		
1	0.00	0.960	-	-	-	-	-	-
2	12.74	0.970	-	-	-	-	-	-
3	23.64	1.130	10-40	8.040E-04	1.000	0.016	160.745	5.634E-04
4	36.72	2.795	1-100	2.493E-03	1.000	0.094	64.722	1.254E-04
5	40.74	3.895	1-150	2.819E-03	1.066	0.122	11.831	5.399E-05
6	44.16	5.480	1-200	3.346E-02	0.653	0.158	18.000	2.374E-04
7	47.74	6.660	1-600	6.186E-02	0.751	0.514	10.190	2.488E-04
8	60.74	7.625	1-800	1.568E-01	0.720	0.900	9.317	4.255E-04
9	71.60	9.830	1-600	1.007E-01	0.715	0.522	11.050	1.305E-04
10	84.65	11.750	1-800	1.366E-01	0.762	0.789	13.870	1.054E-04

Table A.7 Experiment Details: STB22 (400 RPM) 15 June 2007

Sample #	Time (h)	Concentration (g/l)	Shear Rate Range (s^{-1})	Herschel-Bulkley Model			Standard Error of Fit	$K/X^{2.91}$
				K ($Pa.s^n$)	n	Yield Stress (Pa)		
1	0.00	1.040	5-30	9.226E-04	1.000	0.002	9.628	8.231E-04
3	15.96	3.320	1-350	4.992E-02	0.733	0.585	5.261	1.522E-03
4	18.92	4.555	1-600	1.235E-01	0.707	1.390	6.162	1.500E-03
5	23.88	7.340	1-700	2.099E-01	0.680	1.639	5.707	6.364E-04
6	37.47	10.120	1-700	2.808E-01	0.635	0.789	8.512	3.344E-04
7	42.00	10.440	1-700	2.703E-01	0.636	0.737	8.978	2.941E-04
8	47.98	10.680	1-700	3.043E-01	0.640	1.144	12.190	3.099E-04
10	60.93	10.850	1-800	3.084E-01	0.650	1.078	12.440	3.000E-04
12	66.71	12.075	1-800	3.156E-01	0.633	1.148	12.020	2.249E-04
13	71.95	12.875	1-800	4.642E-01	0.600	1.390	9.703	2.744E-04
15	84.93	14.025	1-800	3.895E-01	0.618	1.678	10.660	1.795E-04
17	95.92	13.680	1-800	5.469E-01	0.576	1.508	9.611	2.710E-04
19	108.96	13.800	1-800	4.717E-01	0.597	1.588	9.286	2.279E-04
21	119.90	14.900	1-800	3.966E-01	0.629	1.545	10.300	1.533E-04
23	132.95	16.000	1-800	3.198E-01	0.660	1.262	10.740	1.005E-04

B.2 Reciprocating Plate Bioreactor Data

Table A.8 Experiment Details: RPB16 (0.25 Hz) 16 March 2007

Sample #	Time (h)	Concentration (g/l)	Shear Rate Range (s^{-1})	Herschel-Bulkley Model			Standard Error of Fit	$K/X^{2.91}$
				K ($Pa.s^n$)	n	Yield Stress (Pa)		
1	0.00	1.077	10-30	1.526E-02	1.000	0.015	726.5	1.230E-02
2	13.00	2.115	5-200	2.214E-03	1.000	0.550	93.5	2.504E-04
3	23.32	3.047	10-200	3.379E-03	1.000	0.574	109.3	1.323E-04
4	36.86	3.826	10-200	2.946E-04	1.000	0.573	373.3	5.943E-06
5	48.56	3.800	3-200	3.271E-03	1.000	0.705	646.6	6.731E-05
6	61.61	5.261	1.5-100	2.640E-03	1.000	0.331	107.3	2.108E-05
7	73.27	4.967	1.5-300	1.045E-02	0.944	0.689	29.1	9.869E-05
8	85.52	3.706	1-300	3.735E-02	0.777	0.468	11.8	8.265E-04
9	96.60	4.073	1-300	7.328E-02	0.665	0.357	10.0	1.232E-03
10	109.56	4.000	1-300	6.620E-02	0.661	0.243	8.8	1.173E-03
11	120.31	4.446	1-300	3.821E-02	0.755	0.263	9.4	4.980E-04
12	132.12	4.037	1-300	3.071E-02	0.764	0.209	9.7	5.301E-04
13	143.86	4.608	1-200	2.280E-02	0.789	0.186	9.1	2.678E-04
14	156.84	4.211	1-200	1.658E-02	0.825	0.175	8.5	2.531E-04
15	167.16	4.438	1-200	1.039E-02	0.894	0.180	11.4	1.362E-04
16	180.11	4.280	1-200	6.825E-03	0.954	0.174	8.5	9.933E-05
17	191.05	4.250	1-200	5.042E-03	0.991	0.158	13.7	7.492E-05
18	205.65	4.274	1-200	5.102E-03	1.031	0.140	10.0	7.459E-05
19	215.19	4.225	1-100	4.459E-03	0.947	0.129	18.7	6.741E-05
20	230.96	4.250	1-100	2.715E-03	1.028	0.119	16.6	4.034E-05
21	239.56	4.412	1-100	2.629E-03	1.000	0.115	29.2	3.502E-05

Table A.9 Experiment Details: RPB18 (0.5 Hz) 31 March 2007

Sample #	Time (h)	Concentration (g/l)	Shear Rate Range (s^{-1})	Herschel-Bulkley Model			Standard Error of Fit	$K/X^{2.91}$
				K ($Pa.s^n$)	n	Yield Stress (Pa)		
1	0	0.968	15-30	-	-	-	707.1	-
4	13.32	1.803	15-150	1.161E-02	0.892	0.285	68.01	2.091E-03
11	48.75	5.385	1-100	6.971E-02	0.550	0.839	50.41	5.204E-04
12	60.81	4.734	1-400	1.151E-01	0.654	0.536	5.939	1.250E-03
13	71.74	4.545	1-400	1.429E-01	0.622	0.456	6.066	1.746E-03
14	84.84	4.403	1-400	9.815E-02	0.662	0.398	7.02	1.316E-03
15	95.76	4.770	1-400	8.405E-02	0.681	0.359	8.175	8.926E-04
16	108.81	5.973	1-400	7.129E-02	0.719	0.364	12.08	3.936E-04
17	119.72	8.414	1-400	1.196E-01	0.685	0.774	10.27	2.437E-04
18	133.11	6.876	1-400	6.327E-02	0.737	0.677	9.162	2.319E-04

Table A.10 Experiment Details: RPB19 (0.75Hz) 05 May 2007

Sample #	Time (h)	Concentration (g/l)	Shear Rate Range (s^{-1})	Herschel-Bulkley Model			Standard Error of Fit	$K/X^{2.91}$
				K ($Pa.s^n$)	n	Yield Stress (Pa)		
1	0.00	0.967	3-30	1.060E-03	0.974	1E-04	1.306	1.170E-03
4	12.73	1.814	1-100	1.147E-02	0.748	0.041	13.940	2.028E-03
5	18.32	2.303	1-100	3.295E-03	1.000	0.106	38.950	2.910E-04
6	23.79	4.375	1-100	1.166E-02	0.880	0.521	30.860	1.593E-04
8	36.80	5.383	1-600	1.112E-01	0.705	0.741	5.743	8.307E-04
9	47.74	5.662	1-600	1.609E-01	0.656	0.527	6.342	1.038E-03
10	60.77	6.685	1-400	1.451E-01	0.644	0.390	5.861	5.774E-04
11	71.79	7.016	1-400	8.061E-02	0.711	0.418	8.960	2.787E-04
12	84.77	7.746	1-350	3.895E-02	0.797	0.359	8.766	1.010E-04
13	95.79	8.456	1-300	2.209E-02	0.870	0.330	8.587	4.436E-05
16	107.72	9.563	1-300	1.975E-02	0.886	0.297	7.419	2.774E-05

Table A.11 Experiment Details: RPB20 (1.0 Hz) 21 May 2007

Sample #	Time (h)	Concentration (g/l)	Shear Rate Range (s^{-1})	Herschel-Bulkley Model			Standard Error of Fit	$K/X^{2.91}$
				K ($Pa.s^n$)	n	Yield Stress (Pa)		
1	0.00	1.17	3-30	9.741E-04	0.995	0.002	4.541	6.221E-04
4	12.77	2.01	3-100	4.377E-03	0.888	0.127	101.9	5.744E-04
5	15.82	2.36	-	2.032E-03	1.000	0.068	-	1.671E-04
6	19.83	3.13	1--80	5.658E-03	0.840	0.084	18.04	2.047E-04
7	23.73	5.00	1-300	3.768E-02	0.760	0.393	7.107	3.490E-04
9	36.78	6.12	1-700	2.912E-01	0.635	1.439	6.636	1.498E-03
10	47.73	7.76	1-700	2.295E-01	0.640	0.806	9.85	5.918E-04
11	60.72	10.30	1-700	2.610E-01	0.625	0.938	11.11	2.953E-04
12	71.72	9.24	1-700	2.789E-01	0.610	1.956	29.43	4.328E-04
13	84.70	11.36	1-700	2.033E-01	0.668	0.839	10.97	1.730E-04
14	91.95	14.20	1-600	1.331E-01	0.700	0.854	8.032	5.918E-05

Table A.12 Experiment Details: RPB22 (0.75 Hz) 04 June 2007

Sample #	Time (h)	Concentration (g/l)	Shear Rate Range (s^{-1})	Herschel-Bulkley Model			Standard Error of Fit	$K/X^{2.91}$
				K ($Pa.s^n$)	n	Yield Stress (Pa)		
1	0.00	0.995	8-40	1.309E-03	0.904	0.001	6.214	1.328E-03
2	12.69	1.640	4-50	2.508E-03	0.847	0.005	3.966	5.948E-04
6	36.57	6.517	1-500	9.813E-02	0.716	0.923	9.132	4.205E-04
7	47.40	7.617	1-600	2.705E-01	0.623	1.137	5.364	7.364E-04
9	60.48	8.500	1-600	3.386E-01	0.593	1.332	5.367	6.699E-04
11	71.39	9.250	1-800	2.905E-01	0.635	1.878	8.956	4.494E-04
13	84.47	9.475	1-600	3.281E-01	0.598	1.937	5.203	4.733E-04
15	95.39	9.250	1-700	2.006E-01	0.663	2.187	14.44	3.103E-04
16	110.60	9.925	1-300	4.515E-02	0.732	0.397	11.6	5.691E-05

C. Experimental Runs Raw Data

Table A.13 STB 200 RPM

Sample #	Viscosity Pa.s	Shear stress Pa	Shear rate 1/s	Torque µN.m	Velocity rad/s	Sample #	Viscosity Pa.s	Shear stress Pa	Shear rate 1/s	Torque µN.m	Velocity rad/s	Sample #	Viscosity Pa.s	Shear stress Pa	Shear rate 1/s	Torque µN.m	Velocity rad/s
Sample 1	0.005627	5.627	1000	311.11	68.88	Sample 4	0.009669	9.669	1000	534.57	68.88	Sample 7	0.01489	14.89	1000	823.42	68.88
	0.003468	2.188	631	120.98	43.46		0.008036	5.07	631	280.32	43.46		0.01461	9.216	631	509.54	43.46
	0.002422	0.9642	398	53.31	27.42		0.007166	2.853	398.1	157.73	27.42		0.01521	6.057	398.1	334.88	27.42
	0.001774	0.4455	251	24.63	17.3		0.007976	2.003	251.2	110.76	17.3		0.01677	4.211	251.2	232.84	17.3
	0.001311	0.2078	159	11.49	10.92		0.01023	1.621	158.5	89.64	10.92		0.01955	3.099	158.5	171.34	10.92
	0.001001	0.1001	100	5.53	6.888		0.01615	1.615	100	89.29	6.888		0.02338	2.338	100	129.23	6.888
	0.000726	0.04581	63	2.53	4.346		0.02509	1.583	63.09	87.52	4.346		0.02844	1.795	63.1	99.22	4.346
	0.000644	0.02564	40	1.42	2.742		0.04412	1.756	39.81	97.11	2.742		0.03495	1.391	39.81	76.92	2.742
	0.0005892	0.0148	25	0.82	1.73		0.07188	1.805	25.12	99.82	1.73		0.04244	1.066	25.12	58.94	1.73
	0.0005432	0.008609	16	0.48	1.092		0.1152	1.825	15.85	100.9	1.092		0.05386	0.8536	15.85	47.19	1.092
	0.0005236	0.005236	10	0.29	0.6888		0.1582	1.582	9.998	87.46	0.6887		0.07493	0.7493	10	41.43	0.6888
	0.0005117	0.003229	6	0.18	0.4346		0.278	1.753	6.308	96.94	0.4345		0.1036	0.6535	6.31	36.13	0.4346
	0.0004994	0.001988	4	0.11	0.2742		0.3473	1.383	3.981	76.44	0.2742		0.1476	0.5877	3.981	32.49	0.2742
	0.000457	0.001148	3	0.06	0.173		0.581	1.46	2.512	80.69	0.173		0.2143	0.5382	2.512	29.76	0.173
	0.0002906	0.000461	2	0.03	0.1092		0.8005	1.269	1.585	70.15	0.1092		0.3064	0.4856	1.585	26.84	0.1092
	0.000753	0.000753	1	0.04	0.06889		1.031	1.031	1	56.99	0.06889		0.4743	0.4744	1	26.23	0.06889
Sample 2	0.005655	5.655	1000	312.64	68.88	Sample 5	0.009657	9.657	1000	533.88	68.88	Sample 8	0.01458	14.58	1000	806.09	68.88
	0.003551	2.24	631	123.86	43.46		0.007677	4.844	631	267.81	43.46		0.01383	8.724	631	482.31	43.46
	0.002633	1.048	398.1	57.95	27.42		0.007706	3.068	398.1	169.62	27.42		0.01452	5.78	398.1	319.57	27.42
	0.001888	0.4744	251.2	26.23	17.3		0.009334	2.345	251.2	129.62	17.3		0.01577	3.962	251.2	219.05	17.3
	0.001444	0.2289	158.5	12.65	10.92		0.01187	1.882	158.5	104.02	10.92		0.01766	2.798	158.5	154.7	10.92
	0.001142	0.1142	100	6.31	6.888		0.01672	1.672	100	92.45	6.889		0.02065	2.065	100	114.17	6.888
	0.000979	0.06177	63.1	3.42	4.346		0.02711	1.71	63.09	94.56	4.346		0.02499	1.576	63.1	87.16	4.346
	0.000843	0.03356	39.81	1.86	2.742		0.0452	1.799	39.8	99.46	2.742		0.03108	1.237	39.81	68.41	2.742
	0.0007497	0.01883	25.12	1.04	1.73		0.07242	1.82	25.12	100.6	1.731		0.03874	0.9732	25.12	53.8	1.73
	0.0007103	0.01126	15.85	0.62	1.092		0.08976	1.423	15.85	78.66	1.092		0.04714	0.7471	15.85	41.3	1.092
	0.00139	0.0139	10	0.77	0.6888		0.1698	1.698	9.998	93.88	0.6887		0.06379	0.6379	10	35.27	0.6888
	0.001759	0.0111	6.309	0.61	0.4346		0.2541	1.604	6.31	88.66	0.4347		0.09019	0.569	6.309	31.46	0.4346
	0.003047	0.01213	3.981	0.67	0.2742		0.2456	0.9778	3.981	54.06	0.2742		0.1305	0.5194	3.981	28.72	0.2742
	0.004938	0.0124	2.512	0.69	0.173		0.2374	0.5963	2.512	32.97	0.173		0.1732	0.4351	2.512	24.06	0.173
	0.007051	0.01118	1.585	0.62	0.1092		0.4427	0.7017	1.585	38.79	0.1092		0.2334	0.37	1.585	20.45	0.1092
	0.02392	0.02392	1	1.32	0.06889		0.4348	0.4348	1	24.04	0.06888		0.3341	0.334	1	18.47	0.06888
Sample 3	0.006009	6.009	1000	332.2	68.88	Sample 6	0.01578	15.78	1000	872.37	68.88	Sample 9	0.01384	13.84	1000	765.17	68.88
	0.0044	2.776	631	153.5	43.46		0.01594	10.06	631	556.02	43.46		0.01276	8.048	631	444.96	43.46
	0.003501	1.394	398.1	77.07	27.42		0.01686	6.713	398.1	371.16	27.42		0.01313	5.229	398.1	289.1	27.42
	0.003109	0.7809	251.2	43.17	17.3		0.0193	4.848	251.2	268.04	17.3		0.0143	3.591	251.2	198.54	17.3
	0.003169	0.5023	158.5	27.77	10.92		0.02312	3.664	158.5	202.57	10.92		0.01591	2.521	158.5	139.39	10.92
	0.003386	0.3386	100	18.72	6.888		0.02761	2.761	100	152.62	6.888		0.01807	1.807	100	99.92	6.888
	0.004854	0.3063	63.09	16.93	4.346		0.03471	2.19	63.1	121.09	4.346		0.02165	1.366	63.1	75.52	4.346
	0.006732	0.268	39.81	14.82	2.742		0.04191	1.669	39.81	92.25	2.742		0.02679	1.066	39.81	58.96	2.742
	0.008449	0.2122	25.12	11.73	1.73		0.05654	1.42	25.12	78.52	1.73		0.03453	0.8674	25.12	47.96	1.73
	0.01159	0.1837	15.85	10.16	1.092		0.07805	1.237	15.85	68.38	1.092		0.04215	0.6681	15.85	36.94	1.092
	0.01436	0.1436	10	7.94	0.6888		0.1136	1.136	10	62.79	0.6888		0.05421	0.5421	10	29.97	0.6888
	0.01817	0.1146	6.31	6.34	0.4346		0.1644	1.038	6.31	57.36	0.4346		0.07524	0.4747	6.31	26.25	0.4346
	0.02118	0.08432	3.981	4.66	0.2743		0.2504	0.9969	3.981	55.12	0.2743		0.1111	0.4422	3.981	24.45	0.2742
	0.02686	0.06746	2.512	3.73	0.173		0.3908	0.9817	2.512	54.27	0.173		0.1656	0.4161	2.512	23	0.173
	0.04221	0.0669	1.585	3.7	0.1092		0.5915	0.9374	1.585	51.83	0.1092		0.2326	0.3686	1.585	20.38	0.1092
	0.04173	0.04173	1	2.31	0.06888		0.8633	0.8634	1	47.73	0.06889		0.301	0.301	1	16.64	0.06889

Table A.14 STB 200 RPM

Sample #	Viscosity Pa.s	Shear stress Pa	Shear rate 1/s	Torque µN.m	Velocity rad/s	Sample #	Viscosity Pa.s	Shear stress Pa	Shear rate 1/s	Torque µN.m	Velocity rad/s
Sample 10	0.01434	14.34	1000	793.06	68.88	Sample 13	0.01227	12.27	1000	678.32	68.88
	0.01332	8.407	631	464.77	43.46		0.00996	6.285	631	347.45	43.46
	0.01371	5.457	398.1	301.71	27.42		0.009796	3.9	398.1	215.61	27.42
	0.01498	3.763	251.2	208.05	17.3		0.01028	2.583	251.2	142.79	17.3
	0.01704	2.701	158.5	149.35	10.92		0.01087	1.723	158.5	95.28	10.92
	0.01974	1.974	100	109.11	6.888		0.01213	1.213	100	67.08	6.888
	0.0237	1.495	63.1	82.67	4.346		0.01432	0.9034	63.1	49.95	4.346
	0.02953	1.176	39.81	64.99	2.742		0.01771	0.7051	39.81	38.98	2.742
	0.03811	0.9572	25.12	52.92	1.73		0.02315	0.5816	25.12	32.16	1.73
	0.0475	0.7529	15.85	41.62	1.092		0.03168	0.502	15.85	27.76	1.092
	0.06083	0.6083	10	33.63	0.6888		0.04407	0.4407	10	24.37	0.6888
	0.08317	0.5248	6.31	29.01	0.4346		0.06151	0.3881	6.31	21.45	0.4346
	0.1197	0.4766	3.981	26.35	0.2742		0.08741	0.348	3.981	19.24	0.2742
	0.175	0.4395	2.512	24.3	0.173		0.1239	0.3113	2.512	17.21	0.173
	0.2263	0.3586	1.585	19.83	0.1092		0.178	0.2821	1.585	15.6	0.1092
	0.3051	0.3051	1	16.87	0.06888		0.2738	0.2738	1	15.14	0.06888
Sample 11	0.01315	13.15	1000	726.79	68.88	Sample 14	0.01174	11.74	1000	649.25	68.88
	0.01149	7.249	631	400.75	43.46		0.008903	5.617	631	310.55	43.46
	0.01177	4.684	398.1	258.98	27.42		0.008538	3.399	398.1	187.92	27.42
	0.01269	3.187	251.2	176.2	17.3		0.008682	2.181	251.2	120.57	17.3
	0.01432	2.27	158.5	125.51	10.92		0.009246	1.465	158.5	81.01	10.92
	0.0165	1.65	100	91.22	6.888		0.01031	1.031	100	56.97	6.888
	0.0195	1.23	63.1	68.02	4.346		0.01193	0.7529	63.1	41.63	4.346
	0.02398	0.9548	39.81	52.79	2.742		0.01476	0.5875	39.81	32.48	2.742
	0.03088	0.7757	25.12	42.88	1.73		0.01941	0.4876	25.12	26.96	1.73
	0.04112	0.6517	15.85	36.03	1.092		0.02717	0.4306	15.85	23.81	1.092
	0.05296	0.5296	10	29.28	0.6888		0.03824	0.3823	10	21.14	0.6888
	0.07095	0.4477	6.31	24.75	0.4346		0.05407	0.3411	6.31	18.86	0.4346
	0.09963	0.3967	3.981	21.93	0.2742		0.0783	0.3117	3.981	17.23	0.2742
	0.1465	0.3679	2.512	20.34	0.173		0.1087	0.273	2.512	15.09	0.173
	0.2214	0.351	1.585	19.4	0.1092		0.1572	0.2492	1.585	13.78	0.1092
	0.3063	0.3063	1	16.94	0.06888		0.2301	0.23	1	12.72	0.06888
Sample 12	0.01349	13.49	1000	745.59	68.88						
	0.01202	7.586	631	419.42	43.46						
	0.01208	4.809	398.1	265.87	27.42						
	0.01304	3.276	251.2	181.11	17.3						
	0.01435	2.274	158.5	125.7	10.92						
	0.01657	1.657	100	91.59	6.888						
	0.01978	1.248	63.1	69.01	4.346						
	0.02438	0.9706	39.81	53.66	2.742						
	0.03127	0.7854	25.12	43.42	1.73						
	0.04147	0.6572	15.85	36.33	1.092						
	0.05405	0.5405	10	29.88	0.6888						
	0.07149	0.4511	6.31	24.94	0.4346						
	0.09954	0.3963	3.981	21.91	0.2742						
	0.1464	0.3678	2.512	20.33	0.173						
	0.2196	0.348	1.585	19.24	0.1092						
	0.3166	0.3167	1	17.51	0.06889						

Table A.15 STB 300 RPM

Sample #	Viscosity Pa.s	Shear stress Pa	Shear rate 1/s	Torque mN.m	Velocity rad/s	Sample #	Viscosity Pa.s	Shear stress Pa	Shear rate 1/s	Torque mN.m	Velocity rad/s	Sample #	Viscosity Pa.s	Shear stress Pa	Shear rate 1/s	Torque mN.m	Velocity rad/s
Sample 1	0.003437	3.437	1000	190.02	68.88	Sample 2	0.005587	5.587	1000	308.88	68.88	Sample 4	0.008502	8.502	1000	470.04	68.88
	0.003083	2.449	794.3	135.4	54.72		0.004118	2.964	719.7	163.85	49.57		0.007494	5.393	719.7	298.18	49.57
	0.002752	1.737	631	96.01	43.46		0.003245	1.681	517.9	92.93	35.68		0.006706	3.473	517.9	192.03	35.68
	0.002497	1.251	501.2	69.18	34.52		0.002713	1.011	372.8	55.91	25.68		0.006604	2.462	372.8	136.1	25.68
	0.002234	0.8895	398.1	49.18	27.42		0.002209	0.5926	268.3	32.76	18.48		0.006561	1.76	268.3	97.3	18.48
	0.00199	0.6293	316.2	34.79	21.78		0.001901	0.367	193.1	20.29	13.3		0.006882	1.329	193.1	73.45	13.3
	0.001769	0.4442	251.2	24.56	17.3		0.001801	0.2502	138.9	13.83	9.571		0.006897	0.9583	138.9	52.98	9.571
	0.001527	0.3047	199.5	16.85	13.74		0.001736	0.1736	100	9.6	6.888		0.008109	0.8109	100	44.83	6.888
	0.00129	0.2045	158.5	11.31	10.92		0.001884	0.1356	71.97	7.5	4.957		0.0109	0.7842	71.97	43.35	4.957
	0.00111	0.1398	125.9	7.73	8.672		0.001883	0.09752	51.79	5.39	3.568		0.01461	0.7569	51.79	41.84	3.568
	0.001089	0.1089	100	6.02	6.888		0.001739	0.06481	37.28	3.58	2.568		0.01957	0.7296	37.28	40.34	2.568
	0.001078	0.08559	79.43	4.73	5.472		0.001741	0.0467	26.83	2.58	1.848		0.02641	0.7085	26.83	39.17	1.848
	0.001087	0.06856	63.1	3.79	4.346		0.002087	0.0403	19.31	2.23	1.33		0.0359	0.6931	19.31	38.32	1.33
	0.001082	0.05424	50.12	3	3.452		0.002341	0.03252	13.9	1.8	0.9571		0.05453	0.7578	13.9	41.9	0.9572
	0.001132	0.04508	39.81	2.49	2.742		0.003205	0.03205	10	1.77	0.6888		0.08318	0.8318	10	45.99	0.6889
	0.001152	0.03642	31.62	2.01	2.178		0.004212	0.03031	7.197	1.68	0.4958		0.1128	0.8121	7.198	44.9	0.4958
	0.001173	0.02946	25.12	1.63	1.73		0.006177	0.03199	5.179	1.77	0.3568		0.1421	0.7359	5.179	40.69	0.3567
	0.001195	0.02384	19.95	1.32	1.374		0.008808	0.03283	3.728	1.82	0.2568		0.1858	0.6923	3.727	38.28	0.2567
	0.001279	0.02028	15.85	1.12	1.092		0.01069	0.02869	2.683	1.59	0.1848		0.229	0.6145	2.683	33.97	0.1848
	0.0013	0.01637	12.59	0.91	0.8672		0.01217	0.0235	1.931	1.3	0.133		0.307	0.5928	1.931	32.77	0.133
	0.001395	0.01395	10	0.77	0.6888		0.01321	0.01836	1.389	1.02	0.09571		0.485	0.6739	1.389	37.26	0.09571
	0.001505	0.01196	7.943	0.66	0.5472		0.0194	0.0194	1	1.07	0.06889		0.6071	0.607	1	33.56	0.06888
	0.001571	0.009914	6.31	0.55	0.4346	Sample 3	0.00696	6.96	1000	384.79	68.88	Sample 6	0.01711	17.11	1000	945.75	68.88
	0.001636	0.008197	5.012	0.45	0.3452		0.005878	4.23	719.7	233.88	49.57		0.01743	12.54	719.7	693.35	49.57
	0.001884	0.007502	3.981	0.41	0.2742		0.005147	2.666	517.9	147.38	35.68		0.01894	9.809	517.9	542.28	35.68
	0.002017	0.006378	3.162	0.35	0.2178		0.004866	1.814	372.8	100.27	25.68		0.02112	7.874	372.8	435.32	25.68
	0.002305	0.00579	2.512	0.32	0.173		0.005033	1.35	268.3	74.65	18.48		0.02391	6.414	268.3	354.59	18.48
	0.002143	0.004277	1.995	0.24	0.1374		0.006146	1.187	193.1	65.6	13.3		0.02682	5.178	193.1	286.28	13.3
	0.002792	0.004424	1.585	0.24	0.1092		0.005705	0.7927	138.9	43.83	9.571		0.03217	4.47	139	247.1	9.571
	0.002977	0.003748	1.259	0.21	0.08672		0.006828	0.6828	100	37.75	6.888		0.037	3.7	100	204.58	6.888
	0.002657	0.002657	1	0.15	0.06888		0.008527	0.6137	71.97	33.93	4.958		0.04402	3.168	71.97	175.16	4.957
							0.01043	0.5402	51.79	29.87	3.568		0.05408	2.801	51.8	154.87	3.568
							0.01326	0.4943	37.28	27.33	2.568		0.06661	2.483	37.28	137.29	2.568
							0.01531	0.4107	26.83	22.71	1.848		0.08503	2.281	26.83	126.11	1.848
							0.01562	0.3016	19.31	16.67	1.33		0.1036	2	19.31	110.58	1.33
							0.01849	0.2569	13.89	14.2	0.9571		0.1343	1.866	13.89	103.15	0.9571
							0.02358	0.2358	10	13.04	0.6889		0.184	1.84	9.999	101.74	0.6888
							0.03059	0.2202	7.197	12.17	0.4958		0.2443	1.758	7.197	97.18	0.4957
							0.03802	0.1969	5.179	10.89	0.3568		0.3401	1.762	5.179	97.39	0.3567
							0.04483	0.1671	3.727	9.24	0.2568		0.4558	1.699	3.727	93.92	0.2568
							0.05607	0.1504	2.683	8.32	0.1848		0.6532	1.752	2.683	96.88	0.1848
							0.05779	0.1116	1.931	6.17	0.133		0.7706	1.488	1.93	82.24	0.133
							0.09055	0.1258	1.389	6.96	0.09571		1.087	1.511	1.389	83.52	0.09571
							0.1276	0.1276	1	7.05	0.06889		1.216	1.216	1	67.23	0.06888

Table A.16 STB 300 RPM

Sample	Viscosity	Shear stress	Shear rate	Torque	Velocity	Sample	Viscosity	Shear stress	Shear rate	Torque	Velocity
#	Pa.s	Pa	1/s	mN.m	rad/s	#	Pa.s	Pa	1/s	mN.m	rad/s
Sample 7	0.02134	21.34	1000	1179.9	68.88	Sample 9	0.01393	13.93	1000	770.19	68.88
	0.02217	15.96	719.7	882.11	49.57		0.01201	8.646	719.7	478.01	49.57
	0.02402	12.44	517.9	687.71	35.68		0.01158	5.999	517.9	331.69	35.68
	0.02671	9.957	372.8	550.5	25.68		0.01151	4.292	372.8	237.27	25.68
	0.03053	8.19	268.3	452.77	18.48		0.01181	3.168	268.3	175.14	18.48
	0.03519	6.795	193.1	375.67	13.3		0.01223	2.361	193.1	130.51	13.3
	0.04089	5.681	138.9	314.09	9.571		0.01279	1.777	138.9	98.27	9.571
	0.04804	4.804	100	265.62	6.888		0.01379	1.379	100	76.22	6.888
	0.05623	4.047	71.97	223.72	4.957		0.0153	1.101	71.97	60.88	4.957
	0.06557	3.396	51.79	187.76	3.568		0.01753	0.9079	51.79	50.2	3.568
	0.08001	2.982	37.28	164.89	2.568		0.02089	0.7786	37.28	43.05	2.568
	0.09914	2.66	26.83	147.04	1.848		0.02605	0.6988	26.83	38.64	1.848
	0.1205	2.326	19.31	128.62	1.33		0.03356	0.648	19.31	35.82	1.33
	0.1494	2.076	13.9	114.77	0.9572		0.04185	0.5815	13.89	32.15	0.9571
	0.1818	1.818	10	100.5	0.6889		0.05087	0.5087	10	28.12	0.6888
	0.234	1.684	7.197	93.09	0.4957		0.06355	0.4574	7.197	25.29	0.4957
	0.3007	1.557	5.179	86.09	0.3568		0.08287	0.4292	5.18	23.73	0.3568
	0.3663	1.365	3.728	75.48	0.2568		0.108	0.4026	3.728	22.26	0.2568
	0.483	1.296	2.683	71.64	0.1848		0.1388	0.3723	2.683	20.59	0.1848
	0.7086	1.368	1.931	75.63	0.133		0.1853	0.3578	1.931	19.78	0.133
	0.9272	1.288	1.389	71.22	0.09571		0.2526	0.3509	1.389	19.4	0.09571
	1.465	1.465	1	81.01	0.06889		0.3461	0.3461	1	19.13	0.06888
Sample 8	0.01564	15.64	1000	864.79	68.88						
	0.01456	10.48	719.7	579.24	49.57						
	0.01465	7.589	517.9	419.57	35.68						
	0.01505	5.611	372.8	310.24	25.68						
	0.01603	4.3	268.3	237.71	18.48						
	0.01732	3.344	193.1	184.87	13.3						
	0.01895	2.632	138.9	145.54	9.571						
	0.02112	2.112	100	116.78	6.888						
	0.02398	1.726	71.97	95.42	4.957						
	0.02784	1.442	51.79	79.72	3.568						
	0.03311	1.234	37.28	68.23	2.568						
	0.03966	1.064	26.83	58.83	1.848						
	0.0457	0.8823	19.31	48.78	1.33						
	0.05277	0.7333	13.9	40.54	0.9571						
	0.06463	0.6463	10	35.73	0.6888						
	0.08211	0.5909	7.197	32.67	0.4957						
	0.1074	0.5565	5.179	30.77	0.3568						
	0.1422	0.5301	3.728	29.31	0.2568						
	0.1887	0.5061	2.683	27.98	0.1848						
	0.2281	0.4404	1.931	24.35	0.133						
	0.2587	0.3594	1.389	19.87	0.09571						
	0.31	0.31	1	17.14	0.06888						

Table A.17 STB 400 RPM

Sample	Viscosity	Shear stress	Shear rate	Torque	Velocity	Sample	Viscosity	Shear stress	Shear rate	Torque	Velocity	Sample	Viscosity	Shear stress	Shear rate	Torque	Velocity
#	Pa.s	Pa	1/s	mN.m	rad/s	#	Pa.s	Pa	1/s	mN.m	rad/s	#	Pa.s	Pa	1/s	mN.m	rad/s
Sample 1	3.36E-03	3.356	1000	185.56	68.88	Sample 5	4.70E-03	4.696	1000	259.6	68.88	Sample 7	0.03158	5.005	158.5	276.71	10.92
	2.91E-03	2.095	719.7	115.84	49.57		4.52E-03	3.255	719.7	179.95	49.57		0.03426	4.313	125.9	238.47	8.672
	2.52E-03	1.307	517.9	72.28	35.68		4.76E-03	2.467	517.9	136.4	35.68		0.03727	3.727	100	206.06	6.888
	2.17E-03	0.8082	372.8	44.68	25.68		5.03E-03	1.876	372.8	103.73	25.68		0.04149	3.295	79.43	182.19	5.472
	1.81E-03	0.4855	268.3	26.84	18.48		8.24E-03	0.5933	71.97	32.8	4.957		0.04348	2.743	63.1	151.67	4.346
	1.48E-03	0.2858	193.1	15.8	13.3		9.47E-03	0.4904	51.79	27.11	3.568		0.04911	2.461	50.12	136.07	3.452
	1.10E-03	0.1531	138.9	8.47	9.571		9.86E-03	0.3676	37.28	20.32	2.568		0.05642	2.246	39.81	124.18	2.742
	1.08E-03	0.1075	100	5.94	6.888		1.11E-02	0.2983	26.83	16.49	1.848		0.06524	2.063	31.62	114.05	2.178
	1.07E-03	0.07663	71.97	4.24	4.957		1.18E-02	0.2278	19.31	12.59	1.33		0.0753	1.892	25.12	104.58	1.73
	1.06E-03	0.05508	51.79	3.05	3.568		1.72E-02	0.2391	13.89	13.22	0.9571		0.08865	1.769	19.95	97.79	1.374
	1.07E-03	0.0397	37.28	2.2	2.568		1.86E-02	0.1863	10	10.3	0.6888		0.1054	1.671	15.85	92.37	1.092
	1.08E-03	0.02902	26.83	1.6	1.848		2.96E-02	0.2133	7.196	11.79	0.4957		0.1221	1.538	12.59	85.01	0.8671
	1.12E-03	0.02168	19.31	1.2	1.33		4.13E-02	0.2141	5.18	11.84	0.3568		0.143	1.43	10	79.04	0.6888
	1.20E-03	0.01661	13.89	0.92	0.9571		5.83E-02	0.2171	3.727	12.01	0.2568		0.1591	1.264	7.944	69.87	0.5472
	1.28E-03	0.01282	10	0.71	0.6888		7.69E-02	0.2063	2.683	11.41	0.1848		0.1839	1.16	6.31	64.14	0.4346
	1.46E-03	0.01051	7.197	0.58	0.4957		1.03E-01	0.198	1.931	10.94	0.133		0.2267	1.136	5.012	62.82	0.3452
	1.69E-03	8.73E-03	5.179	0.48	0.3568		1.43E-01	0.199	1.39	11	0.09571		0.3013	1.2	3.981	66.32	0.2742
	1.97E-03	7.36E-03	3.728	0.41	0.2568		1.51E-01	0.1506	1	8.33	0.06888		0.372	1.176	3.162	65.04	0.2178
	2.26E-03	6.07E-03	2.683	0.34	0.1848	Sample 6	7.38E-03	7.381	1000	408.04	68.88		0.4481	1.126	2.512	62.23	0.173
	2.76E-03	5.32E-03	1.931	0.29	0.133		8.34E-03	6.001	719.7	331.75	49.57		0.5139	1.025	1.995	56.69	0.1374
	3.30E-03	4.59E-03	1.39	0.25	0.09571		9.69E-03	5.018	517.9	277.43	35.68		0.6754	1.071	1.585	59.19	0.1092
	4.38E-03	4.38E-03	1	0.24	0.06888		1.12E-02	4.169	372.8	230.51	25.68		0.6981	0.8789	1.259	48.59	0.08672
Sample 4	3.89E-03	3.885	1000	214.79	6.89E+01		0.01277	3.426	268.3	189.4	18.48		0.8116	0.8116	1	44.87	0.06888
	3.48E-03	2.505	719.7	138.51	4.96E+01		0.01585	3.061	193.1	169.23	13.3	Sample 8	0.02346	23.46	1000	1297.03	68.88
	3.16E-03	1.635	517.9	90.37	35.68		0.0184	2.557	139	141.37	9.572		0.02366	17.03	719.7	941.37	49.57
	2.93E-03	1.093	372.8	60.45	25.68		0.02113	2.113	100	116.83	6.888		0.02504	12.97	517.9	717.11	35.68
	2.76E-03	0.7409	268.3	40.96	18.48		0.02591	1.865	71.97	103.11	4.957		2.72E-02	10.14	372.8	560.48	25.68
	2.62E-03	0.5064	193.1	28	13.3		0.02962	1.534	51.79	84.82	3.568		0.0304	8.155	268.3	450.86	18.48
	2.69E-03	0.3737	138.9	20.66	9.571		0.03728	1.39	37.28	76.83	2.568		0.03483	6.725	193.1	371.8	13.3
	2.95E-03	0.2949	100	16.3	6.888		0.04204	1.128	26.83	62.35	1.848		0.04018	5.583	138.9	308.66	9.571
	3.49E-03	0.2513	71.97	13.89	4.957		0.04589	0.886	19.31	48.98	1.33		0.04665	4.665	100	257.92	6.888
	4.20E-03	0.2173	51.79	12.01	3.568		0.05533	0.7688	13.89	42.5	0.9571		0.05425	3.904	71.97	215.83	4.957
	4.85E-03	0.1807	37.28	9.99	2.568		0.06872	0.6872	10	38	0.6889		0.06088	3.153	51.79	174.33	3.568
	5.10E-03	0.1367	26.83	7.56	1.848		0.08553	0.6155	7.197	34.03	0.4957		0.06578	2.452	37.28	135.56	2.568
	5.99E-03	0.1157	19.31	6.4	1.33		0.1116	0.578	5.18	31.96	0.3568		0.07705	2.067	26.83	114.28	1.848
	6.10E-03	0.08473	13.9	4.68	0.9572		0.1327	0.4947	3.728	27.35	0.2568		0.09397	1.814	19.31	100.3	1.33
	1.03E-02	0.1033	10	5.71	0.6889		0.174	0.4667	2.683	25.8	0.1848		0.1149	1.597	13.89	88.27	0.9571
	1.25E-02	0.08995	7.197	4.97	0.4957		0.2423	0.4678	1.931	25.86	0.133		0.1423	1.423	10	78.67	0.6888
	1.79E-02	0.09249	5.179	5.11	0.3568		0.3825	0.5315	1.389	29.39	0.09571		0.1796	1.293	7.197	71.48	0.4957
	2.44E-02	0.09088	3.727	5.02	0.2568		0.4372	0.4373	1	24.17	0.06889		0.2155	1.116	5.179	61.72	0.3568
	2.92E-02	0.0782	2.683	4.32	0.1848	Sample 7	0.01946	19.46	1000	1075.85	68.88		0.2657	0.9906	3.727	54.76	0.2568
	4.50E-02	0.08696	1.931	4.81	0.133		0.01969	15.64	794.3	864.85	54.72		0.3255	0.8733	2.683	48.28	0.1848
	5.07E-02	0.07043	1.389	3.89	0.09571		0.02016	12.72	631	703.19	43.46		0.4133	0.798	1.931	44.12	0.133
	6.39E-02	0.06392	1	3.53	0.06888		2.11E-02	10.57	501.2	584.35	34.52		0.5227	0.7263	1.39	40.15	0.09571
Sample 5	4.70E-03	4.696	1000	259.6	68.88		0.02231	8.882	398.1	491.07	27.42		0.6601	0.66	1	36.49	0.06888
	4.52E-03	3.255	719.7	179.95	49.57		0.02407	7.612	316.2	420.86	21.78	Sample 9	0.02047	20.47	1000	1131.91	68.88
	4.76E-03	2.467	517.9	136.4	35.68		0.02626	6.597	251.2	364.73	17.3		0.01959	14.1	719.7	779.57	49.57
	5.03E-03	1.876	372.8	103.73	25.68		0.02895	5.776	199.5	319.34	13.74		0.02024	10.48	517.9	579.58	35.68

Table A.18 STB 400 RPM

Sample	Viscosity	Shear stress	Shear rate	Torque	Velocity	Sample	Viscosity	Shear stress	Shear rate	Torque	Velocity	Sample	Viscosity	Shear stress	Shear rate	Torque	Velocity
#	Pa.s	Pa	1/s	mN.m	rad/s	#	Pa.s	Pa	1/s	mN.m	rad/s	#	Pa.s	Pa	1/s	mN.m	rad/s
Sample 9	2.12E-02	7.918	372.8	437.75	25.68	Sample 10	0.4683	0.5895	1.259	32.59	0.08672	Sample 13	0.04741	1.499	31.62	82.89	2.178
	0.02299	6.167	268.3	340.93	18.48		0.593	0.5931	1	32.79	0.06889		0.05338	1.341	25.12	74.13	1.73
	0.02557	4.937	193.1	272.93	13.3	Sample 12	0.02246	22.46	1000	1241.7	68.88		0.06055	1.208	19.95	66.79	1.374
	0.02886	4.01	138.9	221.69	9.571		0.02186	17.36	794.3	959.82	54.72		0.06926	1.098	15.85	60.68	1.092
	0.03301	3.301	100	182.51	6.888		0.02176	13.73	631	759.15	43.46		0.07949	1.001	12.59	55.33	0.8672
	0.038	2.735	71.97	151.2	4.957		2.20E-02	11.03	501.2	609.65	34.52		0.09233	0.9233	10	51.04	0.6888
	0.04422	2.29	51.79	126.61	3.568		0.0225	8.959	398.1	495.31	27.42		0.1068	0.848	7.943	46.88	0.5472
	0.05173	1.928	37.28	106.62	2.568		0.02338	7.393	316.2	408.74	21.78		0.1241	0.7829	6.31	43.28	0.4346
	0.06067	1.628	26.83	89.98	1.848		0.02459	6.177	251.2	341.5	17.3		0.1429	0.7161	5.012	39.59	0.3452
	0.06849	1.322	19.31	73.1	1.33		0.0262	5.227	199.5	288.99	13.74		0.1653	0.6579	3.981	36.37	0.2742
	0.07744	1.076	13.89	59.49	0.9571		0.02805	4.446	158.5	245.78	10.92		0.1957	0.6188	3.162	34.21	0.2178
	0.09285	0.9285	10	51.33	0.6888		0.03028	3.812	125.9	210.77	8.672		0.2323	0.5835	2.512	32.26	0.173
	0.1143	0.8226	7.197	45.48	0.4957		0.03284	3.284	100	181.58	6.888		0.2749	0.5485	1.995	30.32	0.1374
	0.1419	0.7352	5.179	40.65	0.3568		0.03563	2.83	79.43	156.46	5.472		0.3263	0.5172	1.585	28.59	0.1092
	0.1856	0.6918	3.728	38.25	0.2568		0.03873	2.444	63.1	135.1	4.346		0.3968	0.4996	1.259	27.62	0.08672
	0.2386	0.6401	2.683	35.39	0.1848		0.04231	2.121	50.12	117.25	3.452		0.4791	0.4791	1	26.49	0.06889
	0.3135	0.6053	1.931	33.47	0.133		0.04647	1.85	39.81	102.27	2.742	Sample 14	0.01263	12.63	1000	698.21	68.88
	0.4048	0.5625	1.389	31.1	0.09571		0.05134	1.623	31.62	89.75	2.178		0.01009	7.259	719.7	401.3	49.57
	0.4869	0.4868	1	26.92	0.06888		0.05716	1.436	25.12	79.37	1.73		9.30E-03	4.819	517.9	266.41	35.68
Sample 10	0.02076	20.76	1000	1147.58	68.88		0.06386	1.274	19.95	70.45	1.374		9.41E-03	3.507	372.8	193.91	25.68
	0.02025	16.09	794.3	889.4	54.72		0.07208	1.142	15.85	63.16	1.092		9.58E-03	2.571	268.3	142.12	18.48
	0.02013	12.7	631	702.22	43.46		0.08172	1.029	12.59	56.88	0.8672		9.87E-03	1.906	193.1	105.35	13.3
	2.01E-02	10.08	501.2	557.35	34.52		0.09186	0.9186	10	50.78	0.6888		0.01038	1.442	138.9	79.72	9.571
	0.02079	8.275	398.1	457.47	27.42		0.1017	0.8076	7.943	44.65	0.5472		0.01118	1.118	100	61.81	6.888
	0.02179	6.892	316.2	381.03	21.78		0.1117	0.705	6.31	38.98	0.4346		0.01251	0.9005	71.97	49.78	4.957
	0.02307	5.795	251.2	320.37	17.3		0.1242	0.6227	5.012	34.43	0.3452		0.01449	0.7506	51.79	41.5	3.568
	0.02465	4.919	199.5	271.97	13.74		0.1409	0.5611	3.981	31.02	0.2742		0.01725	0.643	37.28	35.55	2.568
	0.02653	4.204	158.5	232.43	10.92		0.1617	0.5115	3.162	28.28	0.2178		0.02101	0.5637	26.83	31.17	1.848
	0.02867	3.609	125.9	199.51	8.672		0.1893	0.4755	2.512	26.29	0.173		0.02614	0.5046	19.31	27.9	1.33
	0.03115	3.115	100	172.19	6.888		0.2233	0.4455	1.995	24.63	0.1374		0.03308	0.4596	13.89	25.41	0.9571
	0.03401	2.701	79.43	149.35	5.472		0.2641	0.4185	1.585	23.14	0.1092		0.04259	0.4259	10	23.55	0.6888
	0.0374	2.359	63.1	130.45	4.346		0.3173	0.3995	1.259	22.08	0.08672		0.05514	0.3968	7.197	21.94	0.4957
	0.04143	2.076	50.12	114.79	3.452		0.3818	0.3818	1	21.11	0.06888		0.07183	0.372	5.179	20.57	0.3568
	0.04621	1.84	39.81	101.7	2.742	Sample 13	0.02118	21.18	1000	1170.84	68.88		0.09418	0.3511	3.728	19.41	0.2568
	0.05222	1.651	31.62	91.29	2.178		0.02036	16.17	794.3	894.11	54.72		0.1247	0.3345	2.683	18.49	0.1848
	0.05961	1.497	25.12	82.79	1.73		0.02005	12.65	631	699.46	43.46		0.1623	0.3133	1.931	17.32	0.133
	0.06815	1.36	19.95	75.17	1.374		2.05E-02	10.26	501.2	567.29	34.52		0.2068	0.2874	1.39	15.89	0.09571
	0.07521	1.192	15.85	65.9	1.092		0.02097	8.348	398.1	461.53	27.42		0.27	0.27	1	14.93	0.06888
	0.08155	1.027	12.59	56.76	0.8672		0.02164	6.844	316.2	378.38	21.78						
	0.09119	0.9119	10	50.42	0.6888		0.02263	5.683	251.2	314.21	17.3						
	0.1046	0.8307	7.943	45.93	0.5472		0.02393	4.775	199.5	263.97	13.74						
	0.1226	0.7734	6.31	42.76	0.4346		0.0255	4.041	158.5	223.42	10.92						
	0.146	0.7315	5.012	40.44	0.3452		0.02735	3.443	125.9	190.35	8.672						
	0.1759	0.7005	3.981	38.73	0.2742		0.02922	2.922	100	161.55	6.888						
	0.2084	0.6592	3.162	36.44	0.2178		0.03183	2.529	79.43	139.8	5.472						
	0.2508	0.6301	2.512	34.84	0.173		0.03485	2.199	63.1	121.55	4.346						
	0.3092	0.6169	1.995	34.11	0.1374		0.03829	1.919	50.12	106.11	3.452						
	0.376	0.5959	1.585	32.94	0.1092		0.04246	1.69	39.81	93.44	2.742						

Table A.19 STB 500 RPM

Sample	Viscosity	Shear stress	Shear rate	Torque	Velocity	Sample	Viscosity	Shear stress	Shear rate	Torque	Velocity	Sample	Viscosity	Shear stress	Shear rate	Torque	Velocity
#	Pa.s	Pa	1/s	mN.m	rad/s	#	Pa.s	Pa	1/s	mN.m	rad/s	#	Pa.s	Pa	1/s	mN.m	rad/s
Sample 1	0.003437	3.437	1000	190.02	68.88	Sample 5	0.008264	0.1649	19.95	9.12	1.374	Sample 10	0.02222	22.22	1000	1228.58	68.88
	0.003083	2.449	794.3	135.4	54.72		0.009259	0.1468	15.85	8.11	1.092		0.02265	17.99	794.3	994.55	54.72
	0.002752	1.737	631	96.01	43.46		0.01068	0.1344	12.59	7.43	0.8672		0.02357	14.87	631	822.23	43.46
	0.002497	1.251	501.2	69.18	34.52		0.01211	0.1211	10	6.69	0.6888		2.48E-02	12.43	501.2	687.33	34.52
	0.002234	0.8895	398.1	49.18	27.42		0.01388	0.1102	7.943	6.09	0.5472		0.02665	10.61	398.1	586.67	27.42
	0.00199	0.6293	316.2	34.79	21.78		0.02267	0.143	6.31	7.91	0.4346		0.02901	9.175	316.2	507.27	21.78
	0.001769	0.4442	251.2	24.56	17.3		0.02358	0.1182	5.012	6.53	0.3452		0.03196	8.029	251.2	443.88	17.3
	0.001527	0.3047	199.5	16.85	13.74		0.03166	0.126	3.981	6.97	0.2742		0.0354	7.064	199.5	390.54	13.74
	0.00129	0.2045	158.5	11.31	10.92		0.0373	0.118	3.162	6.52	0.2178		0.03909	6.196	158.5	342.55	10.92
	0.00111	0.1398	125.9	7.73	8.672		0.04688	0.1178	2.512	6.51	0.173		0.0431	5.425	125.9	299.95	8.672
	0.001089	0.1089	100	6.02	6.888		0.05745	0.1146	1.995	6.34	0.1374		0.04753	4.753	100	262.77	6.888
	0.001078	0.08559	79.43	4.73	5.472		0.07735	0.1226	1.585	6.78	0.1092		0.05204	4.133	79.43	228.52	5.472
	0.001087	0.06856	63.1	3.79	4.346		0.09278	0.1168	1.259	6.46	0.08673		0.05572	3.516	63.1	194.38	4.346
	0.001082	0.05424	50.12	3	3.452		0.09147	0.09147	1	5.06	0.06889		0.05745	2.879	50.12	159.18	3.452
	0.001132	0.04508	39.81	2.49	2.742	Sample 9	0.02143	21.43	1000	1184.56	68.88		0.06332	2.521	39.81	139.37	2.742
	0.001152	0.03642	31.62	2.01	2.178		0.0222	17.63	794.3	974.83	54.72		0.07166	2.266	31.62	125.28	2.178
	0.001173	0.02946	25.12	1.63	1.73		0.02343	14.78	631	817.16	43.46		0.08272	2.078	25.12	114.88	1.73
	0.001195	0.02384	19.95	1.32	1.374		2.50E-02	12.55	501.2	693.8	34.52		0.09718	1.939	19.95	107.2	1.374
	0.001279	0.02028	15.85	1.12	1.092		2.72E-02	10.82	398.1	597.94	27.42		0.1158	1.836	15.85	101.48	1.092
	0.0013	0.01637	12.59	0.91	0.8672		3.00E-02	9.47	316.2	523.55	21.78		0.1371	1.725	12.59	95.39	0.8672
	0.001395	0.01395	10	0.77	0.6888		3.31E-02	8.322	251.2	460.12	17.3		0.16	1.6	10	88.43	0.6888
	0.001505	0.01196	7.943	0.66	0.5472		3.66E-02	7.294	199.5	403.25	13.74		0.1788	1.421	7.944	78.53	0.5472
	0.001571	0.009914	6.31	0.55	0.4346		4.01E-02	6.362	158.5	351.71	10.92		0.209	1.319	6.31	72.9	0.4346
	0.001636	0.008197	5.012	0.45	0.3452		4.45E-02	5.599	125.9	309.57	8.672		0.2462	1.234	5.012	68.22	0.3452
	0.001884	0.007502	3.981	0.41	0.2742		5.00E-02	4.995	100	276.14	6.888		0.2958	1.178	3.981	65.1	0.2742
	0.002017	0.006378	3.162	0.35	0.2178		5.60E-02	4.446	79.43	245.82	5.472		0.351	1.11	3.162	61.37	0.2178
	0.002305	0.00579	2.512	0.32	0.173		6.17E-02	3.891	63.1	215.1	4.346		0.4142	1.04	2.512	57.52	0.173
	0.002143	0.004277	1.995	0.24	0.1374		7.08E-02	3.55	50.12	196.24	3.452		0.492	0.9817	1.995	54.28	0.1374
	0.002792	0.004424	1.585	0.24	0.1092		8.40E-02	3.344	39.81	184.89	2.742		0.6297	0.998	1.585	55.18	0.1092
	0.002977	0.003748	1.259	0.21	0.08672		9.70E-02	3.067	31.62	169.58	2.178		0.7924	0.9976	1.259	55.15	0.08672
	0.002657	0.002657	1	0.15	0.06888		1.13E-01	2.84	25.12	157.03	1.73		0.9534	0.9534	1	52.71	0.06888
Sample 5	0.006223	6.223	1000	344.04	68.88		1.29E-01	2.579	19.95	142.58	1.374	Sample 11	0.01939	19.39	1000	1072.02	68.88
	0.005485	4.357	794.3	240.86	54.72		1.48E-01	2.338	15.85	129.27	1.092		0.01926	15.3	794.3	845.68	54.72
	0.005019	3.167	631	175.09	43.46		1.68E-01	2.112	12.59	116.76	0.8672		0.01965	12.4	631	685.44	43.46
	0.004532	2.271	501.2	125.57	34.52		1.97E-01	1.967	10	108.74	0.6888		2.04E-02	10.2	501.2	564.13	34.52
	0.004164	1.658	398.1	91.64	27.42		2.38E-01	1.889	7.943	104.43	0.5472		0.02154	8.575	398.1	474.09	27.42
	0.004057	1.283	316.2	70.92	21.78		2.79E-01	1.759	6.31	97.22	0.4346		0.02302	7.28	316.2	402.48	21.78
	0.00429	1.078	251.2	59.58	17.3		3.41E-01	1.711	5.012	94.57	0.3452		0.02495	6.267	251.2	346.46	17.3
	0.004472	0.8923	199.5	49.33	13.74		4.44E-01	1.768	3.981	97.75	0.2742		0.02736	5.459	199.5	301.78	13.74
	0.004692	0.7436	158.5	41.11	10.92		5.33E-01	1.685	3.162	93.13	0.2178		0.03019	4.785	158.5	264.53	10.92
	0.004737	0.5964	125.9	32.97	8.672		6.98E-01	1.752	2.512	96.86	0.173		0.03322	4.183	125.9	231.24	8.672
	0.005018	0.5018	100	27.74	6.888		8.22E-01	1.64	1.995	90.65	0.1374		0.03659	3.659	100	202.29	6.888
	0.005369	0.4265	79.43	23.58	5.472		9.80E-01	1.553	1.585	85.87	0.1092		0.04018	3.192	79.43	176.47	5.472
	0.005001	0.3155	63.1	17.44	4.346		1.218	1.534	1.259	84.8	0.08671		0.04428	2.794	63.1	154.47	4.346
	0.005646	0.283	50.12	15.64	3.452		1.49	1.49	1	82.38	0.06889		0.04861	2.436	50.12	134.69	3.452
	0.0059	0.2349	39.81	12.99	2.742								0.05172	2.059	39.81	113.83	2.742
	0.006177	0.1953	31.62	10.8	2.178								0.05544	1.753	31.62	96.92	2.178
	0.007264	0.1825	25.12	10.09	1.73								0.06202	1.558	25.12	86.13	1.73

Table A.20 STB 500 RPM

Sample	Viscosity	Shear stress	Shear rate	Torque	Velocity	Sample	Viscosity	Shear stress	Shear rate	Torque	Velocity	Sample	Viscosity	Shear stress	Shear rate	Torque	Velocity
#	Pa.s	Pa	1/s	mN.m	rad/s	#	Pa.s	Pa	1/s	mN.m	rad/s	#	Pa.s	Pa	1/s	mN.m	rad/s
Sample 11	0.07122	1.421	19.95	78.57	1.374	Sample 13	0.02921	29.21	1000	1615.06	68.88	Sample 14	0.1476	2.945	19.95	162.82	1.374
	0.0833	1.32	15.85	72.99	1.092		0.02905	23.08	794.3	1275.89	54.72		0.1599	2.535	15.85	140.14	1.092
	0.09918	1.249	12.59	69.03	0.8672		0.02954	18.64	631	1030.59	43.46		0.1814	2.283	12.59	126.24	0.8672
	0.1194	1.194	10	66	0.6888		3.06E-02	15.33	501.2	847.33	34.52		0.2101	2.101	10	116.17	0.6888
	0.141	1.12	7.943	61.92	0.5472		0.03233	12.87	398.1	711.55	27.42		0.2463	1.957	7.943	108.18	0.5472
	0.1613	1.018	6.31	56.26	0.4346		0.03471	10.98	316.2	606.88	21.78		0.2888	1.822	6.31	100.73	0.4346
	0.1901	0.953	5.012	52.69	0.3452		0.03773	9.478	251.2	524.03	17.3		0.3387	1.697	5.012	93.84	0.3452
	0.216	0.8601	3.981	47.55	0.2742		0.04133	8.246	199.5	455.88	13.74		0.3952	1.573	3.981	86.98	0.2742
	0.2478	0.7835	3.162	43.32	0.2178		0.04531	7.181	158.5	397.01	10.92		0.4629	1.464	3.162	80.93	0.2178
	0.292	0.7336	2.512	40.56	0.173		0.05038	6.342	125.9	350.64	8.672		0.5512	1.385	2.512	76.55	0.173
	0.3464	0.6912	1.995	38.21	0.1374		0.05618	5.618	100	310.6	6.888		0.6752	1.347	1.995	74.49	0.1374
	0.4487	0.7112	1.585	39.32	0.1092		0.06259	4.972	79.43	274.87	5.472		0.8455	1.34	1.585	74.09	0.1092
	0.5597	0.7047	1.259	38.96	0.08673		0.07036	4.439	63.1	245.43	4.346		1.093	1.376	1.259	76.1	0.08672
	0.6808	0.6808	1	37.64	0.06888		0.07972	3.995	50.12	220.88	3.452		1.384	1.384	1	76.5	0.06888
Sample 12	0.02212	22.12	1000	1222.91	68.88		0.09035	3.597	39.81	198.86	2.742	Sample 15	0.03531	35.31	1000	1952.34	68.88
	0.02176	17.29	794.3	955.78	54.72		0.1027	3.248	31.62	179.58	2.178		0.03581	28.45	794.3	1572.76	54.72
	0.02189	13.81	631	763.61	43.46		0.1147	2.881	25.12	159.27	1.73		0.0371	23.41	631	1294.11	43.46
	2.25E-02	11.27	501.2	622.96	34.52		0.1249	2.491	19.95	137.74	1.374		3.93E-02	19.68	501.2	1088.15	34.52
	0.02336	9.298	398.1	514.07	27.42		0.1381	2.188	15.85	120.99	1.092		0.0423	16.84	398.1	931.02	27.42
	0.02471	7.813	316.2	431.97	21.78		0.1558	1.961	12.59	108.41	0.8672		0.04614	14.59	316.2	806.74	21.78
	0.02648	6.65	251.2	367.68	17.3		0.1799	1.799	10	99.43	0.6888		0.05065	12.72	251.2	703.43	17.3
	0.02871	5.728	199.5	316.68	13.74		0.2097	1.666	7.943	92.08	0.5472		0.05592	11.16	199.5	616.9	13.74
	0.03135	4.968	158.5	274.68	10.92		0.2466	1.556	6.31	86.02	0.4346		0.06214	9.849	158.5	544.5	10.92
	0.03445	4.337	125.9	239.79	8.672		0.2895	1.451	5.012	80.22	0.3452		0.06919	8.71	125.9	481.57	8.672
	0.0383	3.83	100	211.72	6.888		0.3389	1.349	3.981	74.58	0.2742		0.07721	7.721	100	426.85	6.888
	0.04284	3.403	79.43	188.15	5.472		0.399	1.262	3.162	69.75	0.2178		0.08661	6.88	79.43	380.36	5.472
	0.04788	3.021	63.1	167.02	4.346		0.4712	1.184	2.512	65.44	0.173		0.09767	6.163	63.1	340.7	4.346
	0.05387	2.7	50.12	149.28	3.452		0.586	1.169	1.995	64.64	0.1374		0.1104	5.534	50.12	305.96	3.452
	0.06075	2.419	39.81	133.71	2.742		0.7346	1.164	1.585	64.37	0.1092		0.1254	4.992	39.81	275.97	2.742
	0.06805	2.152	31.62	118.98	2.178		0.902	1.136	1.259	62.79	0.08672		0.1419	4.486	31.62	248.04	2.178
	0.07319	1.838	25.12	101.64	1.73		1.1	1.1	1	60.83	0.06888		0.158	3.97	25.12	219.48	1.73
	0.07958	1.588	19.95	87.79	1.374	Sample 14	0.03286	32.86	1000	1816.93	68.88		0.1695	3.383	19.95	187.02	1.374
	0.08922	1.414	15.85	78.18	1.092		0.03285	26.09	794.3	1442.42	54.72		0.1814	2.875	15.85	158.94	1.092
	0.1019	1.283	12.59	70.91	0.8672		0.0338	21.32	631	1178.88	43.46		0.2041	2.57	12.59	142.08	0.8672
	0.1183	1.183	10	65.39	0.6888		3.50E-02	17.55	501.2	970.26	34.52		0.2341	2.341	10	129.45	0.6888
	0.1386	1.101	7.943	60.86	0.5472		0.03686	14.68	398.1	811.33	27.42		0.2772	2.202	7.943	121.74	0.5472
	0.1637	1.033	6.31	57.09	0.4346		0.03937	12.45	316.2	688.25	21.78		0.3299	2.081	6.31	115.06	0.4346
	0.1943	0.9739	5.012	53.84	0.3452		0.04253	10.68	251.2	590.61	17.3		0.3904	1.956	5.012	108.16	0.3452
	0.2307	0.9183	3.981	50.77	0.2742		0.04623	9.225	199.5	510	13.74		0.4623	1.841	3.981	101.76	0.2742
	0.2725	0.8616	3.162	47.64	0.2178		0.05066	8.029	158.5	443.91	10.92		0.5515	1.744	3.162	96.41	0.2178
	0.3223	0.8097	2.512	44.76	0.173		0.05591	7.038	125.9	389.13	8.672		0.6705	1.684	2.512	93.12	0.173
	0.3758	0.7498	1.995	41.46	0.1374		0.06221	6.221	100	343.94	6.888		0.8197	1.635	1.995	90.42	0.1374
	0.4196	0.665	1.585	36.77	0.1092		0.06969	5.536	79.43	306.05	5.472		1.017	1.612	1.585	89.12	0.1092
	0.4676	0.5886	1.259	32.54	0.08672		0.07858	4.958	63.1	274.09	4.346		1.251	1.575	1.259	87.07	0.08672
	0.5231	0.5231	1	28.92	0.06888		0.0894	4.481	50.12	247.72	3.452		1.496	1.496	1	82.73	0.06888
							0.1025	4.082	39.81	225.65	2.742						
							0.1178	3.726	31.62	205.98	2.178						
							0.1338	3.361	25.12	185.8	1.73						

Table A.21 STB 500 RPM

Sample	Viscosity	Shear stress	Shear rate	Torque	Velocity	Sample	Viscosity	Shear stress	Shear rate	Torque	Velocity	Sample	Viscosity	Shear stress	Shear rate	Torque	Velocity
#	Pa.s	Pa	1/s	mN.m	rad/s	#	Pa.s	Pa	1/s	mN.m	rad/s	#	Pa.s	Pa	1/s	mN.m	rad/s
Sample 16	0.03431	34.31	1000	1896.71	68.88	Sample 17	0.1932	3.855	19.95	213.1	1.374	Sample 19	0.0184	18.4	1000	1017.03	68.88
	0.03445	27.36	794.3	1512.81	54.72		0.2122	3.362	15.85	185.89	1.092		0.01768	14.05	794.3	776.64	54.72
	0.03556	22.43	631	1240.27	43.46		0.2296	2.89	12.59	159.79	0.8672		0.01754	11.07	631	611.78	43.46
	3.75E-02	18.77	501.2	1037.93	34.52		0.2464	2.464	10	136.21	0.6888		1.76E-02	8.811	501.2	487.14	34.52
	0.04002	15.93	398.1	880.88	27.42		0.2731	2.169	7.943	119.94	0.5472		0.01813	7.219	398.1	399.12	27.42
	0.04326	13.68	316.2	756.3	21.78		0.313	1.975	6.31	109.18	0.4346		0.01858	5.877	316.2	324.91	21.78
	0.0471	11.83	251.2	654.03	17.3		0.3627	1.818	5.012	100.51	0.3452		0.01941	4.875	251.2	269.51	17.3
	0.05146	10.27	199.5	567.7	13.74		0.4243	1.689	3.981	93.38	0.2742		0.02059	4.109	199.5	227.15	13.74
	0.05657	8.965	158.5	495.64	10.92		0.5024	1.589	3.162	87.84	0.2178		0.02208	3.499	158.5	193.44	10.92
	0.0625	7.869	125.9	435.04	8.672		0.605	1.52	2.512	84.02	0.173		0.02407	3.03	125.9	167.54	8.672
	0.0695	6.95	100	384.26	6.888		0.7254	1.447	1.995	80.02	0.1374		0.02658	2.658	100	146.96	6.888
	0.07778	6.178	79.43	341.56	5.472		0.863	1.368	1.585	75.61	0.1092		0.02971	2.36	79.43	130.48	5.472
	0.08756	5.525	63.1	305.43	4.346		1.039	1.308	1.259	72.31	0.08672		0.03356	2.117	63.1	117.07	4.346
	0.09922	4.973	50.12	274.92	3.452		1.285	1.285	1	71.04	0.06888		0.03823	1.916	50.12	105.92	3.452
	0.1134	4.516	39.81	249.65	2.742	Sample 18	0.03317	33.17	1000	1833.96	68.88		0.04392	1.749	39.81	96.68	2.742
	0.1301	4.115	31.62	227.49	2.178		0.03282	26.07	794.3	1441.49	54.72		0.05097	1.612	31.62	89.1	2.178
	0.1491	3.746	25.12	207.1	1.73		0.03349	21.13	631	1168.39	43.46		0.05957	1.496	25.12	82.73	1.73
	0.1656	3.305	19.95	182.7	1.374		3.50E-02	17.54	501.2	969.62	34.52		0.07018	1.4	19.95	77.41	1.374
	0.1804	2.86	15.85	158.09	1.092		0.03731	14.85	398.1	821.21	27.42		0.08315	1.318	15.85	72.85	1.092
	0.2011	2.532	12.59	139.96	0.8672		0.04038	12.77	316.2	705.95	21.78		0.09827	1.237	12.59	68.4	0.8672
	0.2303	2.303	10	127.31	0.6888		0.04396	11.04	251.2	610.55	17.3		0.1163	1.163	10	64.29	0.6888
	0.2707	2.15	7.943	118.87	0.5472		0.04819	9.615	199.5	531.55	13.74		0.1377	1.094	7.943	60.46	0.5472
	0.3224	2.034	6.31	112.47	0.4346		0.05308	8.412	158.5	465.08	10.92		0.1622	1.023	6.31	56.57	0.4346
	0.3814	1.912	5.012	105.68	0.3452		0.0588	7.403	125.9	409.26	8.672		0.1903	0.9535	5.012	52.72	0.3452
	0.4507	1.794	3.981	99.2	0.2742		0.06538	6.538	100	361.47	6.888		0.2212	0.8806	3.981	48.68	0.2742
	0.5274	1.668	3.162	92.21	0.2178		0.073	5.798	79.43	320.57	5.472		0.2596	0.8208	3.162	45.38	0.2178
	0.6363	1.598	2.512	88.37	0.173		0.08215	5.183	63.1	286.56	4.346		0.3059	0.7685	2.512	42.48	0.173
	0.7823	1.561	1.995	86.29	0.1374		0.09273	4.648	50.12	256.95	3.452		0.3626	0.7235	1.995	40	0.1374
	0.9603	1.522	1.585	84.14	0.1092		0.1052	4.188	39.81	231.53	2.742		0.4402	0.6977	1.585	38.57	0.1092
	1.244	1.566	1.259	86.6	0.08672		0.1194	3.775	31.62	208.7	2.178		0.5357	0.6744	1.259	37.29	0.08672
	1.543	1.543	1	85.32	0.06888		0.135	3.39	25.12	187.41	1.73		0.6608	0.6608	1	36.53	0.06888
Sample 17	0.04045	40.45	1000	2236.55	68.88		0.1525	3.043	19.95	168.24	1.374						
	0.04107	32.62	794.3	1803.47	54.72		0.1695	2.686	15.85	148.52	1.092						
	0.04277	26.98	631	1491.83	43.46		0.1869	2.353	12.59	130.1	0.8672						
	4.53E-02	22.7	501.2	1254.81	34.52		0.2034	2.034	10	112.43	0.6888						
	0.04859	19.35	398.1	1069.56	27.42		0.2256	1.792	7.943	99.05	0.5472						
	0.05271	16.67	316.2	921.52	21.78		0.2572	1.623	6.31	89.71	0.4346						
	0.05754	14.45	251.2	799.1	17.3		0.3011	1.509	5.012	83.44	0.3452						
	0.06313	12.6	199.5	696.34	13.74		0.3556	1.416	3.981	78.26	0.2742						
	0.0697	11.05	158.5	610.76	10.92		0.4213	1.332	3.162	73.65	0.2178						
	0.0773	9.731	125.9	537.99	8.672		0.4962	1.246	2.512	68.91	0.173						
	0.08581	8.581	100	474.43	6.888		0.6112	1.22	1.995	67.43	0.1374						
	0.09571	7.602	79.43	420.31	5.472		0.7379	1.169	1.585	64.65	0.1092						
	0.1072	6.763	63.1	373.92	4.346		0.9191	1.157	1.259	63.97	0.08672						
	0.1207	6.049	50.12	334.41	3.452		1.119	1.119	1	61.86	0.06888						
	0.1361	5.42	39.81	299.65	2.742												
	0.1535	4.853	31.62	268.3	2.178												
	0.1724	4.329	25.12	239.35	1.73												

Table A.22 RPB 0.25 Hz

Sample #	Viscosity Pa.s	Shear stress Pa	Shear rate 1/s	Torque mN.m	Velocity rad/s	Sample #	Viscosity Pa.s	Shear stress Pa	Shear rate 1/s	Torque mN.m	Velocity rad/s	Sample #	Viscosity Pa.s	Shear stress Pa	Shear rate 1/s	Torque mN.m	Velocity rad/s
Sample 1	5.62E-03	5.619	1000	310.64	68.88	Sample 4	7.76E-03	7.763	1000	429.2	68.88	Sample 7	9.52E-03	9.517	1000	526.18	68.88
	3.52E-03	2.221	631	122.78	43.46		6.10E-03	3.846	631	212.62	43.46		8.29E-03	5.228	631	289.03	43.46
	2.49E-03	0.9926	398.1	54.88	27.42		5.48E-03	2.18	398.1	120.53	27.42		9.03E-03	3.595	398.1	198.76	27.42
	1.86E-03	0.467	251.2	25.82	17.3		5.88E-03	1.478	251.2	81.7	17.3		1.04E-02	2.615	251.2	144.6	17.3
	1.44E-03	0.228	158.5	12.61	10.92		5.96E-03	0.9447	158.5	52.23	10.92		1.27E-02	2.005	158.5	110.84	10.92
	1.26E-03	0.1258	100	6.96	6.888		6.39E-03	0.639	100	35.33	6.888		1.39E-02	1.392	100	76.98	6.888
	1.15E-03	0.07224	63.1	3.99	4.346		8.59E-03	0.5418	63.1	29.95	4.346		1.85E-02	1.169	63.1	64.62	4.346
	1.09E-03	0.0433	39.81	2.39	2.742		1.42E-02	0.5637	39.81	31.17	2.742		2.57E-02	1.023	39.81	56.54	2.742
	1.19E-03	0.02982	25.12	1.65	1.73		2.33E-02	0.584	25.12	32.29	1.73		3.78E-02	0.9485	25.12	52.44	1.73
	1.94E-03	3.07E-02	15.85	1.7	1.092		3.51E-02	0.556	15.85	30.74	1.092		5.88E-02	0.932	15.85	51.53	1.092
	3.11E-03	3.11E-02	10	1.72	0.6888		6.27E-02	0.6266	10	34.64	0.6889		8.74E-02	0.8735	10	48.3	0.6888
	7.77E-03	4.90E-02	6.309	2.71	0.4346		7.27E-02	0.4587	6.311	25.36	0.4347		1.28E-01	0.8091	6.31	44.73	0.4347
	1.92E-02	7.64E-02	3.981	4.22	0.2742		1.29E-01	0.5131	3.981	28.37	0.2742		1.56E-01	0.6227	3.981	34.43	0.2742
	1.95E-02	4.91E-02	2.512	2.71	0.173		1.92E-01	0.482	2.512	26.65	0.173		2.69E-01	0.6749	2.512	37.31	0.173
	2.69E-02	4.26E-02	1.585	2.35	0.1092		2.44E-01	0.3872	1.585	21.4	0.1092		4.07E-01	0.6442	1.585	35.62	0.1092
	6.16E-02	6.16E-02	1	3.4	0.06888		3.88E-01	0.388	1	21.45	0.06888		5.79E-01	0.579	1	32.01	0.06889
Sample 2	7.29E-03	7.286	1000	402.83	68.88	Sample 5	8.31E-03	8.307	1000	459.26	68.88	Sample 8	0.01089	10.89	1000	601.92	68.88
	5.88E-03	3.708	631	205.01	43.46		6.82E-03	4.305	631	238	43.46		0.01021	6.439	631	355.99	43.46
	5.27E-03	2.097	398.1	115.94	27.42		6.70E-03	2.665	398.1	147.35	27.42		0.011	4.38	398.1	242.16	27.42
	4.96E-03	1.245	251.2	68.85	17.3		7.38E-03	1.854	251.2	102.51	17.3		0.01275	3.202	251.2	177.05	17.3
	5.95E-03	0.9437	158.5	52.17	10.92		8.43E-03	1.335	158.5	73.83	10.92		0.01513	2.399	158.5	132.61	10.92
	7.22E-03	0.7217	100	39.9	6.888		9.21E-03	0.9213	100	50.93	6.888		0.0182	1.82	100	100.59	6.888
	1.04E-02	0.6551	63.1	36.22	4.346		0.01284	0.81	63.1	44.78	4.346		0.0212	1.337	63.1	73.94	4.346
	1.61E-02	0.6407	39.81	35.42	2.742		0.01973	0.7854	39.81	43.42	2.742		0.02749	1.094	39.81	60.51	2.742
	2.34E-02	0.588	25.12	32.51	1.73		0.03224	0.8099	25.12	44.77	1.73		0.03824	0.9605	25.12	53.1	1.73
	3.90E-02	0.6185	15.85	34.19	1.091		0.04845	0.7678	15.85	42.45	1.092		0.05398	0.8555	15.85	47.29	1.092
	5.87E-02	0.5872	9.999	32.47	0.6888		0.08453	0.8452	9.999	46.73	0.6887		0.0728	0.728	10	40.25	0.6888
	9.07E-02	0.5724	6.309	31.64	0.4346		0.1174	0.7409	6.31	40.96	0.4347		0.09673	0.6104	6.31	33.74	0.4346
	1.38E-01	0.5476	3.981	30.27	0.2742		0.1795	0.7146	3.981	39.51	0.2742		0.1335	0.5314	3.981	29.38	0.2742
	2.38E-01	0.5974	2.512	33.03	0.173		0.2726	0.6847	2.512	37.86	0.173		0.2068	0.5194	2.512	28.72	0.173
	2.72E-01	0.4307	1.585	23.81	0.1092		0.3815	0.6046	1.585	33.42	0.1092		0.331	0.5246	1.585	29	0.1092
	3.85E-01	0.3848	1	21.28	0.06888		0.4841	0.4841	1	26.76	0.06888		0.5157	0.5157	1	28.51	0.06888
Sample 3	7.66E-03	7.658	1000	423.4	68.88	Sample 6	7.16E-03	7.16	1000	395.83	68.88	Sample 9	0.01118	11.18	1000	618.07	68.88
	5.88E-03	3.707	631	204.95	43.46		5.93E-03	3.739	631	206.69	43.46		0.01051	6.63	631	366.57	43.46
	5.63E-03	2.242	398.1	123.96	27.42		5.33E-03	2.123	398.1	117.36	27.42		0.01108	4.411	398.1	243.88	27.42
	6.43E-03	1.614	251.2	89.22	17.3		5.60E-03	1.405	251.2	77.7	17.3		1.28E-02	3.221	251.2	178.06	17.3
	7.35E-03	1.165	158.5	64.4	10.92		5.87E-03	0.9302	158.5	51.42	10.92		0.01579	2.503	158.5	138.38	10.92
	8.70E-03	0.8703	100	48.12	6.888		6.32E-03	0.6317	100	34.92	6.888		0.01959	1.959	100	108.31	6.888
	1.14E-02	0.7187	63.1	39.74	4.346		7.40E-03	0.4671	63.1	25.82	4.346		0.02402	1.516	63.1	83.79	4.346
	1.69E-02	0.6707	39.81	37.08	2.742		1.07E-02	0.4272	39.81	23.62	2.742		0.02848	1.134	39.81	62.69	2.742
	2.61E-02	0.6555	25.12	36.24	1.731		1.42E-02	0.3574	25.12	19.76	1.73		0.03808	0.9565	25.12	52.88	1.73
	4.19E-02	0.6641	15.85	36.71	1.092		2.11E-02	0.3342	15.85	18.48	1.092		0.0528	0.8369	15.85	46.27	1.092
	6.65E-02	0.6646	10	36.74	0.6889		3.51E-02	0.3513	10	19.42	0.6889		0.0736	0.736	10	40.69	0.6888
	1.27E-01	0.7981	6.309	44.12	0.4346		5.91E-02	0.3726	6.309	20.6	0.4346		0.09773	0.6166	6.309	34.09	0.4346
	1.56E-01	0.6226	3.981	34.42	0.2742		9.45E-02	0.3762	3.981	20.8	0.2743		0.1305	0.5194	3.981	28.72	0.2742
	1.63E-01	0.4087	2.512	22.6	0.173		1.35E-01	0.3385	2.512	18.71	0.173		0.1878	0.4717	2.512	26.08	0.173
	6.24E-01	0.9889	1.585	54.67	0.1092		2.30E-01	0.3644	1.585	20.14	0.1092		0.2942	0.4663	1.585	25.78	0.1092
	6.52E-01	0.652	1	36.05	0.06888		3.16E-01	0.3154	1	17.44	0.06888		0.4414	0.4414	1	24.4	0.06888

Table A.23 RPB 0.25 Hz

Sample #	Viscosity Pa.s	Shear stress Pa	Shear rate 1/s	Torque mN.m	Velocity rad/s	Sample #	Viscosity Pa.s	Shear stress Pa	Shear rate 1/s	Torque mN.m	Velocity rad/s	Sample #	Viscosity Pa.s	Shear stress Pa	Shear rate 1/s	Torque mN.m	Velocity rad/s
Sample 10	0.01085	10.85	1000	600.13	68.88	Sample 13	9.32E-03	9.321	1000	515.33	68.88	Sample 16	8.64E-03	8.641	1000	477.73	68.88
	9.60E-03	6.059	631	334.99	43.46		7.56E-03	4.767	631	263.54	43.46		6.70E-03	4.228	631	233.75	43.46
	9.95E-03	3.959	398.1	218.9	27.42		7.59E-03	3.02	398.1	166.94	27.42		6.01E-03	2.392	398.1	132.24	27.42
	1.12E-02	2.808	251.2	155.23	17.3		8.19E-03	2.058	251.2	113.77	17.3		6.28E-03	1.577	251.2	87.2	17.3
	0.01321	2.093	158.5	115.73	10.92		9.08E-03	1.44	158.5	79.6	10.92		6.55E-03	1.037	158.5	57.36	10.92
	0.01643	1.643	100	90.83	6.888		0.01024	1.024	100	56.59	6.888		7.14E-03	0.7139	100	39.47	6.888
	0.02044	1.29	63.1	71.31	4.346		0.01225	0.7728	63.1	42.73	4.346		8.24E-03	0.5198	63.1	28.74	4.346
	0.02513	1	39.81	55.31	2.742		0.01523	0.6064	39.81	33.53	2.742		0.01025	0.4083	39.81	22.57	2.742
	0.03018	0.7582	25.12	41.92	1.73		0.01957	0.4915	25.12	27.17	1.73		0.01312	0.3296	25.12	18.22	1.73
	0.04076	0.646	15.85	35.71	1.092		0.02508	0.3976	15.85	21.98	1.092		0.01792	0.284	15.85	15.7	1.092
	0.057	0.57	10	31.51	0.6888		0.03259	0.3259	10	18.02	0.6888		0.02394	0.2394	10	13.23	0.6888
	0.08007	0.5052	6.309	27.93	0.4346		0.04496	0.2837	6.31	15.68	0.4346		0.03329	0.2101	6.31	11.61	0.4346
	0.1054	0.4197	3.981	23.2	0.2742		0.06607	0.263	3.981	14.54	0.2742		0.04911	0.1955	3.981	10.81	0.2742
	0.1389	0.3488	2.512	19.29	0.173		0.09324	0.2342	2.512	12.95	0.173		0.07465	0.1875	2.512	10.37	0.173
	0.1936	0.3069	1.585	16.97	0.1092		0.1336	0.2118	1.585	11.71	0.1092		0.1124	0.1781	1.585	9.84	0.1092
	0.3122	0.3122	1	17.26	0.06889		0.1927	0.1927	1	10.65	0.06888		0.1411	0.1411	1	7.8	0.06888
Sample 11	0.01093	10.93	1000	604.45	68.88	Sample 14	9.03E-03	9.033	1000	499.4	68.88	Sample 17	8.34E-03	8.341	1000	461.13	68.88
	9.43E-03	5.948	631	328.82	43.46		7.27E-03	4.585	631	253.5	43.46		6.36E-03	4.01	631	221.69	43.46
	9.72E-03	3.871	398.1	213.99	27.42		6.91E-03	2.75	398.1	152.05	27.42		5.41E-03	2.152	398.1	118.98	27.42
	1.10E-02	2.763	251.2	152.78	17.3		7.36E-03	1.849	251.2	102.23	17.3		5.65E-03	1.419	251.2	78.47	17.3
	0.01234	1.956	158.5	108.14	10.92		7.99E-03	1.267	158.5	70.04	10.92		5.87E-03	0.9297	158.5	51.4	10.92
	0.01494	1.494	100	82.61	6.888		8.99E-03	0.899	100	49.7	6.888		6.26E-03	0.626	100	34.61	6.888
	0.01834	1.157	63.1	63.99	4.346		0.01059	0.6685	63.1	36.96	4.346		7.14E-03	0.4508	63.1	24.92	4.346
	0.0228	0.9076	39.81	50.18	2.742		0.01306	0.5198	39.81	28.74	2.742		8.82E-03	0.3512	39.81	19.42	2.742
	0.02702	0.6787	25.12	37.52	1.73		0.01685	0.4232	25.12	23.4	1.73		0.01156	0.2904	25.12	16.05	1.73
	0.0356	0.5643	15.85	31.2	1.092		0.02234	0.354	15.85	19.57	1.092		0.01601	0.2538	15.85	14.03	1.092
	0.0488	0.488	10	26.98	0.6888		0.02874	0.2874	10	15.89	0.6888		0.02172	0.2172	10	12.01	0.6888
	0.06899	0.4353	6.31	24.07	0.4346		0.03947	0.249	6.31	13.77	0.4346		0.0305	0.1925	6.31	10.64	0.4346
	0.09651	0.3842	3.981	21.24	0.2742		0.05789	0.2305	3.981	12.74	0.2742		0.04549	0.1811	3.981	10.01	0.2742
	0.131	0.3292	2.512	18.2	0.173		0.08467	0.2127	2.512	11.76	0.173		0.06771	0.1701	2.512	9.4	0.173
	0.1836	0.291	1.585	16.09	0.1092		0.1198	0.1898	1.585	10.49	0.1092		0.1006	0.1595	1.585	8.82	0.1092
	0.2696	0.2696	1	14.91	0.06888		0.1811	0.1811	1	10.01	0.06889		0.1392	0.1392	1	7.7	0.06888
Sample 12	0.01007	10.07	1000	556.83	68.88	Sample 15	8.89E-03	8.889	1000	491.43	68.88	Sample 18	8.81E-03	8.807	1000	486.92	68.88
	8.48E-03	5.353	631	295.96	43.46		6.93E-03	4.371	631	241.66	43.46		7.23E-03	4.559	631	252.05	43.46
	8.54E-03	3.4	398.1	187.98	27.42		6.42E-03	2.556	398.1	141.3	27.42		6.36E-03	2.531	398.1	139.95	27.42
	9.26E-03	2.326	251.2	128.59	17.3		6.89E-03	1.73	251.2	95.66	17.3		6.67E-03	1.675	251.2	92.58	17.3
	0.0104	1.648	158.5	91.14	10.92		7.28E-03	1.153	158.5	63.76	10.92		6.89E-03	1.092	158.5	60.36	10.92
	0.0122	1.22	100	67.44	6.888		7.96E-03	0.7959	100	44	6.888		7.20E-03	0.72	100	39.81	6.888
	0.01484	0.9365	63.1	51.78	4.346		9.39E-03	0.5922	63.1	32.74	4.346		7.86E-03	0.4961	63.1	27.43	4.346
	0.0186	0.7407	39.81	40.95	2.742		0.01163	0.4631	39.81	25.6	2.742		9.17E-03	0.365	39.81	20.18	2.742
	0.02368	0.5948	25.12	32.88	1.73		0.01511	0.3797	25.12	20.99	1.73		0.01138	0.286	25.12	15.81	1.73
	0.0291	0.4612	15.85	25.5	1.092		0.02003	0.3175	15.85	17.55	1.092		0.01526	0.2419	15.85	13.37	1.092
	0.03865	0.3865	10	21.37	0.6888		0.02656	0.2656	10	14.68	0.6888		0.02096	0.2096	10	11.59	0.6888
	0.05608	0.3538	6.309	19.56	0.4346		0.03696	0.2332	6.31	12.89	0.4346		0.02902	0.1831	6.31	10.12	0.4346
	0.07569	0.3013	3.981	16.66	0.2742		0.05389	0.2145	3.981	11.86	0.2742		0.04092	0.1629	3.981	9.01	0.2742
	0.1136	0.2853	2.512	15.77	0.173		0.08249	0.2072	2.512	11.46	0.173		0.06	0.1507	2.512	8.33	0.173
	0.1506	0.2388	1.585	13.2	0.1092		0.111	0.1759	1.585	9.73	0.1092		0.09037	0.1432	1.585	7.92	0.1092
	0.2005	0.2005	1	11.09	0.06889		0.162	0.162	1	8.96	0.06888		0.124	0.124	1	6.86	0.06888

Table A.24 RPB 0.25 Hz

Sample	Viscosity	Shear stress	Shear rate	Torque	Velocity
#	Pa.s	Pa	1/s	mN.m	rad/s
Sample 19	7.93E-03	7.933	1000	438.6	68.88
	5.93E-03	3.744	631	207	43.46
	4.68E-03	1.864	398.1	103.05	27.42
	4.55E-03	1.143	251.2	63.21	17.3
	4.59E-03	0.7268	158.5	40.18	10.92
	4.85E-03	0.4852	100	26.82	6.888
	5.44E-03	0.3435	63.1	18.99	4.346
	6.71E-03	0.267	39.81	14.76	2.742
	8.89E-03	0.2233	25.12	12.35	1.73
	0.01251	0.1982	15.85	10.96	1.092
	0.01789	0.1789	10	9.89	0.6888
	0.02549	0.1608	6.31	8.89	0.4346
	0.03733	0.1486	3.981	8.22	0.2742
	0.05599	0.1406	2.512	7.78	0.173
	0.08421	0.1335	1.585	7.38	0.1092
	0.1172	0.1172	1	6.48	0.06888
Sample 20	7.76E-03	7.756	1000	428.78	68.88
	5.65E-03	3.568	631	197.24	43.46
	4.58E-03	1.822	398.1	100.72	27.42
	4.10E-03	1.029	251.2	56.88	17.3
	4.14E-03	0.6562	158.5	36.28	10.92
	4.33E-03	0.4327	100	23.92	6.888
	4.81E-03	0.3033	63.1	16.77	4.346
	5.83E-03	0.2319	39.81	12.82	2.742
	7.72E-03	0.1939	25.12	10.72	1.73
	0.01089	0.1726	15.85	9.54	1.092
	0.01569	0.1569	10	8.67	0.6888
	0.02263	0.1428	6.31	7.89	0.4346
	0.03365	0.134	3.981	7.41	0.2742
	0.0492	0.1236	2.512	6.83	0.173
	0.07592	0.1203	1.585	6.65	0.1092
	0.1099	0.1099	1	6.08	0.06888
Sample 21	7.66E-03	7.658	1000	423.39	68.88
	5.53E-03	3.489	631	192.89	43.46
	4.44E-03	1.768	398.1	97.72	27.42
	3.88E-03	0.9734	251.2	53.82	17.3
	3.73E-03	0.5911	158.5	32.68	10.92
	3.87E-03	0.3871	100	21.4	6.888
	4.28E-03	0.2701	63.1	14.93	4.346
	5.26E-03	0.2096	39.81	11.59	2.742
	7.13E-03	0.1792	25.12	9.9	1.73
	0.0102	0.1616	15.85	8.93	1.092
	0.0151	0.151	10	8.35	0.6888
	0.02215	0.1398	6.31	7.73	0.4346
	0.03246	0.1292	3.981	7.14	0.2742
	0.0484	0.1216	2.512	6.72	0.173
	0.07307	0.1158	1.585	6.4	0.1092
	0.1088	0.1088	1	6.02	0.06888

Table A.25 RPB 0.5 Hz

Sample	Viscosity	Shear stress	Shear rate	Torque	Velocity	Sample	Viscosity	Shear stress	Shear rate	Torque	Velocity	Sample	Viscosity	Shear stress	Shear rate	Torque	Velocity
#	Pa.s	Pa	1/s	mN.m	rad/s	#	Pa.s	Pa	1/s	mN.m	rad/s	#	Pa.s	Pa	1/s	mN.m	rad/s
Sample 1	5.63E-03	5.625	1000	310.98	68.88	Sample 7	7.59E-03	7.593	1000	419.78	68.88	Sample 11	0.01114	11.14	1000	616.12	68.88
	4.01E-03	2.885	719.7	159.49	49.57		6.53E-03	4.697	719.7	259.7	49.57		0.01082	7.789	719.7	430.63	49.57
	3.02E-03	1.565	517.9	86.54	35.68		5.68E-03	2.941	517.9	162.61	35.68		0.01127	5.837	517.9	322.71	35.68
	2.43E-03	0.9057	372.8	50.07	25.68		5.17E-03	1.927	372.8	106.54	25.68		1.20E-02	4.469	372.8	247.08	25.68
	2.04E-03	0.5481	268.3	30.3	18.48		5.03E-03	1.35	268.3	74.64	18.48		0.01305	3.5	268.3	193.52	18.48
	1.74E-03	0.3358	193.1	18.57	13.3		4.81E-03	0.929	193.1	51.36	13.3		0.01435	2.77	193.1	153.13	13.3
	1.55E-03	0.2149	138.9	11.88	9.571		4.94E-03	0.6867	138.9	37.96	9.571		0.01641	2.28	139	126.04	9.571
	1.43E-03	0.1428	100	7.9	6.888		5.03E-03	0.5029	100	27.8	6.888		0.0194	1.94	100	107.28	6.888
	1.31E-03	0.09452	71.97	5.23	4.957		7.00E-03	0.5035	71.97	27.83	4.957		0.02268	1.632	71.97	90.22	4.957
	1.22E-03	0.06324	51.79	3.5	3.568		9.59E-03	0.4964	51.79	27.44	3.568		0.02791	1.446	51.8	79.93	3.568
	1.32E-03	0.04933	37.28	2.73	2.568		0.01296	0.483	37.28	26.71	2.568		0.0348	1.297	37.28	71.72	2.568
	1.46E-03	0.03912	26.83	2.16	1.848		0.01808	0.485	26.83	26.81	1.848		0.04521	1.213	26.83	67.06	1.848
	1.49E-03	0.02874	19.31	1.59	1.33		0.02936	0.5671	19.31	31.35	1.33		0.05738	1.108	19.31	61.25	1.33
	9.70E-03	0.1347	13.9	7.45	0.9572		0.05381	0.7477	13.9	41.34	0.9571		0.07685	1.068	13.89	59.03	0.9571
	0.01031	0.1031	10	5.7	0.6888		0.09256	0.9256	9.999	51.17	0.6888		0.1178	1.178	10	65.1	0.6888
	0.01186	0.08536	7.198	4.72	0.4958		0.1118	0.8046	7.197	44.49	0.4958		0.1621	1.167	7.196	64.5	0.4957
	0.01519	0.07865	5.179	4.35	0.3567		0.1119	0.5793	5.18	32.03	0.3568		0.2129	1.103	5.179	60.97	0.3568
	0.02373	0.08844	3.727	4.89	0.2567		0.1576	0.5874	3.727	32.48	0.2567		0.2677	0.9979	3.728	55.17	0.2568
	0.0238	0.06384	2.682	3.53	0.1848		0.1611	0.432	2.683	23.89	0.1848		0.3799	1.019	2.683	56.34	0.1848
	0.03448	0.06658	1.931	3.68	0.133		0.3985	0.7694	1.931	42.54	0.133		0.4553	0.879	1.931	48.6	0.133
	0.03955	0.05495	1.39	3.04	0.09571		0.6485	0.9012	1.39	49.82	0.09572		0.5772	0.802	1.389	44.34	0.09571
	0.04858	0.04858	1	2.69	0.06888		0.6114	0.6114	1	33.8	0.06888		0.7039	0.7039	1	38.92	0.06888
Sample 4	6.83E-03	6.834	1000	377.85	68.88	Sample 9	9.29E-03	9.294	1000	513.83	68.88	Sample 12	0.01381	13.81	1000	763.58	68.88
	5.63E-03	4.054	719.7	224.12	49.57		7.91E-03	5.695	719.7	314.86	49.57		0.01405	10.11	719.7	559.01	49.57
	4.83E-03	2.502	517.9	138.35	35.68		7.73E-03	4.002	517.9	221.23	35.68		0.01496	7.747	517.9	428.33	35.68
	4.55E-03	1.697	372.8	93.8	25.68		8.01E-03	2.987	372.8	165.15	25.68		1.64E-02	6.098	372.8	337.12	25.68
	5.92E-03	1.589	268.3	87.84	18.48		8.65E-03	2.319	268.3	128.22	18.48		0.0185	4.964	268.3	274.45	18.48
	6.70E-03	1.293	193.1	71.49	13.3		9.29E-03	1.793	193.1	99.12	13.3		0.02126	4.105	193.1	226.96	13.3
	9.31E-03	1.293	138.9	71.51	9.571		9.96E-03	1.384	138.9	76.54	9.571		0.02482	3.449	138.9	190.67	9.571
	8.62E-03	0.8619	100	47.65	6.888		0.01041	1.041	100	57.56	6.888		0.02916	2.916	100	161.23	6.888
	1.11E-02	0.795	71.97	43.95	4.957		0.01167	0.8396	71.97	46.42	4.957		0.03424	2.464	71.97	136.24	4.957
	1.56E-02	0.8067	51.79	44.6	3.568		0.01451	0.7517	51.8	41.56	3.568		0.0405	2.098	51.8	115.98	3.568
	1.57E-02	0.5848	37.28	32.33	2.568		0.02013	0.7503	37.28	41.48	2.568		0.0456	1.7	37.28	93.97	2.568
	1.81E-02	0.4868	26.83	26.91	1.848		0.02781	0.7459	26.82	41.24	1.848		0.05634	1.511	26.83	83.56	1.848
	2.16E-02	0.4167	19.31	23.04	1.33		0.04222	0.8151	19.3	45.06	1.33		0.06886	1.329	19.31	73.5	1.33
	3.01E-02	0.418	13.89	23.11	0.9571		0.05992	0.8324	13.89	46.02	0.957		0.08629	1.199	13.9	66.29	0.9571
	3.25E-02	0.3249	10	17.96	0.6888		0.08403	0.8402	10	46.45	0.6888		0.1041	1.041	10	57.55	0.6888
	3.86E-02	0.278	7.196	15.37	0.4957		0.1134	0.8162	7.199	45.12	0.4959		0.1278	0.9197	7.197	50.85	0.4957
	4.97E-02	0.2575	5.179	14.24	0.3568		0.1651	0.8551	5.179	47.27	0.3567		0.1638	0.8484	5.18	46.91	0.3568
	1.11E-01	0.4125	3.728	22.8	0.2568		0.1884	0.7021	3.727	38.82	0.2567		0.208	0.7752	3.728	42.86	0.2568
	9.10E-02	0.2441	2.683	13.49	0.1848		0.2276	0.6106	2.682	33.76	0.1848		0.3063	0.8218	2.683	45.44	0.1848
	9.46E-02	0.1826	1.931	10.1	0.133		0.3626	0.7002	1.931	38.71	0.133		0.3854	0.744	1.931	41.13	0.133
	1.09E-01	0.1519	1.389	8.4	0.09571		0.4617	0.6415	1.389	35.46	0.09571		0.4829	0.6709	1.39	37.09	0.09571
	2.16E-01	0.2158	1	11.93	0.06888		0.7036	0.7036	1	38.9	0.06888		0.7164	0.7164	1	39.61	0.06888

Table A.26 RPB 0.5 Hz

Sample	Viscosity	Shear stress	Shear rate	Torque	Velocity	Sample	Viscosity	Shear stress	Shear rate	Torque	Velocity	Sample	Viscosity	Shear stress	Shear rate	Torque	Velocity
#	Pa.s	Pa	1/s	mN.m	rad/s	#	Pa.s	Pa	1/s	mN.m	rad/s	#	Pa.s	Pa	1/s	mN.m	rad/s
Sample 13	0.01423	14.23	1000	786.68	68.88	Sample 15	0.01311	13.11	1000	724.78	68.88	Sample 17	0.01897	18.97	1000	1048.89	68.88
	0.0143	10.29	719.7	568.97	49.57		0.01262	9.08	719.7	501.99	49.57		0.01888	13.58	719.7	751.01	49.57
	0.01521	7.876	517.9	435.41	35.68		0.01296	6.711	517.9	371.03	35.68		0.01971	10.21	517.9	564.43	35.68
	1.66E-02	6.185	372.8	341.93	25.68		1.39E-02	5.169	372.8	285.8	25.68		2.09E-02	7.806	372.8	431.56	25.68
	0.01882	5.049	268.3	279.15	18.48		0.01528	4.098	268.3	226.56	18.48		0.02313	6.205	268.3	343.04	18.48
	0.02177	4.203	193.1	232.39	13.3		0.01722	3.324	193.1	183.75	13.3		0.02637	5.091	193.1	281.46	13.3
	0.02548	3.541	138.9	195.77	9.571		0.01971	2.739	138.9	151.44	9.571		0.03024	4.202	138.9	232.29	9.571
	0.03003	3.003	100	166.03	6.888		0.02284	2.284	100	126.3	6.888		0.03535	3.535	100	195.43	6.888
	0.03559	2.562	71.97	141.62	4.957		0.02674	1.924	71.97	106.39	4.957		0.04352	3.132	71.97	173.17	4.957
	0.04158	2.154	51.79	119.07	3.568		0.03158	1.635	51.79	90.42	3.568		0.05034	2.607	51.79	144.16	3.568
	0.04851	1.808	37.28	99.96	2.568		0.03723	1.388	37.28	76.73	2.568		0.06139	2.288	37.28	126.51	2.568
	0.05575	1.496	26.83	82.69	1.848		0.04423	1.187	26.83	65.6	1.848		0.07291	1.956	26.83	108.14	1.848
	0.06795	1.312	19.31	72.53	1.33		0.04989	0.9631	19.31	53.25	1.33		0.08523	1.645	19.31	90.97	1.33
	0.08507	1.182	13.89	65.35	0.9571		0.06056	0.8414	13.89	46.52	0.9571		0.1048	1.456	13.9	80.51	0.9572
	0.1091	1.091	10	60.33	0.6888		0.07651	0.7651	10	42.3	0.6888		0.1339	1.339	10	74	0.6888
	0.1354	0.9747	7.197	53.89	0.4957		0.09854	0.7092	7.197	39.21	0.4957		0.1764	1.27	7.197	70.19	0.4957
	0.1662	0.8608	5.18	47.59	0.3568		0.1269	0.6571	5.179	36.33	0.3568		0.2383	1.234	5.179	68.24	0.3568
	0.2007	0.748	3.728	41.36	0.2568		0.1626	0.606	3.728	33.5	0.2568		0.3109	1.159	3.728	64.07	0.2568
	0.2581	0.6923	2.683	38.28	0.1848		0.1998	0.5361	2.683	29.64	0.1848		0.3539	0.9494	2.683	52.49	0.1848
	0.3333	0.6435	1.931	35.58	0.133		0.2381	0.4597	1.931	25.42	0.133		0.4617	0.8914	1.931	49.28	0.133
	0.4736	0.6581	1.389	36.38	0.09571		0.3036	0.4218	1.39	23.32	0.09571		0.5987	0.8318	1.39	45.99	0.09572
	0.6336	0.6336	1	35.03	0.06889		0.3808	0.3808	1	21.05	0.06889		1.057	1.057	1	58.45	0.06889
Sample 14	0.01311	13.11	1000	724.54	68.88	Sample 16	0.01382	13.82	1000	763.9	68.88	Sample 18	0.01562	15.62	1000	863.84	68.88
	0.01292	9.298	719.7	514.06	49.57		0.01338	9.633	719.7	532.56	49.57		0.01441	10.37	719.7	573.45	49.57
	0.01336	6.918	517.9	382.48	35.68		0.01362	7.055	517.9	390.05	35.68		0.0146	7.562	517.9	418.1	35.68
	1.45E-02	5.397	372.8	298.38	25.68		1.47E-02	5.48	372.8	302.98	25.68		1.54E-02	5.754	372.8	318.13	25.68
	0.0162	4.347	268.3	240.32	18.48		0.01594	4.277	268.3	236.45	18.48		0.01687	4.525	268.3	250.2	18.48
	0.01836	3.545	193.1	196.01	13.3		0.01771	3.419	193.1	189	13.3		0.01892	3.654	193.1	202	13.3
	0.02124	2.951	138.9	163.15	9.571		0.01971	2.739	138.9	151.4	9.571		0.02178	3.026	138.9	167.28	9.571
	0.02476	2.476	100	136.9	6.888		0.02267	2.267	100	125.32	6.888		0.02552	2.552	100	141.08	6.888
	0.02914	2.097	71.97	115.96	4.957		0.02835	2.04	71.97	112.81	4.957		0.0302	2.173	71.97	120.15	4.957
	0.03436	1.78	51.79	98.4	3.568		0.03162	1.638	51.79	90.55	3.568		0.0362	1.875	51.79	103.65	3.568
	0.04039	1.506	37.28	83.24	2.568		0.03766	1.404	37.27	77.6	2.568		0.04389	1.636	37.28	90.45	2.568
	0.04665	1.252	26.83	69.19	1.848		0.04345	1.166	26.83	64.44	1.848		0.05407	1.451	26.83	80.2	1.848
	0.05415	1.045	19.31	57.8	1.33		0.04669	0.9014	19.31	49.83	1.33		0.06721	1.298	19.31	71.74	1.33
	0.06745	0.9373	13.89	51.82	0.9571		0.05704	0.7926	13.89	43.82	0.9571		0.08437	1.172	13.89	64.82	0.9571
	0.08587	0.8587	10	47.48	0.6888		0.07275	0.7275	10	40.22	0.6888		0.1048	1.048	10	57.93	0.6889
	0.1112	0.8002	7.197	44.24	0.4957		0.0945	0.6801	7.197	37.6	0.4957		0.1308	0.9414	7.197	52.05	0.4958
	0.1432	0.7417	5.179	41	0.3568		0.1249	0.6471	5.179	35.78	0.3568		0.1667	0.8634	5.18	47.74	0.3568
	0.1782	0.6644	3.728	36.73	0.2568		0.158	0.5888	3.728	32.55	0.2568		0.2191	0.8166	3.728	45.15	0.2568
	0.2065	0.554	2.683	30.63	0.1848		0.188	0.5044	2.683	27.89	0.1848		0.2909	0.7803	2.683	43.14	0.1848
	0.2603	0.5026	1.931	27.79	0.133		0.225	0.4345	1.931	24.02	0.133		0.3829	0.7393	1.931	40.87	0.133
	0.3589	0.4988	1.39	27.57	0.09571		0.2935	0.4078	1.39	22.55	0.09572		0.5131	0.713	1.39	39.42	0.09572
	0.4893	0.4893	1	27.05	0.06888		0.4054	0.4054	1	22.41	0.06889		0.6156	0.6156	1	34.03	0.06888

Table A.27 RPB 0.75 Hz

Sample	Viscosity	Shear stress	Shear rate	Torque	Velocity	Sample	Viscosity	Shear stress	Shear rate	Torque	Velocity	Sample	Viscosity	Shear stress	Shear rate	Torque	Velocity
#	Pa.s	Pa	1/s	mN.m	rad/s	#	Pa.s	Pa	1/s	mN.m	rad/s	#	Pa.s	Pa	1/s	mN.m	rad/s
Sample 1	3.39E-03	3.387	1000	187.27	68.88	Sample 4	2.40E-02	0.06037	2.512	3.34	0.173	Sample 6	0.07901	0.6277	7.944	34.7	0.5472
	2.94E-03	2.115	719.7	116.93	49.57		2.81E-02	0.05602	1.995	3.1	0.1374		0.0989	0.6239	6.309	34.49	0.4346
	2.53E-03	1.309	517.9	72.4	35.68		3.30E-02	0.05226	1.585	2.89	0.1092		0.1283	0.6429	5.012	35.54	0.3452
	2.16E-03	0.8037	372.8	44.44	25.68		3.83E-02	0.04816	1.259	2.66	0.08672		0.1454	0.5787	3.981	32	0.2742
	1.81E-03	0.4849	268.3	26.81	18.48		4.88E-02	0.04877	1	2.7	0.06888		0.1791	0.5662	3.162	31.3	0.2178
	1.45E-03	0.2801	193.1	15.49	13.3	Sample 5	6.18E-03	6.176	1000	341.44	68.88		0.2255	0.5663	2.512	31.31	0.173
	1.07E-03	0.1483	138.9	8.2	9.571		4.95E-03	3.562	719.7	196.91	49.57		0.2777	0.5541	1.995	30.63	0.1374
	1.03E-03	0.1034	100	5.72	6.888		4.35E-03	2.254	517.9	124.64	35.68		0.3386	0.5366	1.585	29.67	0.1092
	1.01E-03	0.07266	71.97	4.02	4.957		4.26E-03	1.589	372.8	87.84	25.68		0.3613	0.4548	1.259	25.15	0.08672
	9.89E-04	0.05121	51.79	2.83	3.568		4.36E-03	1.168	268.3	64.58	18.48		0.4516	0.4516	1	24.97	0.06889
	9.85E-04	0.03673	37.28	2.03	2.568		4.64E-03	0.8961	193.1	49.54	13.3	Sample 8	0.01673	16.73	1000	925.01	68.88
	9.77E-04	0.02621	26.83	1.45	1.848		5.28E-03	0.7331	138.9	40.53	9.571		0.01736	13.79	794.3	762.15	54.72
	9.86E-04	0.01903	19.31	1.05	1.33		4.55E-03	0.4552	100	25.17	6.888		0.01817	11.46	631	633.68	43.46
	9.95E-04	0.01382	13.89	0.76	0.9571		4.68E-03	0.3369	71.97	18.63	4.957		1.95E-02	9.766	501.2	539.92	34.52
	1.01E-03	0.01009	10	0.56	0.6888		4.93E-03	0.2551	51.79	14.1	3.568		0.02082	8.288	398.1	458.21	27.42
	1.03E-03	7.41E-03	7.197	0.41	0.4957		5.91E-03	0.2203	37.28	12.18	2.568		0.02235	7.067	316.2	390.71	21.78
	1.03E-03	5.34E-03	5.179	0.3	0.3568		6.76E-03	0.1813	26.83	10.02	1.848		0.02443	6.138	251.2	339.32	17.3
	1.05E-03	3.90E-03	3.728	0.22	0.2568		9.72E-03	0.1877	19.31	10.38	1.33		0.02689	5.366	199.5	296.67	13.74
	9.97E-04	2.67E-03	2.683	0.15	0.1848		9.72E-03	0.1351	13.9	7.47	0.9571		0.02984	4.73	158.5	261.49	10.92
	1.10E-03	2.13E-03	1.931	0.12	0.133		1.52E-02	0.1521	10	8.41	0.6888		0.03297	4.151	125.9	229.47	8.672
	1.13E-03	1.57E-03	1.39	0.09	0.09571		2.06E-02	0.148	7.197	8.18	0.4957		0.03642	3.642	100	201.37	6.888
	9.80E-04	9.80E-04	1	0.05	0.06888		2.63E-02	0.1364	5.179	7.54	0.3568		0.04027	3.199	79.43	176.87	5.472
Sample 4	6.27E-03	6.269	1000	346.57	6.89E+01		3.16E-02	0.1176	3.728	6.5	0.2568		0.04497	2.837	63.1	156.86	4.346
	5.23E-03	4.157	794.3	229.85	5.47E+01		4.90E-02	0.1314	2.683	7.27	0.1848		0.05006	2.509	50.12	138.71	3.452
	4.59E-03	2.893	631	159.93	43.46		6.36E-02	0.1228	1.931	6.79	0.133		0.05598	2.229	39.81	123.22	2.742
	4.09E-03	2.052	501.2	113.43	34.52		8.99E-02	0.125	1.389	6.91	0.09571		0.06214	1.965	31.62	108.65	2.178
	3.76E-03	1.497	398.1	82.76	27.42		1.41E-01	0.1411	1	7.8	0.06888		0.07238	1.818	25.12	100.52	1.73
	3.56E-03	1.124	316.2	62.16	21.78	Sample 6	8.98E-03	8.983	1000	496.64	68.88		0.08466	1.689	19.95	93.39	1.374
	3.62E-03	0.9089	251.2	50.25	17.3		8.29E-03	6.586	794.3	364.11	54.72		0.09923	1.573	15.85	86.95	1.092
	3.70E-03	0.7377	199.5	40.78	13.74		8.09E-03	5.102	631	282.08	43.46		0.1181	1.486	12.59	82.18	0.8672
	3.91E-03	0.6194	158.5	34.25	10.92		8.34E-03	4.179	501.2	231.05	34.52		0.132	1.32	10	72.96	0.6888
	3.92E-03	0.493	125.9	27.26	8.672		8.63E-03	3.436	398.1	189.96	27.42		0.156	1.239	7.943	68.51	0.5472
	4.05E-03	0.4047	100	22.37	6.888		9.05E-03	2.862	316.2	158.25	21.78		0.1768	1.115	6.31	61.66	0.4346
	4.43E-03	0.352	79.43	19.46	5.472		9.49E-03	2.385	251.2	131.84	17.3		0.2128	1.066	5.012	58.95	0.3452
	4.59E-03	0.2896	63.1	16.01	4.346		9.99E-03	1.992	199.5	110.16	13.74		0.2413	0.9605	3.981	53.1	0.2742
	4.91E-03	0.246	50.12	13.6	3.452		0.01073	1.701	158.5	94.04	10.92		0.2842	0.8987	3.162	49.69	0.2178
	5.37E-03	0.2139	39.81	11.83	2.742		0.01149	1.447	125.9	79.97	8.672		0.3637	0.9135	2.512	50.51	0.173
	6.03E-03	0.1908	31.62	10.55	2.178		0.01216	1.216	100	67.24	6.888		0.447	0.8918	1.995	49.3	0.1374
	6.70E-03	0.1683	25.12	9.3	1.73		0.01345	1.068	79.43	59.07	5.472		0.587	0.9304	1.585	51.44	0.1092
	7.45E-03	0.1487	19.95	8.22	1.374		0.01529	0.9648	63.1	53.34	4.346		0.7525	0.9474	1.259	52.38	0.08672
	8.64E-03	0.1369	15.85	7.57	1.092		0.01726	0.8648	50.12	47.81	3.452		0.7806	0.7806	1	43.16	0.06888
	9.72E-03	0.1224	12.59	6.77	0.8672		0.0201	0.8002	39.81	44.24	2.742	Sample 9	0.01821	18.21	1000	1006.98	68.88
	1.09E-02	0.1093	10	6.04	0.6889		0.02386	0.7545	31.62	41.72	2.178		0.01848	14.68	794.3	811.67	54.72
	1.31E-02	0.104	7.944	5.75	0.5472		0.02802	0.7039	25.12	38.92	1.73		0.0192	12.12	631	669.85	43.46
	1.48E-02	0.09331	6.31	5.16	0.4346		0.03326	0.6637	19.95	36.69	1.374		2.03E-02	10.19	501.2	563.14	34.52
	1.59E-02	0.07976	5.012	4.41	0.3452		0.03997	0.6336	15.85	35.03	1.092		0.02167	8.625	398.1	476.85	27.42
	1.87E-02	0.0744	3.981	4.11	0.2742		0.05031	0.6333	12.59	35.01	0.8672		0.02342	7.406	316.2	409.43	21.78
	2.21E-02	0.0698	3.162	3.86	0.2178		0.06489	0.6489	10	35.88	0.6888		0.02574	6.466	251.2	357.48	17.3

Table A.28 RPB 0.75 Hz

Sample	Viscosity	Shear stress	Shear rate	Torque	Velocity	Sample	Viscosity	Shear stress	Shear rate	Torque	Velocity	Sample	Viscosity	Shear stress	Shear rate	Torque	Velocity
#	Pa.s	Pa	1/s	mN.m	rad/s	#	Pa.s	Pa	1/s	mN.m	rad/s	#	Pa.s	Pa	1/s	mN.m	rad/s
Sample 9	0.02852	5.69	199.5	314.59	13.74	Sample 10	0.01676	16.76	1000	926.79	68.88	Sample 11	0.01522	15.22	1000	841.53	68.88
	0.03169	5.022	158.5	277.64	10.92		0.01645	13.07	794.3	722.59	54.72		0.01458	11.58	794.3	640.07	54.72
	0.03499	4.405	125.9	243.53	8.672		0.01679	10.59	631	585.55	43.46		0.01453	9.169	631	506.93	43.46
	0.03886	3.886	100	214.82	6.888		1.76E-02	8.812	501.2	487.17	34.52		1.50E-02	7.518	501.2	415.66	34.52
	0.0432	3.432	79.43	189.73	5.472		0.01841	7.328	398.1	405.13	27.42		0.01565	6.232	398.1	344.53	27.42
	0.048	3.029	63.1	167.43	4.346		0.01986	6.28	316.2	347.22	21.78		0.01645	5.201	316.2	287.53	21.78
	0.05306	2.659	50.12	147.01	3.452		0.02163	5.434	251.2	300.42	17.3		0.01758	4.415	251.2	244.09	17.3
	0.05731	2.281	39.81	126.13	2.742		0.02372	4.733	199.5	261.67	13.74		0.01906	3.803	199.5	210.24	13.74
	0.0638	2.018	31.62	111.55	2.178		0.02603	4.126	158.5	228.1	10.92		0.02089	3.311	158.5	183.04	10.92
	0.07256	1.823	25.12	100.76	1.73		0.02879	3.625	125.9	200.41	8.672		0.02297	2.892	125.9	159.91	8.672
	0.08226	1.641	19.95	90.74	1.374		0.03199	3.199	100	176.84	6.888		0.02532	2.532	100	140	6.888
	0.09553	1.514	15.85	83.7	1.092		0.03569	2.835	79.43	156.72	5.472		0.02808	2.231	79.43	123.32	5.472
	0.1114	1.402	12.59	77.52	0.8672		0.04007	2.528	63.1	139.76	4.346		0.0313	1.975	63.1	109.18	4.346
	0.1304	1.304	10	72.07	0.6888		0.04491	2.251	50.12	124.43	3.452		0.03505	1.757	50.12	97.13	3.452
	0.153	1.215	7.943	67.19	0.5472		0.05055	2.013	39.81	111.27	2.742		0.03963	1.578	39.81	87.22	2.742
	0.179	1.13	6.31	62.45	0.4346		0.05631	1.781	31.62	98.45	2.178		0.04497	1.422	31.62	78.63	2.178
	0.2017	1.011	5.012	55.89	0.3452		0.06228	1.564	25.12	86.49	1.73		0.05117	1.285	25.12	71.07	1.73
	0.2343	0.9328	3.981	51.57	0.2742		0.06888	1.374	19.95	75.98	1.374		0.05806	1.158	19.95	64.04	1.374
	0.2643	0.8358	3.162	46.21	0.2178		0.07578	1.201	15.85	66.4	1.092		0.06467	1.025	15.85	56.67	1.092
	0.3087	0.7755	2.512	42.87	0.173		0.08582	1.08	12.59	59.74	0.8672		0.07164	0.9018	12.59	49.86	0.8672
	0.3692	0.7367	1.995	40.73	0.1374		0.09942	0.9942	10	54.96	0.6888		0.08103	0.8103	10	44.8	0.6888
	0.4417	0.7001	1.585	38.7	0.1092		0.1169	0.9283	7.943	51.32	0.5472		0.09484	0.7533	7.943	41.65	0.5472
	0.5596	0.7045	1.259	38.95	0.08672		0.1379	0.8702	6.31	48.11	0.4346		0.1122	0.7077	6.31	39.13	0.4346
	0.672	0.672	1	37.15	0.06888		0.1637	0.8203	5.012	45.35	0.3452		0.1334	0.6687	5.012	36.97	0.3452
							0.1979	0.788	3.981	43.57	0.2742		0.1595	0.6348	3.981	35.1	0.2742
							0.2347	0.7421	3.162	41.03	0.2178		0.194	0.6136	3.162	33.92	0.2178
							0.2708	0.6802	2.512	37.61	0.173		0.2294	0.5762	2.512	31.86	0.173
							0.309	0.6165	1.995	34.08	0.1374		0.2715	0.5417	1.995	29.95	0.1374
							0.3623	0.5743	1.585	31.75	0.1092		0.3068	0.4863	1.585	26.88	0.1092
							0.3996	0.5031	1.259	27.82	0.08672		0.325	0.4091	1.259	22.62	0.08672
							0.4892	0.4892	1	27.04	0.06888		0.3736	0.3736	1	20.65	0.06888

Table A.29 RPB 0.75 Hz

Sample	Viscosity	Shear stress	Shear rate	Torque	Velocity	Sample	Viscosity	Shear stress	Shear rate	Torque	Velocity	Sample	Viscosity	Shear stress	Shear rate	Torque	Velocity
#	Pa.s	Pa	1/s	mN.m	rad/s	#	Pa.s	Pa	1/s	mN.m	rad/s	#	Pa.s	Pa	1/s	mN.m	rad/s
Sample 12	0.01388	13.88	1000	767.43	68.88	Sample 13	0.01356	13.56	1000	749.77	68.88	Sample 16	0.01347	13.47	1000	744.86	68.88
	0.01274	10.12	794.3	559.7	54.72		0.01192	9.471	794.3	523.59	54.72		0.01186	9.424	794.3	520.99	54.72
	0.01254	7.914	631	437.54	43.46		0.01143	7.211	631	398.69	43.46		0.01119	7.063	631	390.48	43.46
	1.27E-02	6.384	501.2	352.94	34.52		1.15E-02	5.781	501.2	319.61	34.52		1.11E-02	5.578	501.2	308.4	34.52
	0.01302	5.182	398.1	286.51	27.42		0.01165	4.639	398.1	256.47	27.42		0.01133	4.512	398.1	249.43	27.42
	0.01343	4.248	316.2	234.87	21.78		0.01186	3.751	316.2	207.39	21.78		0.0115	3.637	316.2	201.05	21.78
	0.01406	3.531	251.2	195.23	17.3		0.01225	3.076	251.2	170.08	17.3		0.01179	2.961	251.2	163.71	17.3
	0.01489	2.97	199.5	164.2	13.74		0.01279	2.553	199.5	141.14	13.74		0.01225	2.443	199.5	135.08	13.74
	0.01583	2.51	158.5	138.74	10.92		0.01342	2.127	158.5	117.57	10.92		0.01291	2.047	158.5	113.15	10.92
	0.01695	2.134	125.9	118	8.672		0.0141	1.776	125.9	98.17	8.672		0.01364	1.717	125.9	94.93	8.672
	0.01849	1.849	100	102.25	6.888		0.01514	1.514	100	83.7	6.888		0.01443	1.443	100	79.8	6.888
	0.02037	1.618	79.43	89.44	5.472		0.01643	1.305	79.43	72.15	5.472		0.01544	1.227	79.43	67.82	5.472
	0.02247	1.418	63.1	78.38	4.346		0.01801	1.136	63.1	62.81	4.346		0.01677	1.058	63.1	58.5	4.346
	0.02503	1.254	50.12	69.35	3.452		0.0199	0.9975	50.12	55.15	3.452		0.01848	0.9261	50.12	51.2	3.452
	0.02807	1.117	39.81	61.77	2.742		0.0223	0.8879	39.81	49.09	2.742		0.02054	0.8179	39.81	45.22	2.742
	0.03173	1.003	31.62	55.47	2.178		0.02513	0.7947	31.62	43.94	2.178		0.02302	0.7279	31.62	40.24	2.178
	0.03597	0.9036	25.12	49.96	1.73		0.02859	0.718	25.12	39.7	1.73		0.02608	0.655	25.12	36.21	1.73
	0.04136	0.8252	19.95	45.62	1.374		0.03285	0.6554	19.95	36.23	1.374		0.02991	0.5969	19.95	33	1.374
	0.04798	0.7605	15.85	42.05	1.092		0.03833	0.6075	15.85	33.58	1.092		0.03474	0.5506	15.85	30.44	1.092
	0.05556	0.6994	12.59	38.67	0.8672		0.04484	0.5646	12.59	31.21	0.8672		0.04071	0.5126	12.59	28.34	0.8672
	0.06414	0.6415	10	35.46	0.6888		0.05272	0.5272	10	29.15	0.6888		0.04802	0.4802	10	26.55	0.6888
	0.07405	0.5882	7.943	32.52	0.5472		0.06176	0.4906	7.943	27.12	0.5472		0.05669	0.4503	7.943	24.9	0.5472
	0.08481	0.5351	6.31	29.58	0.4346		0.07226	0.4559	6.31	25.21	0.4346		0.06634	0.4186	6.31	23.14	0.4346
	0.09857	0.494	5.012	27.31	0.3452		0.0847	0.4245	5.012	23.47	0.3452		0.07794	0.3906	5.012	21.59	0.3452
	0.1153	0.459	3.981	25.38	0.2742		0.09919	0.3949	3.981	21.83	0.2742		0.09167	0.365	3.981	20.18	0.2742
	0.1368	0.4325	3.162	23.91	0.2178		0.1172	0.3707	3.162	20.49	0.2178		0.1082	0.3423	3.162	18.92	0.2178
	0.1656	0.4159	2.512	22.99	0.173		0.1403	0.3524	2.512	19.48	0.173		0.1274	0.3201	2.512	17.69	0.173
	0.2032	0.4054	1.995	22.41	0.1374		0.1677	0.3346	1.995	18.5	0.1374		0.1529	0.305	1.995	16.86	0.1374
	0.2485	0.3939	1.585	21.78	0.1092		0.2078	0.3294	1.585	18.21	0.1092		0.186	0.2948	1.585	16.3	0.1092
	0.2935	0.3695	1.259	20.43	0.08672		0.259	0.326	1.259	18.03	0.08672		0.2233	0.2811	1.259	15.54	0.08672
	0.3383	0.3383	1	18.7	0.06888		0.3034	0.3034	1	16.78	0.06888		0.269	0.269	1	14.87	0.06888

Table A.30 RPB 1 Hz

Sample	Viscosity	Shear stress	Shear rate	Torque	Velocity	Sample	Viscosity	Shear stress	Shear rate	Torque	Velocity	Sample	Viscosity	Shear stress	Shear rate	Torque	Velocity
#	Pa.s	Pa	1/s	mN.m	rad/s	#	Pa.s	Pa	1/s	mN.m	rad/s	#	Pa.s	Pa	1/s	mN.m	rad/s
Sample 1	3.46E-03	3.459	1000	191.23	68.88	Sample 4	9.17E-03	0.183	19.95	10.12	1.374	Sample 6	4.02E-03	2.016	501.2	111.44	34.52
	3.06E-03	2.433	794.3	134.51	54.72		1.31E-02	0.2072	15.85	11.46	1.092		3.76E-03	1.496	398.1	82.68	27.42
	2.75E-03	1.734	631	95.86	43.46		2.41E-02	0.303	12.59	16.75	0.8672		3.46E-03	1.094	316.2	60.46	21.78
	2.44E-03	1.221	501.2	67.49	34.52		1.77E-02	0.1772	9.999	9.79	0.6888		3.24E-03	0.8145	251.2	45.03	17.3
	2.14E-03	0.8532	398.1	47.17	27.42		1.93E-02	0.1531	7.943	8.46	0.5471		3.25E-03	0.648	199.5	35.83	13.74
	1.92E-03	0.6079	316.2	33.61	21.78		2.17E-02	0.1371	6.31	7.58	0.4347		3.35E-03	0.5302	158.5	29.31	10.92
	1.73E-03	0.4348	251.2	24.04	17.3		2.62E-02	0.1311	5.012	7.25	0.3452		3.45E-03	0.4337	125.9	23.98	8.672
	1.51E-03	0.3007	199.5	16.62	13.74		2.75E-02	0.1096	3.981	6.06	0.2742		3.65E-03	0.3645	100	20.15	6.888
	1.26E-03	0.1995	158.5	11.03	10.92		3.19E-02	0.101	3.162	5.58	0.2178		3.91E-03	0.3107	79.43	17.18	5.472
	1.07E-03	0.1348	125.9	7.45	8.672		5.98E-02	0.1501	2.512	8.3	0.173		4.16E-03	0.2627	63.1	14.52	4.346
	1.05E-03	0.1045	100	5.78	6.888		4.64E-02	0.09258	1.995	5.12	0.1374		4.73E-03	0.2371	50.12	13.11	3.452
	1.02E-03	0.08136	79.43	4.5	5.472		4.35E-02	0.0689	1.585	3.81	0.1092		5.33E-03	0.2123	39.81	11.73	2.742
	1.01E-03	0.06388	63.1	3.53	4.346		4.46E-02	0.05618	1.259	3.11	0.08672		5.82E-03	0.1839	31.62	10.17	2.178
	1.01E-03	0.0505	50.12	2.79	3.452		5.55E-02	0.05547	1	3.07	0.06888		6.33E-03	0.159	25.12	8.79	1.73
	1.01E-03	0.0403	39.81	2.23	2.742	Sample 5	5.59E-03	5.589	1000	308.97	68.88		7.58E-03	0.1512	19.95	8.36	1.374
	1.04E-03	0.03293	31.62	1.82	2.178		4.50E-03	3.576	794.3	197.72	54.72		8.85E-03	0.1402	15.85	7.75	1.092
	1.03E-03	0.02579	25.12	1.43	1.73		3.86E-03	2.434	631	134.58	43.46		0.01034	0.1302	12.59	7.2	0.8672
	1.05E-03	0.0209	19.95	1.16	1.374		3.43E-03	1.72	501.2	95.1	34.52		0.01294	0.1294	10	7.15	0.6888
	1.07E-03	0.01687	15.85	0.93	1.092		3.26E-03	1.298	398.1	71.77	27.42		0.01453	0.1154	7.943	6.38	0.5472
	1.10E-03	0.01379	12.59	0.76	0.8672		2.95E-03	0.9341	316.2	51.64	21.78		0.01802	0.1137	6.31	6.28	0.4346
	1.14E-03	0.01142	10	0.63	0.6888		2.74E-03	0.6887	251.2	38.07	17.3		0.02253	0.1129	5.012	6.24	0.3452
	1.19E-03	9.47E-03	7.943	0.52	0.5472		2.66E-03	0.5302	199.5	29.31	13.74		0.02759	0.1098	3.981	6.07	0.2742
	1.24E-03	7.84E-03	6.31	0.43	0.4346		2.78E-03	0.4408	158.5	24.37	10.92		0.03331	0.1053	3.162	5.82	0.2178
	1.30E-03	6.52E-03	5.012	0.36	0.3452		2.77E-03	0.3489	125.9	19.29	8.672		0.03765	0.09457	2.512	5.23	0.173
	1.34E-03	5.34E-03	3.981	0.3	0.2742		2.95E-03	0.2945	100	16.28	6.888		0.0452	0.0902	1.995	4.99	0.1374
	1.57E-03	4.96E-03	3.162	0.27	0.2178		3.07E-03	0.2437	79.43	13.47	5.472		0.05368	0.08508	1.585	4.7	0.1092
	1.64E-03	4.13E-03	2.512	0.23	0.173		3.04E-03	0.1918	63.1	10.6	4.346		0.06438	0.08105	1.259	4.48	0.08672
	1.90E-03	3.80E-03	1.995	0.21	0.1374		3.20E-03	0.1604	50.12	8.87	3.452		0.08965	0.08965	1	4.96	0.06888
	2.06E-03	3.26E-03	1.585	0.18	0.1092		3.41E-03	0.1356	39.81	7.5	2.742	Sample 7	9.55E-03	9.545	1000	527.73	68.88
	2.23E-03	2.81E-03	1.259	0.16	0.08672		4.11E-03	0.1301	31.62	7.19	2.178		9.22E-03	7.323	794.3	404.88	54.72
	2.01E-03	2.01E-03	1	0.11	0.06888		4.75E-03	0.1193	25.12	6.59	1.73		9.53E-03	6.012	631	332.39	43.46
Sample 4	5.81E-03	5.81	1000	321.22	6.89E+01		5.56E-03	0.1108	19.95	6.13	1.374		9.98E-03	5.004	501.2	276.64	34.52
	4.97E-03	3.948	794.3	218.26	5.47E+01		7.11E-03	0.1126	15.85	6.23	1.092		0.01048	4.171	398.1	230.6	27.42
	4.48E-03	2.827	631	156.32	43.46		7.39E-03	0.09304	12.59	5.14	0.8672		0.01105	3.494	316.2	193.18	21.78
	4.01E-03	2.01	501.2	111.1	34.52		8.93E-03	0.08928	10	4.94	0.6888		0.0117	2.939	251.2	162.5	17.3
	3.72E-03	1.48	398.1	81.85	27.42		1.02E-02	0.08094	7.943	4.47	0.5472		0.01249	2.491	199.5	137.73	13.74
	3.60E-03	1.137	316.2	62.87	21.78		1.30E-02	0.08194	6.309	4.53	0.4346		0.01349	2.139	158.5	118.24	10.92
	3.62E-03	0.9094	251.2	50.28	17.3		1.62E-02	0.08125	5.012	4.49	0.3452		0.01476	1.858	125.9	102.72	8.672
	3.78E-03	0.7548	199.5	41.73	13.74		3.04E-02	0.121	3.981	6.69	0.2742		0.01625	1.625	100	89.82	6.888
	3.89E-03	0.6165	158.5	34.08	10.92		4.21E-02	0.1331	3.162	7.36	0.2178		0.01804	1.433	79.43	79.2	5.472
	3.91E-03	0.4919	125.9	27.2	8.672		4.52E-02	0.1136	2.512	6.28	0.173		0.01978	1.248	63.1	69.01	4.346
	4.24E-03	0.4236	100	23.42	6.888		4.31E-02	0.08609	1.995	4.76	0.1374		0.02243	1.124	50.12	62.16	3.452
	3.99E-03	0.3172	79.43	17.53	5.472		5.68E-02	0.09	1.585	4.98	0.1092		0.0257	1.023	39.81	56.56	2.742
	4.43E-03	0.2795	63.1	15.45	4.346		5.99E-02	0.07539	1.259	4.17	0.08672		0.02962	0.9366	31.62	51.78	2.178
	5.14E-03	0.2577	50.12	14.25	3.452		6.73E-02	0.06728	1	3.72	0.06888		0.03303	0.8296	25.12	45.86	1.73
	5.85E-03	0.2329	39.81	12.88	2.742	Sample 6	5.85E-03	5.853	1000	323.58	68.88		0.0386	0.7701	19.95	42.58	1.374
	6.20E-03	0.1959	31.62	10.83	2.178		4.93E-03	3.914	794.3	216.39	54.72		0.04642	0.7357	15.85	40.67	1.092
	6.90E-03	0.1734	25.12	9.58	1.73		4.37E-03	2.757	631	152.43	43.46		0.05433	0.684	12.59	37.82	0.8672

Table A.31 RPB 1 Hz

Sample	Viscosity	Shear stress	Shear rate	Torque	Velocity	Sample	Viscosity	Shear stress	Shear rate	Torque	Velocity	Sample	Viscosity	Shear stress	Shear rate	Torque	Velocity
#	Pa.s	Pa	1/s	mN.m	rad/s	#	Pa.s	Pa	1/s	mN.m	rad/s	#	Pa.s	Pa	1/s	mN.m	rad/s
Sample 7	0.0633	0.633	10	35	0.6888	Sample 10	0.023	23	1000	1271.32	68.88	Sample 11	0.0241	24.1	1000	1332.59	68.88
	0.07438	0.5908	7.943	32.66	0.5472		0.02348	18.65	794.3	1031.02	54.72		0.02464	19.57	794.3	1082.07	54.72
	0.08631	0.5446	6.31	30.11	0.4346		0.02441	15.4	631	851.35	43.46		0.02556	16.13	631	891.69	43.46
	0.1051	0.5269	5.012	29.13	0.3452		2.57E-02	12.89	501.2	712.63	34.52		2.71E-02	13.58	501.2	750.58	34.52
	0.1226	0.4882	3.981	26.99	0.2742		0.02789	11.1	398.1	613.78	27.42		0.02916	11.61	398.1	641.73	27.42
	0.1544	0.4883	3.162	26.99	0.2178		0.03052	9.65	316.2	533.53	21.78		0.03216	10.17	316.2	562.17	21.78
	0.1853	0.4655	2.512	25.74	0.173		0.03383	8.498	251.2	469.83	17.3		0.03571	8.969	251.2	495.86	17.3
	0.2225	0.4439	1.995	24.54	0.1374		0.03779	7.539	199.5	416.81	13.74		0.03977	7.936	199.5	438.74	13.74
	0.2666	0.4225	1.585	23.36	0.1092		0.04227	6.699	158.5	370.36	10.92		0.04447	7.048	158.5	389.65	10.92
	0.3166	0.3985	1.259	22.03	0.08672		0.04747	5.976	125.9	330.41	8.672		0.05005	6.301	125.9	348.35	8.672
	0.4067	0.4067	1	22.49	0.06888		0.0533	5.33	100	294.7	6.888		0.05665	5.665	100	313.22	6.888
Sample 9	0.02683	26.83	1000	1483.4	68.88		0.05994	4.761	79.43	263.21	5.472		0.06428	5.106	79.43	282.27	5.472
	0.0282	22.4	794.3	1238.55	54.72		0.06737	4.251	63.1	235	4.346		0.07313	4.614	63.1	255.1	4.346
	0.03009	18.98	631	1049.56	43.46		0.07529	3.774	50.12	208.63	3.452		0.08342	4.181	50.12	231.14	3.452
	3.26E-02	16.33	501.2	902.77	34.52		0.08347	3.323	39.81	183.72	2.742		0.09478	3.773	39.81	208.61	2.742
	0.03609	14.37	398.1	794.3	27.42		0.09012	2.85	31.62	157.55	2.178		0.1077	3.405	31.62	188.27	2.178
	0.04023	12.72	316.2	703.32	21.78		0.09942	2.497	25.12	138.06	1.73		0.1217	3.058	25.12	169.06	1.73
	0.04498	11.3	251.2	624.69	17.3		0.1124	2.243	19.95	123.99	1.374		0.1346	2.685	19.95	148.44	1.374
	0.05028	10.03	199.5	554.59	13.74		0.1293	2.049	15.85	113.29	1.092		0.1512	2.396	15.85	132.48	1.092
	0.05628	8.919	158.5	493.1	10.92		0.1507	1.897	12.59	104.86	0.8672		0.1724	2.17	12.59	119.97	0.8672
	0.06261	7.882	125.9	435.74	8.672		0.1784	1.784	10	98.62	0.6888		0.197	1.97	10	108.91	0.6888
	0.06905	6.905	100	381.74	6.888		0.2129	1.691	7.943	93.47	0.5472		0.2286	1.816	7.943	100.38	0.5472
	0.07607	6.042	79.43	334.06	5.472		0.2547	1.607	6.31	88.84	0.4346		0.2692	1.699	6.31	93.9	0.4346
	0.0828	5.225	63.1	288.85	4.346		0.306	1.534	5.012	84.79	0.3452		0.3188	1.598	5.012	88.33	0.3452
	0.09318	4.67	50.12	258.2	3.452		0.3607	1.436	3.981	79.38	0.2742		0.379	1.509	3.981	83.42	0.2742
	0.1081	4.302	39.81	237.83	2.742		0.4127	1.305	3.162	72.15	0.2178		0.4521	1.43	3.162	79.03	0.2178
	0.1264	3.996	31.62	220.93	2.178		0.4732	1.189	2.512	65.71	0.173		0.5381	1.352	2.512	74.73	0.173
	0.1466	3.682	25.12	203.55	1.73		0.5561	1.11	1.995	61.34	0.1374		0.6537	1.304	1.995	72.11	0.1374
	0.1743	3.478	19.95	192.27	1.374		0.656	1.04	1.585	57.48	0.1092		0.7746	1.228	1.585	67.87	0.1092
	0.2025	3.21	15.85	177.47	1.092		0.7808	0.9829	1.259	54.34	0.08672		0.9041	1.138	1.259	62.93	0.08672
	0.2342	2.949	12.59	163.04	0.8672		0.9795	0.9795	1	54.15	0.06888		1.06	1.06	1	58.6	0.06888
	0.2742	2.742	10	151.57	0.6888												
	0.3169	2.517	7.943	139.15	0.5472												
	0.3709	2.34	6.31	129.39	0.4346												
	0.4297	2.154	5.012	119.06	0.3452												
	0.5355	2.132	3.981	117.87	0.2742												
	0.6342	2.006	3.162	110.88	0.2178												
	0.8081	2.03	2.512	112.23	0.173												
	0.9592	1.914	1.995	105.81	0.1374												
	1.17	1.854	1.585	102.51	0.1092												
	1.506	1.897	1.259	104.85	0.08672												
	2.024	2.024	1	111.88	0.06888												

Table A.32 RPB 1 Hz

Sample	Viscosity	Shear stress	Shear rate	Torque	Velocity	Sample	Viscosity	Shear stress	Shear rate	Torque	Velocity	Sample	Viscosity	Shear stress	Shear rate	Torque	Velocity
#	Pa.s	Pa	1/s	mN.m	rad/s	#	Pa.s	Pa	1/s	mN.m	rad/s	#	Pa.s	Pa	1/s	mN.m	rad/s
Sample 12	0.02572	25.72	1000	1422.03	68.88	Sample 13	0.02504	25.04	1000	1384.59	68.88	Sample 14	0.02169	21.69	1000	1199.16	68.88
	0.02597	20.63	794.3	1140.39	54.72		0.02524	20.05	794.3	1108.42	54.72		0.02141	17.01	794.3	940.23	54.72
	0.02711	17.11	631	945.69	43.46		0.02601	16.41	631	907.42	43.46		0.0218	13.75	631	760.34	43.46
	2.89E-02	14.49	501.2	800.84	34.52		2.75E-02	13.76	501.2	760.55	34.52		2.28E-02	11.42	501.2	631.11	34.52
	0.03098	12.33	398.1	681.94	27.42		0.0293	11.66	398.1	644.81	27.42		0.02413	9.608	398.1	531.19	27.42
	0.03379	10.69	316.2	590.78	21.78		0.03175	10.04	316.2	555	21.78		0.02596	8.209	316.2	453.82	21.78
	0.03746	9.408	251.2	520.16	17.3		0.03483	8.749	251.2	483.72	17.3		0.02826	7.098	251.2	392.43	17.3
	0.04211	8.402	199.5	464.53	13.74		0.03843	7.668	199.5	423.92	13.74		0.03088	6.161	199.5	340.62	13.74
	0.04794	7.597	158.5	420.03	10.92		0.04265	6.759	158.5	373.69	10.92		0.03399	5.388	158.5	297.87	10.92
	0.05518	6.947	125.9	384.08	8.672		0.04754	5.985	125.9	330.89	8.672		0.03768	4.743	125.9	262.23	8.672
	0.06406	6.406	100	354.18	6.888		0.05318	5.318	100	293.99	6.888		0.04201	4.201	100	232.26	6.888
	0.07738	6.146	79.42	339.77	5.471		0.05967	4.739	79.43	262.03	5.472		0.04695	3.729	79.43	206.17	5.472
	0.09083	5.731	63.09	316.82	4.346		0.06702	4.228	63.1	233.77	4.346		0.0527	3.325	63.1	183.82	4.346
	0.1069	5.36	50.14	296.31	3.454		0.07561	3.789	50.12	209.5	3.452		0.05944	2.979	50.12	164.71	3.452
	0.1355	5.397	39.84	298.38	2.744		0.08568	3.411	39.81	188.58	2.742		0.06737	2.682	39.81	148.29	2.742
	0.1551	4.903	31.62	271.05	2.178		0.09749	3.083	31.62	170.45	2.178		0.07681	2.429	31.62	134.28	2.178
	0.1789	4.496	25.13	248.55	1.731		0.1109	2.787	25.12	154.07	1.73		0.08807	2.212	25.12	122.3	1.73
	0.2115	4.219	19.95	233.27	1.374		0.1265	2.524	19.95	139.57	1.374		0.1014	2.024	19.95	111.88	1.374
	0.2347	3.721	15.85	205.7	1.092		0.1433	2.272	15.85	125.59	1.092		0.1176	1.864	15.85	103.08	1.092
	0.2966	3.735	12.6	206.5	0.8676		0.1617	2.036	12.59	112.57	0.8672		0.1369	1.724	12.59	95.31	0.8672
	0.33	3.3	10	182.44	0.6888		0.1821	1.821	10	100.7	0.6888		0.1597	1.597	10	88.28	0.6888
	0.3843	3.054	7.945	168.82	0.5473		0.2032	1.614	7.943	89.23	0.5472		0.1854	1.473	7.943	81.41	0.5472
	0.4264	2.691	6.31	148.78	0.4347		0.2301	1.452	6.31	80.26	0.4346		0.2146	1.354	6.31	74.84	0.4346
	0.5517	2.766	5.013	152.89	0.3453		0.2644	1.325	5.012	73.25	0.3452		0.2511	1.258	5.012	69.57	0.3452
	0.631	2.512	3.98	138.87	0.2742		0.3126	1.244	3.981	68.8	0.2742		0.2932	1.167	3.981	64.53	0.2742
	0.7552	2.388	3.163	132.05	0.2179		0.3693	1.168	3.162	64.57	0.2178		0.3441	1.088	3.162	60.15	0.2178
	0.7925	1.99	2.512	110.04	0.173		0.4375	1.099	2.512	60.75	0.173		0.4043	1.016	2.512	56.15	0.173
	0.9719	1.939	1.995	107.21	0.1374		0.524	1.046	1.995	57.8	0.1374		0.4863	0.9702	1.995	53.64	0.1374
	1.024	1.623	1.585	89.72	0.1092		0.6367	1.009	1.585	55.79	0.1092		0.5983	0.9482	1.585	52.42	0.1092
	1.056	1.33	1.259	73.52	0.08671		0.7686	0.9676	1.259	53.5	0.08672		0.7193	0.9056	1.259	50.06	0.08672
	2.692	2.692	1	148.83	0.06889		0.8829	0.8829	1	48.81	0.06888		0.8477	0.8477	1	46.87	0.06888